



Dipòsit legal: B.8847-2009  
ISBN:

**microRNA-mediated regulation of the full-length  
and truncated isoforms  
of human neurotrophic tyrosine kinase receptor  
type 3 (NTRK3)**

**Monica Guidi**

Doctoral Thesis  
Universitat Pompeu Fabra  
2008

Thesis Directors

Dr. Xavier Estivill  
Center for Genomic Regulation  
(CRG)  
Barcelona

Dr. Yolanda Espinosa-Parrilla  
Center for Genomic Regulation  
(CRG)  
Barcelona









*Life on other planets is difficult,  
sooooo difficult  
E.N.*



# Contents

|                                                                   |    |
|-------------------------------------------------------------------|----|
| <b>ACKNOWLEDGEMENTS</b>                                           | IX |
| <b>ABSTRACT</b>                                                   | XI |
| <b>1.INTRODUCTION</b>                                             | 1  |
| <b>1. Neurotrophin signaling in the vertebrate nervous system</b> | 3  |
| Neurotrophins and their receptors                                 | 3  |
| Neurotrophins and disease                                         | 6  |
| p75NTR signaling                                                  | 8  |
| Trk signaling                                                     | 9  |
| Trk receptors and cancer                                          | 12 |
| TrkC (NTRK3)                                                      | 13 |
| <b>2. microRNAs</b>                                               | 18 |
| Non-coding RNAs                                                   | 18 |
| microRNA-mediated gene silencing                                  | 19 |
| microRNAs in development and differentiation                      | 23 |
| microRNAs in metabolism regulation and stress response            | 24 |
| microRNAs and cancer                                              | 25 |
| microRNAs in the nervous system                                   | 28 |
| microRNA target prediction methods                                | 35 |
| <b>2. OBJECTIVES</b>                                              | 39 |
| <b>3. MATERIALS AND METHODS</b>                                   | 43 |
| 3'UTR cloning                                                     | 45 |
| Cell culture                                                      | 46 |
| Optimization of transfection conditions                           | 47 |
| Luciferase assay                                                  | 48 |
| Protein extraction                                                | 49 |
| Differentiation of SH-SY5Y cells                                  | 49 |
| Transfection of SH-SY5Y cells                                     | 50 |

|                                                                                                            |    |
|------------------------------------------------------------------------------------------------------------|----|
| Western blot optimization for NTRK3                                                                        | 51 |
| Western blotting                                                                                           | 53 |
| Purification of total RNA                                                                                  | 55 |
| miRNA expression analysis using custom oligonucleotide microarrays (Agilent, 11k)                          | 56 |
| Whole-genome expression analysis using beadchip microarrays (Illumina HumanRef-8 v3.0)                     | 56 |
| Real-time quantitative RT-PCR ( <i>NTRK3</i> )                                                             | 57 |
| miRNA quantitative RT-PCR                                                                                  | 57 |
| Cell counting                                                                                              | 58 |
| MTT cell viability assay                                                                                   | 58 |
| Flow cytometry                                                                                             | 59 |
| Computational methods                                                                                      | 59 |
| <b>4. RESULTS</b>                                                                                          | 61 |
| <b>1. Screening of <i>NTRK3</i>'s putative miRNA target sites using a luciferase reporter-based system</b> | 63 |
| Target predictions and tested miRNAs                                                                       | 63 |
| Optimization of the luciferase assay                                                                       | 65 |
| Validation of predicted target sites using luciferase reporter constructs                                  | 67 |
| miRNAs targeting pGL4.13-TR do not act synergistically                                                     | 71 |
| <b>2. miRNA-mediated regulation of endogenous NTRK3</b>                                                    | 72 |
| Expression profile of FL-NTRK3 and TR-NTRK3 in SH-SY5Y cells                                               | 72 |
| miRNA expression in HeLa and SH-SY5Y cells                                                                 | 74 |
| Validation of miRNA target predictions on endogenous NTRK3 by miRNA mimic overexpression                   | 74 |
| miRNA-mediated repression of FL-NTRK3 affects downstream NT3-induced signaling                             | 77 |
| Effects of miR-128 and miR-509 overexpression in undifferentiated SH-SY5Y cells                            | 78 |
| Expression profiles of miR-128 and miR-509 in different human tissues and in SH-SY5Y cells                 | 82 |
| <b>3. Effects of miR-128 and miR-509 overexpression on the transcriptome of SH-SY5Y cells</b>              | 83 |
| Overlapping between miRNA target predictions and deregulated genes                                         | 84 |
| Analysis of deregulated pathways                                                                           | 87 |

|                                                                                                            |     |
|------------------------------------------------------------------------------------------------------------|-----|
| <b>4. miR-124a regulates the expression of the two NTRK3 isoforms through the splicing repressor PTBP1</b> | 103 |
| <b>5. DISCUSSION</b>                                                                                       | 107 |
| <b>6. CONCLUSIONS</b>                                                                                      | 121 |
| <b>7. REFERENCES</b>                                                                                       | 125 |
| <b>ABBREVIATIONS</b>                                                                                       | 144 |





# Acknowledgements

I would like to acknowledge, first and foremost, Dr. Yolanda Espinosa for supervising this thesis, for her generous and continuous assistance and for having been crucial to making this project work.

Dr. Xavier Estivill for giving me the opportunity to join his laboratory for my thesis research. Birgit Kagerbauer for her precious hands-on help, especially in these last months of PhD. Margarita Muiños for being such a cheerful and optimistic NTRK3 fellow :). Dr. Eulàlia Martí, Dr. Mónica Bañez, Dr. Silvia Porta and Elena Miñones for their always helpful advice. Dr. Mara Dierssen for her sympathetic interest in the progression of this thesis. Dr. Heidi C. Howard for her constant encouragement and for being a good friend. All members of lab 521 and of the Genes and Disease Program at CRG, for being a great group of people to work with and making everyday life in the lab enjoyable during five long years.

Thanks to everyone who contributed, directly or indirectly, to the completion of this thesis with their scientific, technical or moral support.

Special thanks to my family and friends in Italy, Spain or wherever for being there.



# Abstract

Neurotrophins and their receptors are key molecules in the development of the nervous system. Neurotrophin-3 binds preferentially to its high-affinity receptor NTRK3, which exists in two major isoforms in humans, the full-length kinase-active form (150 kDa) and a truncated non-catalytic form (50 kDa). The two variants show different 3'UTR regions, indicating that they might be differentially regulated at the post-transcriptional level. In this work we explore how microRNAs take part in the regulation of full-length and truncated NTRK3, demonstrating that the two isoforms are targeted by different sets of microRNAs. We analyze the physiological consequences of the overexpression of some of the regulating microRNAs in human neuroblastoma cells. Finally, we provide preliminary evidence for a possible involvement of miR-124 - a microRNA with no putative target site in either NTRK3 isoform - in the control of the alternative splicing of NTRK3, through the downregulation of the splicing repressor PTBP1.

*Las neurotrofinas y sus receptores constituyen una familia de factores cruciales para el desarrollo del sistema nervioso. La neurotrofina 3 ejerce su función principalmente a través de una unión de gran afinidad al receptor NTRK3, del cual se conocen dos isoformas principales, una larga de 150KDa con actividad de tipo tirosina kinasa y una truncada de 50KDa sin dicha actividad. Estas dos isoformas no comparten la misma región 3'UTR, lo que sugiere la existencia de una regulación postranscripcional diferente. En el presente trabajo se ha explorado como los microRNAs intervienen en la regulación de NTRK3, demostrando que las dos isoformas son reguladas por diferentes miRNAs. Se han analizado las consecuencias fisiológicas de la sobreexpresión de dichos microRNAs utilizando células de neuroblastoma. Finalmente, se ha estudiado la posible implicación del microRNA miR-124 en el control del splicing alternativo de NTRK3 a través de la regulación de represor de splicing PTBP1.*







# **1.Introduction**





## **1. Neurotrophin signaling in the vertebrate nervous system**

### **Neurotrophins and their receptors**

Neurotrophins are a family of growth factors that play important roles in the nervous system; they can exert multiple functions such as promoting neuronal survival, differentiation or apoptosis as well as axon and dendrite growth, depending – among other factors – on the type of neurotrophin and the expression pattern of the corresponding receptors.

Neurotrophins regulate the proliferation and differentiation of neuronal precursors and mediate the survival and maintenance of central and peripheral neurons during development and adulthood, being crucial in the control of neuronal numbers and connections. They are highly expressed in the nervous system but are also released by innervated target organs, being captured by nerve terminals once secreted; here they act locally to regulate nerve terminal function and after internalization they can be transported to neuronal cell bodies where they act at a distance mediating survival and/or differentiation (Reichardt, 2006). Similarly, during development the secretion of neurotrophins by innervated target areas - either structures belonging to the nervous system or peripheral organs - controls neuronal survival. As neurons are produced in excess in early developmental stages, this process helps match the size of neuronal populations with the territory they innervate (Oppenheim, 1991), allowing innervating neurons to escape elimination and grow proportionally with the organism. Moreover, neurotrophin expression is important after injury, when the elevated production of neurotrophic factors is believed to be essential for the survival and regeneration of injured neurons. More recent evidence has indicated that neurotrophins - especially BDNF - also act as synaptic modulators with a key role in synaptic plasticity, showing that they are also involved in cognitive processes, learning and memory formation. They in fact mediate activity-dependent functional and structural modifications of synaptic connections like long-term potentiation (LTP) and long-term depression (LTD) (Lu et al., 2005).

In mammals the neurotrophin family consists of four members, including nerve growth factor (NGF, the first identified neurotrophin discovered in the 1950s by Levi-Montalcini), brain-derived neurotrophic factor (BDNF), neurotrophin-3 (NT3)

and neurotrophin-4/5 (NT4/5); all are produced as longer precursors known as proneurotrophins (30-35 kDa), which undergo intracellular proteolytic cleavage giving rise to mature, secreted ligands that have a size of ~13 kDa and act as non-covalently linked homodimers. The four proteins share a highly homologous structure with features - like the tertiary fold - that are present in several other growth factors (Reichardt, 2006); their genes share sequence homologies, and the flanking genomic segments show as well a similar organization.

With the exception of *NT4/5*, neurotrophin genes are highly conserved in mammals. Sequence comparison among vertebrates suggests that *NGF/NT3* and *BDNF/NT4/5* evolved from separate duplication events involving a portion of the genome derived from an ancestral chordate; accordingly, neurotrophin receptor genes seem to have coevolved with neurotrophins (Hallbook, 1999).

Neurotrophins can interact with two entirely distinct classes of transmembrane receptors (Fig.1), tropomyosin-related kinase (Trk) receptors and the neurotrophin receptor p75 (p75NTR); this dual system allows the transduction of different signals that can be as contrasting as promoting cell death through p75 and cell survival through Trk receptors.

p75NTR was the first neurotrophin receptor to be discovered and was identified as a low affinity receptor for NGF, but it was later shown to bind each neurotrophin with similar affinity ( $\sim 10^{-9}$  M) (Rodriguez-Tebar et al., 1990). It is a member of the tumor necrosis factor superfamily and contains four extracellular cysteine repeats that form the ligand-binding domain, a single transmembrane domain and a cytoplasmic so-called 'death' domain, similar to those present in other members of this family (Liepinsh et al., 1997). p75NTR receptors do not exhibit any intrinsic catalytic activity, but they transduce the signal by associating with, or

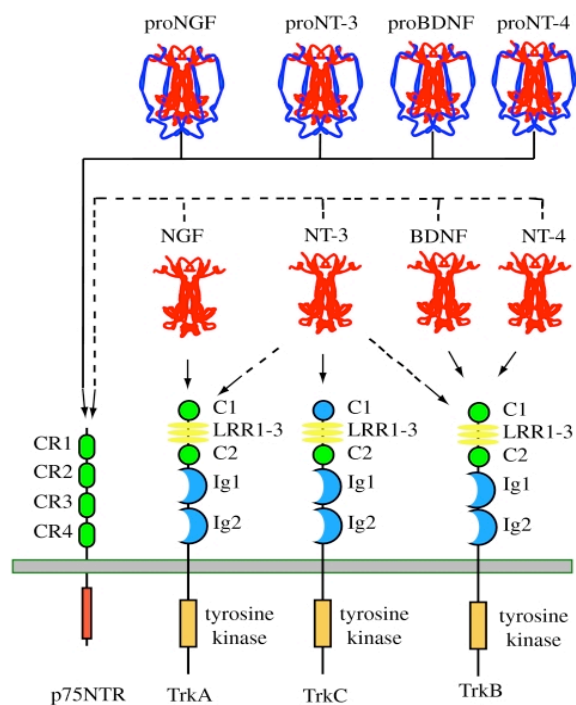


**Fig.1** Major interactions of the four mammalian neurotrophins. Continuous line: high-affinity binding. Dashed line: low-affinity binding. Reichardt, 2006.

dissociating from, cytoplasmic interactors; the cytoplasmic domain contains in fact several protein association motifs. The three-dimensional structure of the p75NTR extracellular domain associated with an NGF homodimer (He and Garcia, 2004) demonstrated that ligand binding occurs along the interface between NGF monomers and causes a conformational change on the opposite side of the dimer, precluding the binding of another p75NTR monomer. Trk receptors on the other hand bind to a different portion of the neurotrophin dimer, suggesting that Trk and p75NTR monomers may simultaneously bind the same neurotrophin dimer, which may contribute to the cross talk between the two classes of receptors.

It is worth noticing that although proneurotrophins were long considered to be just inactive neurotrophin precursors subject to intracellular cleavage, it has been relatively recently shown that the proforms of NGF and BDNF can as well be secreted and cleaved by specific extracellular proteases; furthermore, proneurotrophins are high-affinity ligands that preferentially activate p75NTR to mediate apoptosis, while mature forms activate Trk receptors to promote survival. Proteolytic cleavage therefore regulates the biological action of neurotrophins, and the regulation of neurotrophin maturation is an important posttranslational control point (Lee et al., 2001).

Trk receptors belong to the family of receptor tyrosine kinases, and three Trk genes have been identified in mammals: *TrkA* (also called *NTRK1*, neurotrophic tyrosine kinase receptor type 1), *TrkB* (also called *NTRK2*, neurotrophic tyrosine kinase receptor type 2) and *TrkC* (also called *NTRK3*, neurotrophic tyrosine kinase receptor type 3). NTRK is the official gene symbol approved by the HUGO Gene Nomenclature Committee (HGNC); yet due to historical reasons Trk remains the most commonly used alias. To avoid confusion, we will mostly use the alias Trk throughout this introductory chapter, as this is how neurotrophin receptors are mainly referred to in the literature; however, once we focus on the work done on our gene of interest (*TrkC*) we will apply the official symbol *NTRK3*.

NGF is the preferred ligand for TrkA, BDNF and NT4/5 are preferred for TrkB and NT3 for TrkC (Barbacid, 1994); these specificities are not absolute, and NT3 can also activate TrkA and TrkB, even if with lower efficiency (Fig.1). The extracellular domain of Trk receptors consists of a cysteine-rich cluster followed by three leucine-rich repeats, another cysteine-rich cluster and two immunoglobulin-like domains. Each receptor spans the membrane once and ends with a cytoplasmic tyrosine kinase (TK) domain surrounded by several tyrosines that serve as phosphorylation-dependent docking sites for cytoplasmic adaptors and enzymes; whereas the

tyrosine kinase domains of the three receptors are highly related (~80% amino acid identity), the extracellular domains are more divergent (~30% identity). In contrast with p75NTR, neurotrophin binding causes a dimerization of Trk receptors, resulting in activation through the phosphorylation of the tyrosines present in their cytoplasmic domains.

As a first approximation, the expression of a specific Trk receptor confers responsiveness to the neurotrophins to which it binds, but splicing introduces some limitations to this generalization: alternative splicing can in fact alter ligand specificity through the insertion of short amino acid sequences into the juxtamembrane portions of the extracellular domains, which has been shown, at least for TrkA and TrkB, to enhance the binding of receptors to non-preferred ligands (Clary and Reichardt, 1994; Strohmaier et al., 1996).

## Neurotrophins and disease

In agreement with the variety of processes in which neurotrophins are entailed, neurotrophic signaling has been implicated in many diseases, especially in the nervous system.

First of all, neurotrophins exert neuroprotective activity against different paradigms of neuronal cell death, including different models of apoptosis *in vitro* or *in vivo* (Hetman et al., 1999; Koh et al., 1995; Yao and Cooper, 1995); this has linked neurotrophic factors, in particular NGF, to neurodegenerative disorders like amyotrophic lateral sclerosis (ALS) and Alzheimer's disease, as well as neuropathy and pain (Schulte-Herbruggen et al., 2007). A recent study indicates a possible connection between neurotrophic signaling and autism: mice with a defect in the cerebellar release of BDNF and NT3 in fact exhibit pronounced impairments in cerebellar development and functions (including neuronal differentiation and survival, morphogenesis, synaptic function and motor learning/control), with autistic-like cellular and behavioral phenotypes (Sadakata et al., 2007).

Several neurotrophic factors play a key role in the etiology of psychiatric and mood disorders, as indicated by evidence coming from association studies and murine models. Neurotrophic factors themselves do not control mood, but they act in the activity-dependent modulation of networks whose function determines how plastic changes can influence it (Castren et al., 2007). For example, BDNF and its receptor have been implicated in the neurobiology of depression (Nestler et al.,

2002; Saarelainen et al., 2003) and are associated with eating disorders (Ribases et al., 2004) and obsessive-compulsive disorder (Alonso et al., 2008). In particular, the Val66Met BDNF variant, which is associated with eating disorders, has impaired intracellular trafficking and is not properly sorted within the cell; knock-in mice that homozygously express Met66 BDNF show increased anxiety-like behavior (Chen et al., 2006b) and greater resilience to behavioral and molecular changes after social defeat (Krishnan et al., 2007). Post-mortem data from depressed patients have shown that depression is associated with a decrease in the amount of BDNF in the hippocampus and an increase in the nucleus accumbens (Karege et al., 2005); antidepressant drugs increase the synthesis and signaling of BDNF, and BDNF signaling appears to be both sufficient and necessary for the antidepressant-induced behavioral effects (Castren, 2004). Furthermore, transgenic mice overexpressing the BDNF receptor TrkB show improved learning and memory and reduced anxiety (Koponen et al., 2004). On the contrary, antidepressants decrease the expression of NT3 in the locus coeruleus (LC), a brain nucleus involved in the response to stress and panic, while stress increases NT3 levels (Smith et al., 1995). Transgenic mice overexpressing the NT3 receptor TrkC show increased anxiety-like behavior and panic reaction, as well as an increase in the number and density of noradrenergic neurons in the LC and substantia nigra (Dierssen et al., 2006); transgenic mice also exhibit enhanced panicogenic sensitivity to anxiogenic drugs (Sahun et al., 2007). BDNF and NT3 have as well been proposed as susceptibility genes for schizophrenia (Lin and Tsai, 2004) and bipolar disorder (Tadokoro et al., 2004), and a role for neurotrophic factors in the responses produced by addictive drugs has also been demonstrated (Castren, 2004). For instance, administration of exogenous neurotrophins opposes the effects of chronic morphine treatment, and morphine withdrawal after chronic exposure leads to an increase in *BDNF* mRNA and a decrease in *NT3* mRNA in the LC, indicating that these neurotrophins may be involved in opiate-induced plasticity (Numan et al., 1998).

Finally, in the past few years a diversity of roles has emerged for neurotrophins outside the nervous system, in cardiac development (Lin et al., 2000), neovascularization (Coppola et al., 2004) and immune system function (Kermani et al., 2005), where they are thought to mediate the reciprocal cross talk between the nervous system and the different immune cell subtypes.

## **p75NTR signaling**

As previously mentioned, p75NTR binds unprocessed proneurotrophins with high affinity, ligand engagement resulting in dramatically different consequences, such as apoptosis, than those triggered by Trk receptors (Lee et al., 2001); mature neurotrophins are also able to bind p75NTR, with ~1000-fold lower affinity. Three major signaling pathways are activated by p75NTR following neurotrophin binding (Fig.2) and the function of this receptor varies considerably depending on the cellular context in which it is expressed, maybe as a consequence of the use of numerous cytoplasmic interactors and adaptor proteins for signal transduction.

One major pathway is the Jun-kinase signaling cascade, which results in p53 activation and apoptosis; the Jun-kinase cascade also induces the expression of Fas ligand, again promoting apoptosis through the activation of the Fas receptor. Pro-apoptotic actions of p75NTR appear to require the presence of sortilin, a multi-ligand receptor that functions as a co-receptor for neurotrophins (Chen et al., 2005). Several essential intermediates in the activation of the Jun-kinase cascade have been identified, such as the E3 ubiquitin ligase TRAF6 (TNF receptor-associated factor 6), NRIF (neurotrophin receptor-interacting factor), MAGE (melanoma-associated antigen), NRAGE (neurotrophin receptor interacting MAGE homologue) and SC1 (Schwann cell factor 1); on the other hand, in PC12 cells and sympathetic neurons Jun-kinase activation involves Cdc42 and the MAP kinase kinase kinase ASK1 (apoptosis signal-regulated kinase 1) (Kanamoto et al., 2000); in oligodendrocytes, p75NTR-mediated apoptosis requires Rac activation, indicating that different cell types may use different Rho GTPases as intermediates in the activation of the Jun-kinase cascade (Harrington et al., 2002). Furthermore, p75NTR controls the activity of the Rho family of GTPases; it in fact constitutively activates RhoA through a direct interaction, inhibiting neurite outgrowth (Yamashita et al., 1999). Neurotrophin binding to p75NTR extinguishes the activation of RhoA and stimulates neurite outgrowth.

Neurotrophin binding to p75NTR also promotes the activation of the NFkB complex, through a series of specific adaptors and kinases like TRAF6 and Ikb kinase beta (IKK- $\beta$ ); NFkB activation results in the transcription of several genes that mediate neuronal survival (Middleton et al., 2000). Finally, p75NTR is known to activate sphingomyelin hydrolysis, which results in ceramide production. Ceramide is another mediator of p75NTR signaling as it controls many signaling pathways

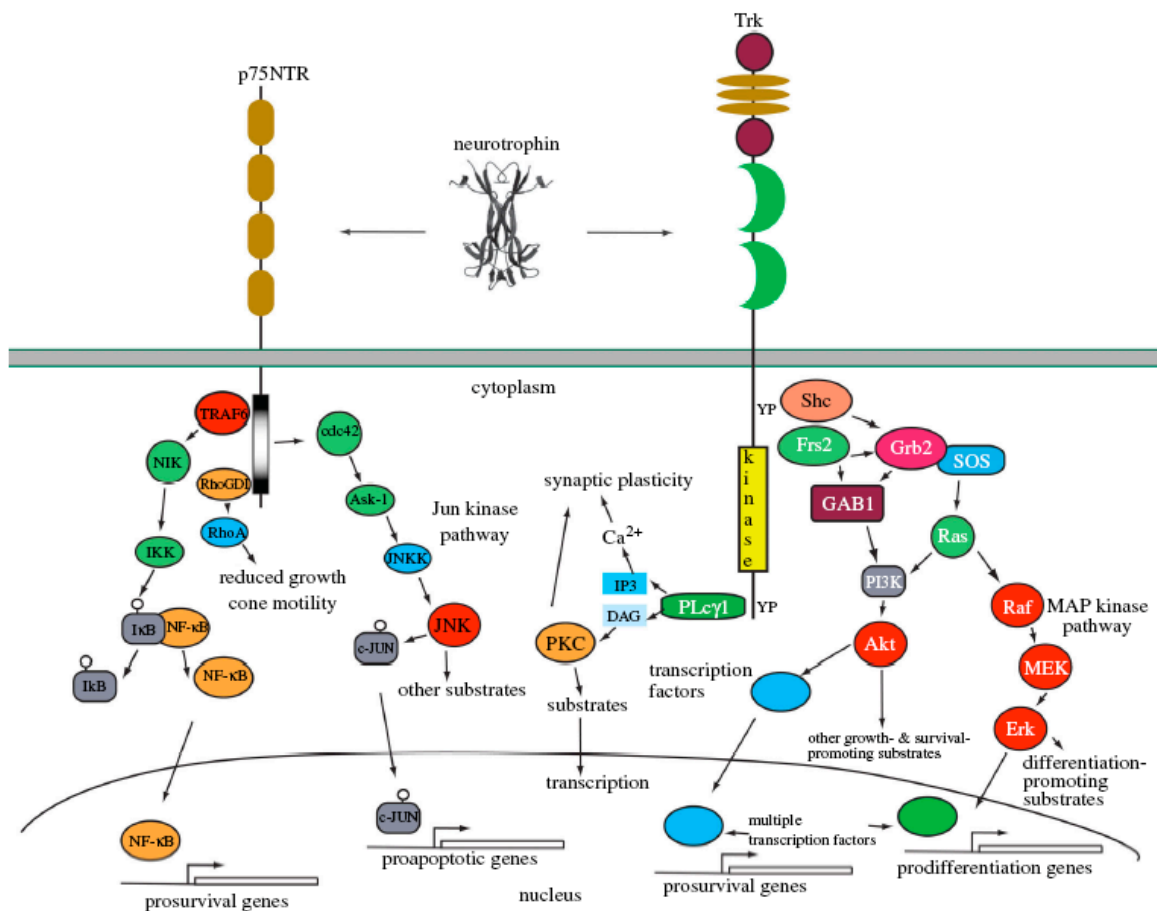


**Fig.2** Major intracellular signaling pathways activated by neurotrophins through p75NTR and Trk receptors. *Reichardt, 2006.*

such as ERK, Jun kinase and NFκB cascades, as well as TrkA activity through the phosphorylation of TrkA serine residues, therefore promoting both apoptotic and prosurvival pathways (Song and Posse de Chaves, 2003).

## Trk signaling

Trk receptors are typical receptor tyrosine kinases; they are activated by neurotrophin-mediated dimerization, which leads to the transphosphorylation of three specific tyrosines located in the autoregulatory activation loop of the tyrosine kinase domain (Y670, Y674 and Y675 in human TrkA). They are specifically regulated by mature neurotrophins and not by their precursors, so the proteases that control proneurotrophin processing also control Trk receptor responsiveness. Phosphorylation of the activation loop tyrosines leads to an open conformation of

the receptor and elevated tyrosine kinase activity, which results in the phosphorylation of several additional conserved tyrosine residues. These tyrosines, once phosphorylated, form binding sites for scaffold proteins and enzymes containing PTB (phosphotyrosine binding) or SH2 (Src homology 2) domains that mediate intracellular signaling cascades; among the tyrosines that are not in the activation loop two are the major sites for endogenous phosphorylation: Y490 and Y785.

There are three main signaling pathways activated by Trk receptors (Fig.2): the Ras/Raf/MEK/MAPK pathway, which promotes differentiation and neurite outgrowth, PI3K (phosphoinositide 3-kinase), which promotes survival, and PLC- $\gamma$ 1 (phospholipase C gamma 1), which is involved in activity-dependent plasticity. Phospho-Y490 provides a docking site for both Shc and Frs2, two adaptor proteins that are phosphorylated by activated Trks and provide the link to Ras via the recruitment of the Grb2/SOS complex (Grb2 being an adaptor protein and SOS the Ras guanine-nucleotide exchange factor son of sevenless). Other adaptor molecules seem to form complexes with Grb2 or directly with Trk receptors, creating alternative connections to the MAPK pathway. This complexity allows a sustained activation of the pathway in response to neurotrophins, as well as a fine-tuning of the responses (Reichardt, 2006).

Phospho-Y490, Shc and Frs2 also provide a link to the PI3K pathway; PI3-kinases generate P3-phosphorylated phosphoinositides and are especially implicated in neuronal survival via the activation of the kinase PKB/AKT, which results in the phosphorylation and inactivation of proapoptotic proteins such as BAD (Datta et al., 1997). PI3K can be activated through Ras-dependent and -independent pathways, and the relative importance of the two mechanisms varies in different subsets of neurons; Ras-independent pathways involve the recruitment of adaptor proteins like IRS (insulin receptor substrates IRS1 and IRS2) and Gab1 (Grb associated binder 1), which mediate the association and activation of PI3K (Holgado-Madruga et al., 1997). In addition, PI3K activation has many targets that promote axon growth and pathfinding as well as neuronal differentiation; the 3-phosphoinositides generated by PI3K recruit in fact many signaling molecules to the membrane, including guanine-nucleotide exchange factors (GEFs) for Cdc42, Rac and Rho, which control F-actin cytoskeleton organization and most likely account for the ability of neurotrophin gradients to guide growth cones (Yuan et al., 2003).

PLC- $\gamma$ 1 on the other hand is recruited to a docking site surrounding phosphorylated Y785 on TrkA and similar sites on TrkB and TrkC. Docked PLC- $\gamma$ 1 is phosphorylated



by Trk and then hydrolyses PtdIns(4,5)P<sub>2</sub> to generate IP3 and DAG. The presence of IP3 results in Ca<sup>2+</sup> release from cytoplasmic stores and DAG stimulates DAG-regulated isoforms of protein kinase C (PKC); together these signaling molecules activate many intracellular enzymes, including almost all PKC isoforms, Ca<sup>2+</sup>-calmodulin-dependent kinases and other Ca<sup>2+</sup>-calmodulin-regulated targets. Signaling through this pathway controls the expression and/or activity of many proteins, including ion channels and transcription factors, and seems to play an important role in neurotrophin-mediated release of neurotrophins and in synaptic plasticity (Canossa et al., 1997).

As mentioned at the beginning, an interesting and neuron-specific aspect of neurotrophin signaling is the retrograde transport of signals from axon terminals to the cell bodies of neurons. Neurotrophin binding stimulates Trk receptor internalization through clathrin-coated pits and micropinocytosis; after internalization, neurotrophins co-localize with Trk receptors in endosomal compartments that recruit signaling intermediates such as Shc and trigger downstream signaling events, which promote axon growth at the axon terminal and retrograde transport and nuclear signaling at the cell soma. Trk internalization is regulated by ubiquitination; very interestingly, the presence of p75NTR has been recently shown to facilitate the ubiquitination and subsequent internalization of Trk receptors through the recruitment of an E2-E3 ubiquitin ligase complex (Geetha et al., 2005), suggesting that one of the major functions of p75NTR *in vivo* may be regulating Trk internalization and consequently axon growth on one side and nuclear signaling on the other.

The complexity of the Trk family increases as each member presents different protein isoforms generated by alternative splicing. As previously mentioned, splicing can occur in the extracellular domain conferring different ligand-binding specificities; nevertheless pre-mRNA processing can also act upon the cytoplasmic domain, with consequences on the kinase activity of the receptors. Truncated isoforms lacking the cytoplasmic tyrosine kinase domain - also called non-catalytic isoforms - have been reported for both TrkB and TrkC, and are well conserved across species (Kaplan and Miller, 2000). Different hypotheses have been raised regarding their potential roles: a) they may bind to neurotrophins and either present them to catalytic receptors leading to signal transduction or mediate neurotrophin clearance after internalization; b) they may have a dominant negative effect on signaling over catalytic receptors; c) they may interact with cytoplasmic

proteins not yet identified and be involved in signal transduction pathways (Menn et al., 1998). Further details about TrkC isoforms are given hereafter.

## Trk receptors and cancer

As for many other growth factors, deregulation of neurotrophin signal transduction is found in a number of tumors, where it can contribute to malignant transformation. Curiously, *Trk* was one of the first transforming oncogenes identified in human cancers; the first *Trk* oncogene was isolated in colon carcinoma as a fusion gene composed of *TrkA* and the tropomyosin gene in the extracellular domain (hence the name Trk) resulting from a chromosomal translocation (Barbacid et al., 1991). The same kind of *TrkA* rearrangement was then found in other types of cancer such as myeloid leukemia and thyroid papillary carcinomas, and a similar translocation involving the *TrkC* gene and the transcription factor *ETV6* (Ets variant gene 6) was reported in acute myeloid leukemia (Eguchi et al., 1999). In both cases, the alteration of the extracellular domain leads to a constitutive activation of the tyrosine kinase activity of the receptor and subsequently of downstream signaling pathways. Trk fusion genes are considered as oncogenes, whereas wild-type Trk receptors are commonly referred to as proto-oncogenes.

Besides *Trk* oncogenes, wild-type receptors and neurotrophins have been implicated in several types of cancers not only of neuronal origin, where Trk

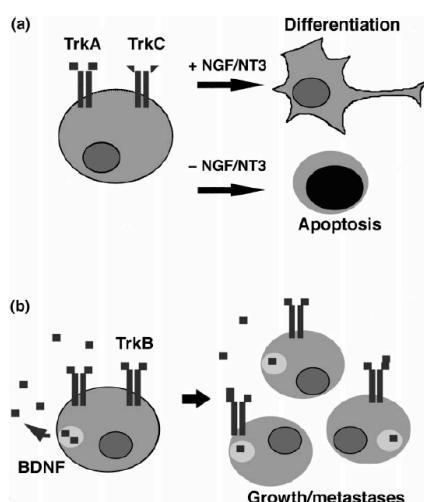


**Fig.3** Function of Trk receptors in favorable (a) and unfavorable (b) neuroblastomas. Yamashiro et al., 1997.

receptor activation can either support or suppress tumor growth, depending on the tumor type (Kruttgen et al., 2006). For instance, the expression of neurotrophins and/or their receptors is altered in malignancies like neuroblastoma (NB), medulloblastoma (MDB), lung cancer, prostate and breast cancer, epithelial ovarian cancer as well as in the formation of brain metastasis and in angiogenesis, and in some cases their expression levels can be used as prognostic markers.

As an example of the mechanisms by which neurotrophic signaling can take part in

cancer biology, TrkA, TrkB and TrkC were identified as major players in the pediatric brain tumor NB. TrkA, and to a lower extent TrkC, are highly expressed in NBs with good prognosis and highly correlate with patient survival; on the other hand, in aggressive NBs (which usually have amplification of the MYCN oncogene) TrkA expression is strongly downregulated, whereas both TrkB and its ligand BDNF are highly expressed.

Although further investigation is needed, a model that could explain how neurotrophic signaling can affect the favorable/unfavorable outcome of NB lies on the differences in the expression patterns of Trk receptors and their downstream signaling molecules (Fig.3): in favorable tumors expressing TrkA and TrkC the addition of NGF or NT3 would promote differentiation, while NGF or NT3 deprivation would lead to cell death. On the other hand, unfavorable NBs express little or no TrkA and TrkC, so they don't respond to NGF or NT3; in this case the concomitant expression of BDNF and TrkB would produce an autocrine loop of BDNF/TrkB resulting in cell proliferation and metastases (Yamashiro et al., 1997).

Of particular interest is also the recent finding that the nervous system directly interacts with tumor cells, raising the hypothesis that tumors are able to stimulate their own innervation through the release of neurotrophic factors; this process, similar to angiogenesis and lymphoangiogenesis, has been termed neoneurogenesis (Entschladen et al., 2008). The growth of nerve endings into tumors leads in turn to the release of neurotransmitters, providing stimuli for the migration of tumor cells and facilitating metastasis formation.

### **TrkC (NTRK3)**

The human *NTRK3* gene is located on chromosome 15q25 and spans ~380 kb of genomic DNA (chr15:86,220,992-86,600,665, March 2006, hg18). It contains 19 introns and, as previously mentioned, undergoes alternative splicing. Although a number of different *TrkC* isoforms have been described in vertebrates, the splicing patterns appear to be relatively simpler in humans, where three variants have been well characterized (Fig.4): a full-length catalytic form containing a tyrosine kinase domain (145-150 kDa), a full-length isoform with an insertion of 14 amino acids in the TK domain, adjacent to the autoregulatory activation loop, and a single non-catalytic truncated form that completely lacks the TK domain (Shelton et al., 1995). The isoform with the insert in the TK domain is less efficient at ligand-induced

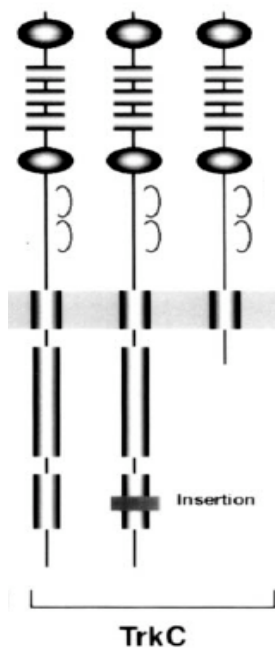


**Fig.4** TrkC isoforms in humans. Adapted from Nagakawara et al., 2001.

autophosphorylation and kinase activity relative to the canonical full-length form; it is less abundant than the full-length isoform, shows reduced signaling potential and its function is thought to be mainly regulatory (Tsoulfas et al., 1996). The truncated isoform on the other hand has no tyrosine kinase activity whatsoever, and the transcript annotated in humans corresponds to a predicted protein of 612 amino acids including a putative signal peptide of 31 amino acids. Accordingly, two major protein isoforms have been detected in human brain samples: the full-length 150 kDa receptor and one truncated isoform of 50 kDa (Beltaifa et al., 2005).

The expression patterns of the full-length and truncated isoforms in the nervous system have been analyzed in mice (Menn et al., 1998), where both transcripts have been detected during embryonic development, starting at day E11.5 and increasingly in later stages. In the embryo full-length and truncated *TrkC* transcripts are coexpressed in several regions, like the telencephalon, mesencephalon, rhombencephalon, in the spinal chord and in neural crest derivatives in the peripheral nervous system; on the

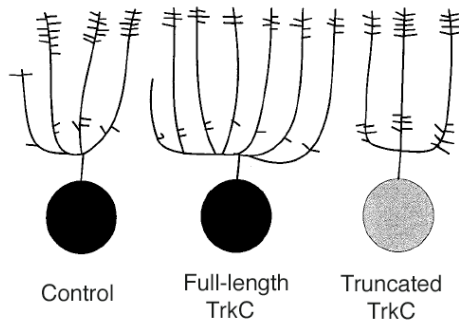


**Fig.5** Schematic diagrams of the effects of full-length and truncated TrkC when overexpressed in primary neurons. Adapted from Ichinose et al., 2000.

other hand only the catalytic form is present in the diencephalon. In adults the two isoforms are codistributed in many brain structures (cerebral cortex, hippocampus, cerebellum and olfactory bulb) but the truncated form is totally absent in the thalamus and hypothalamus. Little is known about the function of the truncated isoform. Transfection of the two variants into primary neurons has shown that different ratios of catalytic and non-catalytic receptors are associated with different axonal morphology (Fig.5): the overexpression of the full-length isoform in fact increases the formation of axonal primary processes, while the overexpression of the truncated isoform reduces it and shifts the distribution of branch points to the proximal region of axons (Ichinose and Snider, 2000). Immunohistochemistry and

immunofluorescence experiments have demonstrated that the relative expression of the two isoforms and their subcellular localization varies throughout neural development. For example, the catalytic isoform is the only one present in proliferating neural stem cells, where TrkC is thought to mediate precursor survival rather than proliferation (Lachyankar et al., 1997); in contrast, the truncated receptor starts to be detected in neurons as they begin to differentiate, and both isoforms are expressed in oligodendrocytes and astrocytes. In differentiating neurons only catalytic receptors are expressed in the growth cone, whereas extending neurites express both variants; in mature neurons the dendritic compartment shows a predominance of truncated receptors but in the axonal compartment both isoforms coexist. This has raised the hypothesis that the catalytic isoform may mediate axon guidance whereas the truncated receptor may play a role in the maintenance of the differentiated state, especially of the dendritic arborization, being possibly involved in short-term and long-term synaptic plasticity (Menn et al., 2000).

From a molecular perspective the main function that has long been attributed to the truncated isoform is the inhibition of catalytic receptors, which is achieved through either a dominant-negative or a ligand-sequestering mechanism. In fact, mice overexpressing truncated TrkC die in the first postnatal day and show severe developmental defects in the peripheral nervous system and in the heart that closely relate this mouse model to the NT3-deficient one (Palko et al., 1999). On the other hand, TrkC-deficient mice show as well a high proportion of sensory neuron loss, which are more severe in mice lacking all TrkC isoforms than in those carrying only the kinase-negative mutation, implicating additional important functions for the truncated receptor (Liebl et al., 1997). Mice lacking all TrkC isoforms also present multiple cardiac malformations involving structures whose formation during development depends on cardiac neural crest function (Youn et al., 2003). The high level of sequence conservation of the intracellular domains of truncated receptors across species actually supports the hypothesis of other functions, such as the interaction with adaptor proteins and the activation of specific signaling pathways. A recent work has identified a new signaling pathway activated by the truncated isoform, linking NT3 to downstream molecules affecting acting cytoskeleton organization and membrane trafficking (Fig.6); Esteban et al. show in fact that truncated TrkC binds to the scaffold protein tamalin and that NT3-induced initiation of this complex leads to activation of the Rac1 GTPase through adenosine diphosphate-ribosylation factor 6 (Arf6). NT3 binding to TrkC-tamalin induces Arf6

translocation to the membrane, which in turn causes membrane ruffling and the formation of cellular protrusions (Esteban et al., 2006).

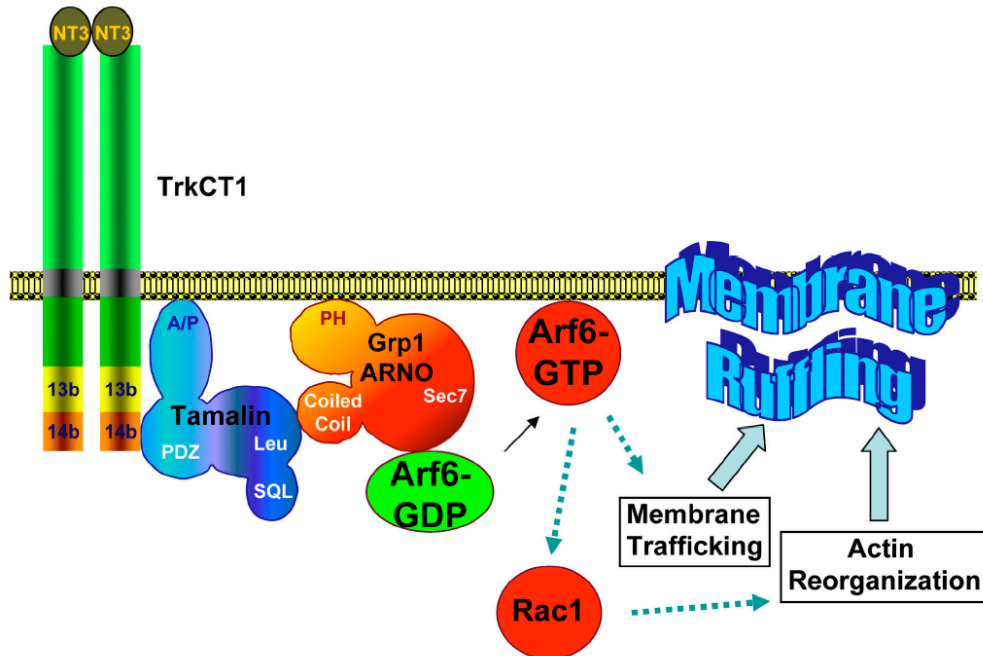


**Fig.6** Schematic representation of the newly identified signaling pathway activated by NT3 through the truncated TrkC receptor. *Esteban et al., 2006*.

Evidence from a study that has examined the expression of TrkC protein and mRNA in human prefrontal cortex post-mortem samples from individuals ranging from 1 month to 86 years of age indicates that the full-length receptor is expressed at low but relatively constant levels throughout development, while the truncated receptor is expressed at moderate levels early in development and increases to reach mature levels by adolescence; in contrast, both full-length and truncated transcripts are uniformly expressed throughout postnatal life and decline in ageing (Beltaifa et al., 2005). The discrepancy between the developmental changes in TrkC protein and mRNA levels suggest that some other post-transcriptional regulation mechanism may play a role in controlling the expression of the two isoforms in addition to alternative splicing. Post-transcriptional gene regulation affords a mechanism for rapid changes in the cellular proteome, and in particular microRNAs (miRNAs) are a well-studied example of post-transcriptional control that has been implicated in the development of the nervous system (Kosik, 2006). miRNAs are

known to regulate gene expression by means of partial complementarity to miRNA binding sites (called miRNA target sites) located in the 3' untranslated regions (3'UTRs) of target genes. It has been reported that genes with long 3'UTRs are more prone to miRNA-mediated regulation as compared to genes with short 3'UTRs, which tend to be specifically deprived of miRNA target sites (Stark et al., 2005). Interestingly, the full-length and truncated TrkC transcripts show completely different 3'UTRs: the former has in fact a short 178 base pairs (bp) 3'UTR sequence and the latter a relatively long 1981 bp 3'UTR sequence (Fig.7), supporting the hypothesis that the two TrkC isoforms may be differentially regulated by miRNAs.

In this context interesting results have recently emerged from a study focusing on miRNA expression in a neuroblastoma cell line differentiated with retinoic acid. This work demonstrates that miR-9 and miR-125a/b are induced upon retinoic acid treatment and are able to regulate the expression of the truncated isoform of the TrkC receptor (Laneve et al., 2007).

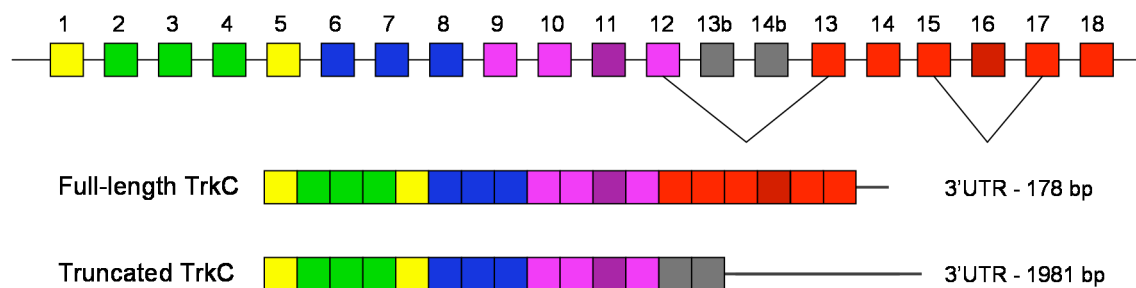


**Fig.7** Schematic representation of the human *NTRK3* gene with the alternative splicing patterns. Colors represent the distribution of exons across the receptor functional domains: cystein clusters (yellow), leucine-rich motifs (green), immunoglobulin-like domains (blue), transmembrane (dark purple) and juxtamembrane (light purple) domains, tyrosine kinase domain (red) of the full-length isoform with the alternatively spliced 14aa insert (exon 16) and intracellular domain of the truncated receptor (grey).

## 2. microRNAs

### Non-coding RNAs

Recent data about the transcriptional activity of the human genome indicate that approximately half of it is transcribed (Szymanski et al., 2005); however, only ~2% of human transcripts are actually protein-coding, while ~98% consists of non-coding RNAs (ncRNAs), the importance of which is highlighted by the fact that increasing organism complexity along the evolutionary scale is accompanied by the accumulation of DNA sequences that are not translated. The term ncRNA includes all RNAs that do not code for proteins and directly function as RNAs; for several decades, only a limited number of ncRNAs, such as ribosomal and transfer RNA, have been studied in depth. In the last few years additional species of ncRNAs have increasingly been discovered, among which small ncRNAs attract particular attention because of their role in processes such as RNA silencing and modification (Kawaji and Hayashizaki, 2008). RNA molecules can have several functions, including catalytic activity and the ability to act as structural components. A common way in which ncRNAs contribute to biological processes is through ribonucleoprotein (RNP) complexes, where they guide the recognition of nucleic acid target sequences relying upon sequence complementarity. Small RNAs are widely utilized in this type of machinery.

Endogenous small RNAs related with RNA silencing are diverse and can be categorized into three main classes: microRNAs (miRNAs), small interfering RNAs (siRNAs) and Piwi-interacting RNAs (piRNAs). Both miRNAs and siRNAs (~22 nucleotides in length) guide sequence-specific gene silencing at the posttranscriptional level; as the active forms are sometimes biochemically or functionally indistinguishable, they are classified based on their origins: miRNAs are generated from the double-stranded RNA (dsRNA) region of hairpin-shaped precursors while siRNAs are derived from long dsRNAs (Kim, 2005). Furthermore, miRNAs recognize target mRNAs by partial complementarity, whereas siRNAs show perfect complementarity to their target mRNA sequences. piRNAs are slightly longer (25-29 nucleotides), are produced by a Dicer-independent mechanism and associate with Piwi-class Argonaute proteins (see below). They are implicated in germline development, silencing of selfish DNA elements, and in maintaining germline DNA



integrity. Whether piRNAs primarily control chromatin organization, gene transcription, RNA stability or RNA translation is not yet well understood, neither is piRNA biogenesis (Klattenhoff and Theurkauf, 2008).

### **microRNA-mediated gene silencing**

microRNAs (miRNAs) are a very abundant class of small RNAs in animals. They were first discovered in 1993 through genetic screens in *C. elegans* and were subsequently shown to play a role in gene regulation in virtually all eukaryotes; through experimental approaches and bioinformatics, thousands of miRNAs have in fact been identified across all species examined. They are widely expressed in practically all tissues and at all stages of development, and more than one third of all human genes have been predicted to be miRNA targets (Lewis et al., 2005).

First described as having a role in the development of worms and flies, miRNAs have since been associated with nearly every cellular process, and contribute to guarantee the normal development and functioning of the body. They are expressed at different levels and often in a tissue-specific manner and, although they have only been studied intensively for the last six years, they have been shown to be related to as diverse functions as development and differentiation of tissues in mammals (Anderson et al., 2006), learning and memory (Fiore and Schratt, 2007), maintenance of germline stem cells in *Drosophila* (Park et al., 2007), cell cycle progression and apoptosis (Carleton et al., 2007) as well as diseases like cancer (He and Hannon, 2004; O'Donnell et al., 2005), cardiac hypertrophy (van Rooij and Olson, 2007), neurological diseases (Barbato et al., 2008) and diabetes (Poy et al., 2004). Furthermore, some viruses have been shown to encode miRNAs, which can regulate host gene expression (Stern-Ginossar et al., 2007).

miRNA genes represent about 1-2% of known eukaryotic genomes; computational predictions estimate that each miRNA can target more than 200 transcripts and that a single mRNA can be regulated by multiple miRNAs, suggesting that miRNAs and their targets are part of complex regulatory circuitries (Lindow and Gorodkin, 2007). In mammals, miRNAs are found throughout the genome in all chromosomes with the exception of the Y chromosome (Ro et al., 2007); miRNA genes are often not randomly dispersed, but are found in clusters that in some cases share a common regulatory region, resulting in the transcription of polycistronic RNA. miRNAs belonging to the same cluster may be functionally related

by targeting the same gene, members of the same gene family or members of the same pathway. miRNA genes are found in intergenic regions as well as in introns or exons of protein coding mRNAs and in introns of non-coding RNA (Rodriguez et al., 2004). The majority of miRNAs identified thus far have orthologs in other species, indicating that miRNA-mediated regulation is evolutionarily conserved.

Most miRNA genes are transcribed by RNA polymerase II, contain a 5'-methyl7G cap structure and are polyadenylated much like mRNAs (Cai et al., 2004). Their promoters share many characteristics with typical targets of polymerase II such as TATA boxes and contain conserved motifs that may serve as transcription factor-binding sites (Kim and Nam, 2006); miRNA promoter regions are twice as conserved as mRNA promoters in animals, underscoring the importance of miRNAs in the regulation of gene expression (Mahony et al., 2007). Furthermore, like coding RNAs, they are susceptible to epigenetic regulation (Calin and Croce, 2007) and canonical mRNA transcription factors are actually utilized in the regulation of miRNA expression. However, a small fraction of miRNA genes may be instead transcribed by RNA polymerase III, being regulated independently of canonical mRNA transcription units (Zhou et al., 2007).

Structurally, mature miRNAs are single-stranded RNA molecules of approximately 22 nucleotides. They are transcribed as longer primary miRNAs (pri-miRNAs), which can be hundreds to thousands nucleotides long and present hairpin structures (Fig.8). Pri-miRNAs are processed in the nucleus by a complex

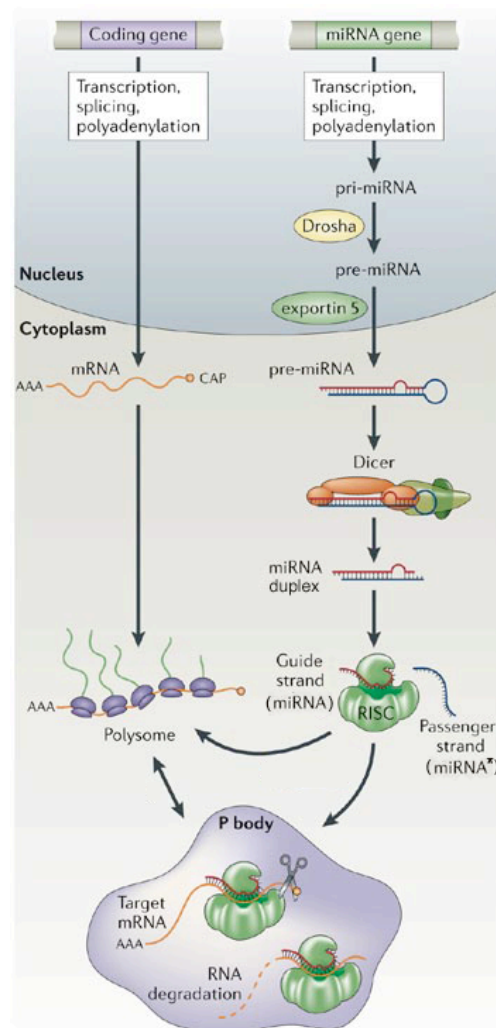


**Fig.8** microRNA biogenesis pathway. miRNA genes generally have RNA polymerase II promoters, and their transcripts can undergo 5' capping, polyadenylation and splicing. The cellular structure most closely associated with the RISC is the P-body, which is visible at the light microscopy level. Adapted from Kosik, 2006.

composed of the RNaseIII enzyme Drosha and a double-stranded RNA-binding protein called DGCR8 (DiGeorge syndrome critical region gene 8). Drosha cleaves near the base of the double-stranded structure to release a stem-loop structure of 60-80 nucleotides called precursor miRNA (pre-miRNA). The excised hairpin is then exported to the cytoplasm by a heterodimer consisting of the transport factor Exportin-5 and its cofactor Ran. Once in the cytoplasm, the pre-mRNA is processed by another RNaseIII enzyme called Dicer, which removes the loop region of the hairpin, releasing an imperfect RNA duplex known as the miRNA:miRNA\* duplex. Dicer also interacts with RNA-binding cofactors that are not required for the cleavage reaction, but stabilize the miRNA and facilitate the formation of a multi-protein complex called RISC (RNA-induced silencing complex), which mediates RNA silencing. During the assembly of the RISC complex, the miRNA strand with lower stability base pairing at nucleotides 2-4 at the 5' end is preferentially loaded onto the RISC and becomes the active miRNA, while the complementary miRNA\* strand is in general removed and degraded. In some cases, two different mature miRNA sequences can be excised from opposite arms of the same hairpin precursor; such mature sequences are currently named using the extensions -5p (5' arm) and -3p (3' arm) depending on which arm of the hairpin they derive from (for example miR-17-5p and miR-17-3p) (Griffiths-Jones, 2006). Mature miRNAs loaded onto the RISC are ready to direct their activity on target mRNAs by binding miRNA-responsive elements usually located in the 3'UTR of the transcript (Hudder and Novak, 2008). The association of the RISC complex with the target mRNA can lead to gene silencing through two different mechanisms, mRNA cleavage or translational repression. Although initial studies suggested that in animals the levels of miRNA-inhibited mRNAs remain mostly unchanged, more recent work has shown that the repression of many mRNA targets is frequently associated with their destabilization. In fact, microarray studies of transcript levels in cells and tissues in which miRNA expression was experimentally altered revealed changes in dozens of validated or predicted miRNA targets, consistent with a role for miRNAs in mRNA destabilization. Destabilization appears to occur by deadenylation, which is followed by decapping and degradation (Filipowicz et al., 2008).

It is thought that the degree of complementarity between mRNA and miRNA determines whether the mRNA will be degraded or repressed, perfect base-pairing generally resulting in mRNA cleavage and imperfect base-pairing in translational repression (Meister and Tuschl, 2004). Nevertheless, even in the case of translational repression good complementarity with the first eight nucleotides at the

5' end of the miRNA - known as the seed region - seems to be crucial for the recognition of target mRNAs, whereas pairing at the 3' end can be more variable (Doench and Sharp, 2004).

The exact composition of the RISC complex is currently unknown, but all the biochemical purifications performed so far have revealed the presence of at least one member of the Argonaute (Ago) family of proteins. Ago proteins (Ago1-4 in humans) are highly basic proteins, which contain an N-terminal domain, a PAZ domain that binds the single-stranded 3' end of miRNAs, a Mid domain and a PIWI domain resembling that of the RNase H endonuclease (Hutvagner and Simard, 2008). However, only Ago2 has endonucleolytic activity and can therefore cleave mRNA, suggesting that near-perfect pairing between miRNA and target mRNA provides a good substrate for recognition and cleavage by Ago2, whereas when internal mismatched bulges are present other Ago proteins are recruited and translation is repressed. Translationally suppressed mRNAs can be found associated with actively translated ribosomes (Maroney et al., 2006) or sequestered from the translation apparatus in the cytoplasm. In either case, the 5' cap structure of the mRNA is involved in translational repression, as cap-independent translation is not repressed by miRNAs; furthermore, a motif (named MC) similar to that of the cap binding domain of the translation initiation factor eIF4E has been recently identified within the Mid domain of Ago proteins (Kiriakidou et al., 2007), suggesting that Ago can compete for message binding and exclude eIF4E. eIF4E is a subunit of the eukaryotic translation initiation factor eIF4F responsible for the recognition of the mRNA 5'-terminal cap structure leading to translational initiation.

RISC complexes along with suppressed mRNAs accumulate in the cytoplasm in foci called processing bodies (P-bodies), which contain decapping proteins and the exoribonuclease *Xrn I*. Recent evidence suggests that repression may be reversible, meaning that once in P-bodies mRNAs can either be stored for later translational activation (Bhattacharyya et al., 2006) or decapped and subsequently degraded by exonucleolytic decay. Similar to P-bodies, stress granules (SGs) are sites of accumulated non-translating mRNAs associated with ribosomes, which form in response to osmotic stress, oxidative stress or heat shock (Anderson and Kedersha, 2006); when the cell recovers from stress, the mRNA can re-enter polyribosomes to resume translation or transfer to P-bodies for degradation.

As mentioned before, miRNAs are involved in the regulation of very diverse cellular processes. Their impact in development and differentiation is certainly fundamental, and it is becoming more and more evident that miRNAs are involved

in regulating most if not all cellular mechanisms, as they hold major roles in most regulatory pathways. It is therefore not surprising that the aberrant expression of miRNAs is associated with cellular dysfunction and disease.

## microRNAs in development and differentiation

miRNA-mediated regulation plays an important role during the development of multicellular organisms, which is the context where miRNAs were originally discovered. A frequently found theme during development is the use of miRNAs to avoid unwanted re-expression of genes that are no longer needed after differentiation; for example, if during differentiation a given gene is downregulated, it is common to find a concomitant upregulation of a miRNA targeting that gene. This is an important mechanism to stabilize the commitment of differentiating cells and to prevent them from erroneously switching towards an inappropriate fate, even if spurious gene transcription should occur (Aumiller and Forstemann, 2008). During embryogenesis many miRNAs show tissue-specific expression patterns, whereas stem cells express specific sets of miRNAs that conversely become

| Name of miRNA | Function                                     | Target gene                                         |
|---------------|----------------------------------------------|-----------------------------------------------------|
| Lin-4         | <i>Caenorhabditis elegans</i> development    | Lin-14, lin-28                                      |
| Let-7         | <i>C. elegans</i> development                | Lin-14, lin-28, lin-41, lin-42, daf-12              |
| miR-196       | Embryo patterning                            | HOXD8                                               |
| miR-1         | Cardiomyocyte differentiation                | HDAC4<br>Myostatin                                  |
| miR-133       | Suppression of cardiomyocyte differentiation | Serum response factor                               |
| miR-124       | Neuronal differentiation                     | Laminin gamma 1<br>Integrin beta 1<br>SCP1<br>PTBP1 |
| miR-34        | Dendritic spine development                  | Limk1                                               |
| miR-133b      | Maturation of dopaminergic neurons           | Pitx3                                               |
| miR-181       | B lymphocyte differentiation                 | Not known                                           |
|               | Myoblast differentiation                     | HOX-A11                                             |
| miR-375       | Insulin secretion                            | Myotrophin                                          |
| miR-122       | Liver development and function               | Many genes                                          |
| miR-143       | Adipocyte differentiation                    | ERK5                                                |

**Table 1** Roles of miRNAs in development. *Adapted from Dalmay, 2008.*

downregulated during differentiation (Suh et al., 2004). Examples of miRNA activity at an early stage (Table 1) are the targeting of HOX genes (a family of genes involved in developmental patterning) by miR-196 (Yekta et al., 2004), the promotion of muscle differentiation by the muscle-specific miR-1, which targets a repressor of muscle gene transcription (Chen et al., 2006a), the regulation of B-lymphocyte and myoblast differentiation by miR-181, liver development and function by miR-122 and adipocyte differentiation by miR-143 (Dalmy, 2008). Furthermore, miRNAs play a major role in the in the development of the nervous system, which will be discussed in more detail in the following chapters.

### **microRNAs in metabolism regulation and stress response**

Genes involved in metabolic processes seem to have a lower propensity to be targeted by miRNAs than genes with a role in development and cell specification. Many housekeeping genes have in fact short 3'UTR sequences with little or no miRNA complementarity: the term 'antitarget' was coined to illustrate this phenomenon (Stark et al., 2005). Nevertheless, even among the so-called antitargets regulation by miRNAs does occur, but it just happens less frequently (Aumiller and Forstemann, 2008). As a matter of fact, more and more evidence is emerging that implicates miRNAs in the regulation of metabolism, and some examples are given below.

Endocrine regulation of energy homeostasis is dependent on the effects of insulin and glucagon. In all of the major tissues involved in energy homeostasis - pancreas, liver, muscle and adipose tissue - specific miRNAs have been identified that regulate mammalian metabolic processes. For instance, insulin secretion from the pancreas is regulated by miR-375 (Poy et al., 2004): miR-375 inhibits the translation of the myotrophin gene, which controls glucose-stimulated insulin exocytosis regulating blood glucose levels. Another miRNA expressed in pancreatic beta-cells is miR-124a, which represses the expression of a transcription factor controlling the preproinsulin gene (Baroukh et al., 2007). A study on the skeletal muscle of diabetic rats identified 4 upregulated and 11 downregulated miRNAs, one of the four (miR-29a) being upregulated also in the liver and adipose tissue (He et al., 2007a); in *Drosophila*, mutants lacking miR-278 are defective in fat storage and are insulin resistant; in mouse, the inhibition of miR-122, which is particularly abundant in the liver, has been reported to reduce plasma cholesterol and

triglycerides levels and to downregulate many cholesterol biosynthesis genes, probably as a secondary effect caused by the upregulation of direct miR-122 targets (Esau et al., 2006). Finally, studies on cultured human cells have provided evidence for an involvement of miRNAs – namely miR-29b - in the regulation of amino acid metabolism.

Stress responses can also involve miRNAs, as different types of cellular stress have been shown to alter miRNA levels. For example, hypoxia-responsive transcription factors such as nuclear factor-kappa B and p53 induce miRNA genes (He et al., 2007b; Taganov et al., 2006). In general, studies on oxidative stress, cold stress and nutrient deprivation indicate that long-term stress may have an impact on miRNAs and on global gene expression, perhaps leaving tissues more susceptible to pathogenic processes. Given the role of miRNAs in metabolism and signal transduction, it is thought that chronic stress can initiate cellular reprogramming through alterations in miRNA expression or activity, leading to sustained changes in gene expression and cellular physiology (Hudder and Novak, 2008).

### **microRNAs and cancer**

As miRNAs affect gene expression, they have been considered since their discovery as good candidates for keeping the balance between tumor suppressors and oncogenes, becoming with good reason a much-hyped topic in cancer research. miRNA expression profiling has demonstrated that many miRNAs are deregulated in human cancers and several oncogenes, tumor suppressors and other cancer-related genes controlling cell cycle progression, apoptosis, cell migration and angiogenesis have been shown to undergo miRNA-mediated repression. Much effort has been invested in the last years in exploring the possible applications of miRNA profiles as a diagnostic tool and in developing routes to interfere with miRNAs as novel cancer therapies. Single miRNAs or miRNA signatures could in fact serve as prognostic biomarkers of the different types of tumor. On the other hand, the therapeutic potential of miRNA relies on the possibility of blocking oncogenic miRNAs by means of miRNA inhibitors (the so-called 'antagomirs') or overexpressing miRNAs with tumor suppressor activity. The two approaches showed promising results in cell culture but need to be improved in animal models; the major challenges in both



cases are the specific delivery of oligonucleotides into the tumor tissue and the minimization of unwanted off-target effects.

The first evidence for a direct link between miRNAs and human cancer came from chronic lymphocytic leukemia (CLL), which is characterized by a deletion at chromosome 13q14. The smallest region that is commonly missing from CLL patients was found to contain two miRNA genes, miR-15a and miR-16, which derive from the same primary transcript that was downregulated in CLL (Calin et al., 2002). Both miR-15a and miR-16 were later shown to recognize target sites on the 3'UTR of *BCL2*, a well known anti-apoptotic oncogene, indicating that the increased expression of *BCL2* caused by the deletion leads to CLL (Cimmino et al., 2005).

miRNAs, namely let-7, are also involved in lung cancer: reduced expression of let-7 shows good correlation with shortened postoperative survival, while its overexpression in lung carcinoma cell lines suppresses cell proliferation (Takamizawa et al., 2004). The tumor suppressor activity of let-7 was elucidated by the validation of two predicted target genes, *MYC* and *RAS*, which contain several let-7 target sites and are key oncogenes in lung cancer (Johnson et al., 2005).

miRNAs can also behave as oncogenes, as is the case for the miR-17-92 cluster, a miRNA polycistron (also called 'OncomiR-1') that comprises six miRNAs (miR-17, miR-18a, miR-19a, miR-20a, miR-19b-1, miR-92-1) and resides in intron 3 of the *C13orf25* gene at 13q31.3. Two paralogous clusters also exist, the miR-106a-92 cluster (Xq26.2) and the miR-106b-25 cluster, found on chromosome 7 and X respectively. The expression of the miR-17-92 cluster is upregulated in small-cell lung cancer and in B-cell lymphoma; furthermore, a study demonstrated that the oncogenic transcription factor *MYC* directly binds to and regulates the miR-17-92 cluster in cell culture. At the same time two miRNAs of this cluster (miR-17-5p and miR-20a) regulate the expression of the transcription factor *E2F1*, an additional *MYC* target implicated in the control of cell cycle progression (O'Donnell et al., 2005). This suggests a complex picture, probably involving several E2F proteins and feedback loops between E2F and *MYC* and between E2F and the miR-17-92 cluster. In addition, inhibitors of angiogenesis like thrombospondin 1 and connective tissue growth factor were identified as targets of this cluster (Dews et al., 2006), indicating that miRNAs may be also involved in the regulation of metastasis formation; finally, the two tumor suppressors *PTEN* and *RB2*, although not experimentally validated yet, are as well predicted targets.

Even if little is known about the actual targets and affected pathways, other types of cancer have been associated with miRNAs, mainly through the information



| Name of miRNA          | Up or down regulation | Type of cancer                | Target gene |
|------------------------|-----------------------|-------------------------------|-------------|
| miR-15, 16             | Down                  | chronic lymphocytic leukaemia | BCL2        |
| Let-7                  | Down                  | Lung                          | RAS, MYC    |
| miR-17-92 cluster      | Up                    | Lung                          | PTEN, RB2   |
| miR-221, 222, 146      | Up                    | papillary thyroid carcinoma   | KIT         |
| miR-143, 145           | Down                  | colorectal neoplasia          | Not known   |
| miR-21, 125b, 145, 155 | Down                  | Breast                        | Not known   |
| miR-21, 221            | Up                    | Glioblastoma multiforme       | Not known   |
| miR-181                | down                  | Glioblastoma multiforme       | Not known   |
| miR-155                | Up                    | B-cell lymphoma               | Not known   |
| miR-17-92 cluster      | Not known             | Not known                     | Tsp1, CTGF  |
| miR-10b                | Up                    | Metastatic breast cancer      | HOXD10      |

CTGF, connective tissue growth factor.

**Table 2** miRNAs involved in different types of cancer. *Adapted from Dalmay, 2008.*

coming from miRNA profiling (Table 2). For example, miR-143 and miR-145 show reduced expression in different stages of colorectal neoplasia (Michael et al., 2003); several miRNAs (miR-21, miR-125b, miR-145 and miR-155) show reduced accumulation in breast cancer samples, which moreover correlates with the progression of the tumor (Ciafre et al., 2005); three miRNAs (miR-146, miR-221 and miR-222) accumulate in thyroid tumors (He et al., 2005) and miR-155 is upregulated in B-cell-derived lymphomas (Eis et al., 2005).

Of particular interest is also the intervention of miRNAs in brain cancers. Glioblastomas (GBM), the most malignant and lethal brain tumors, are characterized by upregulation of miR-21 and miR-221 and downregulation of miR-124, miR-137 and miR-181; in particular, miR-21 overexpression was found to lead to increased caspase-dependent cell death in cultured glioblastoma cells (Chan et al., 2005; Silber et al., 2008). MDB, a pediatric brain tumor, shows significantly decreased expression of miR-124a, a brain-enriched miRNA with a fundamental role in the development of the nervous system (see the following chapter). Interestingly, miR-124a has recently been shown to inhibit MDB cell growth and to repress cyclin dependent kinase 6 (CDK6), which is upregulated in MDB and mediates the G1-S cell cycle transition (Pierson et al., 2008).

Differential miRNA expression has also been observed in neuroblastoma; all studies focusing on miRNA analysis to date have identified at least two miRNAs with *bona fide* tumor suppressor or oncogenic function in NB, the miR-34 family and the miR-17-92 cluster respectively. Several independent studies have linked members of the miR-34 family with the p53 pathway, and miR-34a in particular is a direct

target of p53. Moreover, both miR-34a and miR-34b are located in regions that are commonly deleted in NB. On the other hand, as described above the miR-17-92 cluster is involved in the fine-tuning of MYC signaling, which is an important pathway altered in NB (Schulte et al., 2008).

## **microRNAs in the nervous system**

### **Development and differentiation**

In the last few years, miRNAs have emerged as important players in gene regulation in the nervous system; a major progress in assessing their role has come from the analysis of miRNA expression profiles. Several works have revealed a spatially and/or temporally restricted distribution of miRNAs in the developing and adult nervous system, suggesting that they may contribute to the fine-tuning of neuronal gene expression. The embryonic central nervous system is patterned following spatial dimensions (anterior-posterior, dorso-ventral and left-right axes) as well as a temporal dimension; it is likely that miRNAs are involved in all of these developmental dimensions.

The engagement of miRNAs in neural development was clearly demonstrated by genetic analyses in zebrafish that addressed the role of Dicer. Maternal-zygotic Dicer mutant embryos showed in fact altered patterns of brain morphogenesis and neuronal differentiation caused by the failure to produce mature miRNAs. These developmental defects were partially rescued by the injection into the mutant fish of miRNAs of the miR-430 family, which are expressed at the onset of zygotic transcription and are required for clearing maternal mRNAs (Giraldez et al., 2005). To date, the exact role of Dicer in mammal neurodevelopment is not known as Dicer-deficient mice die at embryonic day 7.5, before neurulation (Bernstein et al., 2003). However, the conditional knock-down of Dicer in mouse Purkinje cells (Schaefer et al., 2007) and dopaminergic neurons (Kim et al., 2007) has been shown to cause progressive death of neuronal cells. Furthermore, Dicer expression is upregulated during the maturation of cultured cerebellar granule neurons and during the differentiation of hippocampal neurons *in vitro* (Barbato et al., 2007), suggesting that the biosynthesis of miRNAs is indeed needed in neural cell differentiation and in the maintenance of neuronal identity in the mature nervous system.

A number of miRNAs have been identified that are specifically expressed or enriched in brain tissues in mammals. In a pivotal study published in 2004, Sempere et al. characterized the expression of over 100 miRNAs in adult organs from mouse and human. They could identify seven brain-specific (i.e. exclusively detected in brain) miRNAs including miR-9, miR-124a and miR-124b and seven brain-enriched (i.e. whose expression was at least two-fold higher in brain than in other organs) miRNAs including miR-9\*, miR-125a, miR-125b and miR-128, with a high conservation of expression between mouse and human. In general, there was a high percentage of brain-specific and brain-enriched miRNAs compared to other organs, as well as an overall prevalence of miRNAs expressed in the brain. To determine which of the brain-expressed miRNAs were associated with neuronal differentiation, in the same study they analyzed miRNA expression in human and mouse embryonic carcinoma cells, using two cell lines that differentiate into neurons upon retinoic acid (RA) treatment. All of the brain-specific and brain-enriched miRNAs listed above were found to be induced by RA exposure, indicating that they might contribute to the specification of neuronal identity. In addition, other brain-non-enriched miRNAs were as well upregulated, like let-7a and let-7b among others (Sempere et al., 2004). Interestingly, the brain-enriched miR-125 is a lin-4 ortholog; lin-4 and let-7 were the first two miRNAs to be described, and were discovered in *C.elegans* where they control temporal cell fates during larval development (Rougvie, 2001). Both lin-4 and let-7 have lin-28 among their targets in *C.elegans* (Table 1); in mammals, LIN28 is downregulated as embryonic development progresses, and was later shown to be indeed modulated by miR-125 (Wu and Belasco, 2005).

Other important evidence for the role of miRNAs in establishing and maintaining neuronal cell identity comes from studies carried out in mouse embryonic stem cells. Krichevsky et al. demonstrated that neuronal differentiation of embryonic stem cell is accompanied by the upregulation of several miRNAs. Among them miR-9, miR-9\*, miR-22, miR-124a and miR-125b are highly expressed in brain and in primary neurons. In particular, overexpression of miR-9 and miR-124a in neural precursors alters the neuron-to-astroglia ratio during neural lineage differentiation, reducing the number of astrocytes, while inhibition of the two miRNAs causes a reduction in the number of neurons (Krichevsky et al., 2006). Finally, profiling experiments performed to define the temporal expression of miRNAs in the mouse brain consistently showed that neuronal-specific miR-124, miR-125 and miR-128 accumulate in parallel to neuronal maturation, while miR-23

and miR-29 are expressed in astrocytes and at low levels in embryonic development (Smirnova et al., 2005).

As a consequence of these results, a number of experiments have been performed to address the specific functions of neuronal miRNAs; the best studied is certainly miR-124, which constitutes 25-50% of total miRNAs expressed in the brain (Johnston and Hobert, 2003) and is involved in the silencing of non-neuronal genes. Overexpression of miR-124 in HeLa cells downregulates more than 100 non-neuronal mRNAs, producing a neuron-like expression profile (Lim et al., 2005). On the other hand, in cortical neurons several non-neuronal mRNA transcripts are increased upon miR-124 knockdown (Conaco et al., 2006), and during chicken spinal cord development miR-124 is needed to preserve neuronal identity (Visvanathan et al., 2007).

Two miR-124 targets have been functionally validated to date, both affecting pathways involved in transcriptional regulation. One such target is SCP1 (small C-terminal domain phosphatase-1), an activator of REST (RE1 silencing transcription factor) involved in the antineural REST pathway. REST is a transcriptional repressor of neural genes in non-neuronal tissues, including the miR-124 gene (Conaco et al., 2006); decreased levels of REST along with increased miR-124 expression lead to terminal differentiation of neuronal cells. In non-neuronal cells and neuronal precursors, REST and SCP1 repress the expression of miR-124 and other neuronal genes that are derepressed during neural differentiation; timely down-regulation of SCP1 is critical for inducing neurogenesis, and miR-124 contributes to this process at least in part by down-regulating SCP1 expression (Visvanathan et al., 2007). The other validated miR-124 target is the polypyrimidine tract-binding protein PTBP1 (also called PTB), an important splicing regulator that represses alternative pre-mRNA splicing in non-neuronal cells. During neuronal differentiation PTBP1 expression is substituted by that of its neuronal homolog PTBP2 (also called nPTB), and this switch has substantial consequences on the splicing patterns of genes

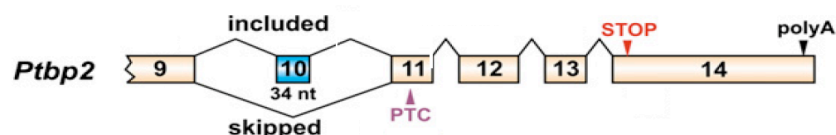


**Fig.9** Diagram of the *PTBP2* gene. In non-neuronal cells, where PTBP1 is expressed, exon 10 is skipped and a premature termination codon (PTC) is created. In neuronal cells exon 10 is included and the correct stop codon (STOP) can be used. *Makeyev et al., 2007*

involved in neuronal functions. Among the targets of PTBP1 is a critical exon (exon 10, Fig.9) in the pre-mRNA of *PTBP2* itself: when this exon is skipped, *PTBP2* undergoes nonsense-mediated decay. During neuronal differentiation miR-124 reduces PTBP1 levels, leading to the accumulation of correctly spliced *PTBP2*, which has a weaker splicing-repressor activity and allows the transition from non-neuronal to neuronal-specific splicing patterns (Makeyev et al., 2007). On the other hand, during muscle development *PTBP2* is directly regulated by the muscle-enriched miR-133, mirroring the example of miR-124 in the nervous system (Boutz et al., 2007).

### **Synaptic plasticity**

The term synaptic plasticity refers to the ability of a synapse to change its efficiency and anatomical organization in response to repeated stimulation, resulting in increased synaptic strength; likewise, if a synapse has not been used for some time its strength will decrease. It is now believed that long-term modification of synapses requires local translation of key synaptic proteins (Sutton and Schuman, 2006), and that the corresponding mRNAs need to be transported to the dendritic compartment in a translationally silenced state (within multiribonucleoprotein complexes called neuronal RNA granules), to be then locally activated for translation at individual synapses in a stimulus-dependent manner. At the neuromuscular junction in *Drosophila*, increased neural activity correlates with increased levels of translational components. Furthermore, the overexpression of the translation initiation factor eIF4E and PABP (polyA-binding protein) results in increased synaptic size and efficiency (Sigrist et al., 2000). In this context, the main question is how differential expression of specific dendritic mRNAs is achieved; it is thought that miRNAs could mediate at least in part this post-transcriptional regulation (Kosik, 2006). In support to this hypothesis, some miRNAs have been shown to be enriched in the dendritic compartment (Kye et al., 2007).

Evidence for the participation of miRNAs in synaptic mRNA expression was first observed in *Drosophila*. Two initial studies found that *dFmr1*, the *Drosophila* ortholog of mammalian Fragile X protein (*FMRP*), interacts with the RNA interference machinery, in particular with Ago2. Fragile X syndrome (FX) is one of the most common forms of mental retardation, and is characterized by abnormalities in the structural development of dendritic spines (Penagarikano et al., 2007). It is caused by a CGG repeat in the 5'UTR of the *FMR1* gene, which is located on the long arm of chromosome X. The condition becomes clinically manifest when the repeat expands as the gene is passed from generation to generation, until its transcription is

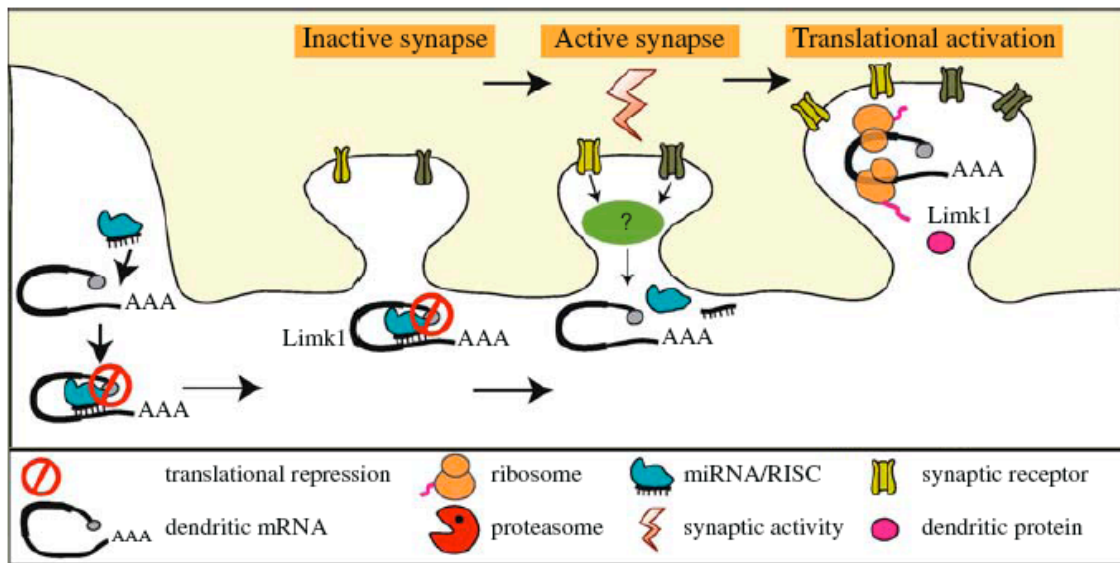


**Fig.10** Model of the mechanism of action of miRNAs in synaptic plasticity. *LIMK1* mRNA is subject to miR-134-mediated translational repression, and is transported from the soma through the dendrite. Upon synaptic activation, the miRNA/RISC complex is inactivated and translational silencing is relieved. Modified from Barbato et al., 2008.

completely shut down in the full-blown syndrome. The current view is that FMRP acts as a translational repressor of a subset of dendritic mRNAs and that the disease is caused by the deregulated expression of its targets, which encode factors required for synaptic plasticity and development. Following the results obtained in *Drosophila*, the interactors of FMRP were further investigated in mammalian cells, revealing that it associates with endogenous miRNAs and with Ago1 (Jin et al., 2004) and supporting the hypothesis that miRNAs might take part in FMRP-mediated silencing of neuronal mRNAs. Furthermore, another study carried out in *Drosophila* has shown an interesting overlapping between the composition of FMRP-containing neuronal granules and P-bodies, which suggests that these classes of granules might be similar not only in composition but also in function (Hillebrand et al., 2007). Additional evidence for a link between miRNA function and synaptic plasticity in *Drosophila* has been recently provided by the finding that *CaMKII* mRNA (Calcium/Calmodulin-dependent protein kinase II), an mRNA involved in plasticity, is subject to RISC-mediated translational repression (Ashraf and Kunes, 2006).

The prime example of a miRNA implicated in synaptic plasticity in mammalian neurons is miR-134, which localizes to dendrites close to synapsin-positive *puncta*. Its overexpression causes a significant decrease in dendritic spine size, while its depletion leads to a small increase in spine volume. miR-134 targets *LIMK1* (Lim-domain-containing protein kinase 1), whose activity is controlled by

BDNF and which is involved in actin filament dynamics, a key step in the cytoskeletal modifications of spines associated with plasticity. The concomitant overexpression of miR-134 with a mutated form of *LIMK1* that has a defective target site rescues the alterations in spine morphology, indicating that the spine size defects caused by miR-134 are indeed due to the deregulation of *LIMK1*. Furthermore, miR-134-mediated repression of *LIMK1* is relieved upon BDNF stimulation of synaptic plasticity (Schratt et al., 2006), showing that neuronal activation intervenes to put a brake on miRNA-mediated silencing (Fig.10).

Finally, another indication of the involvement of microRNAs in controlling local protein translation and synaptic function comes from a recent study that demonstrated that miR-128 is deregulated in HIV-1 encephalopathy (a manifestation of HIV-1 infection that often results in neuronal damage and dysfunction) and that mir-128a inhibits the expression of SNAP25, a pre-synaptic protein that regulates Ca<sup>++</sup> responsiveness (Eletto et al., 2008).

### **Nervous system diseases**

miRNAs have been implicated in several neurological disorders including polyglutamine expansions, Parkinson's and Alzheimer's diseases and the Tourette syndrome and Fragile X syndrome, opening a novel line of research that investigates the potential contribution of miRNAs to mental and psychiatric illnesses. Known miRNA-related nervous system diseases can be schematically grouped based on the specific aspect that is altered; they can be in fact associated with structural alterations involving genes that are important in miRNA biogenesis (e.g FX and DiGeorge syndromes), changes in specific miRNA expression (e.g Parkinson's disease, Alzheimer's disease and schizophrenia) or mutations in target mRNA sequences (e.g. Tourette syndrome, Parkinson's disease).

The biochemical mechanisms underlying the FX syndrome have been mentioned previously; studies on *Drosophila* and mammals indicate that FMRP and miRNAs cooperate in repressing dendritic mRNA expression, even if evidence for a direct participation of miRNAs in the insurgence or development of the FX syndrome is still lacking.

DiGeorge syndrome is a developmental disorder characterized by structural and functional palate anomalies, conotruncal cardiac malformations, immunodeficiency, hypocalcemia, and typical facial anomalies. Most cases result from a deletion of chromosome 22q11.2 (the DiGeorge syndrome chromosome region, or DGCR); interestingly, the deletion includes the DiGeorge syndrome critical



region gene 8 (*DGCR8*), which, as explained before, is required for the maturation of miRNA primary transcripts. *DGCR8* knockdown results in fact in accumulation of pri-miRNAs and reduction of pre-miRNAs and mature miRNAs (Landthaler et al., 2004), indicating a plausible involvement of miRNAs in the etiology of the disease. Schizophrenia might be associated with altered miRNA expression profiles; in postmortem prefrontal cortex from schizophrenia patients several miRNAs were in fact found expressed at lower levels (Perkins et al., 2007), and genetic variants of the brain-expressed miR-198 and miR-206 were found to be associated with the disorder (Hansen et al., 2007).

An increase in miR-9, miR-125b and miR-128 levels has been detected in the hippocampus of Alzheimer's disease brains (Lukiw, 2007); furthermore, a recent work on miRNAs and AD has shown that miR-107 could be a regulator of BACE1 (beta-site amyloid precursor protein cleaving enzyme 1), whose mRNA levels increase as miR-107 levels decrease in the progression of the disease (Wang et al., 2008b); these studies suggest that miRNAs may be important for neuronal survival in the context of human neurodegenerative diseases.

In addition, reduced expression of miR-133b has been observed in dopaminergic neurons in Parkinson's disease patients and has thus been associated with the degeneration of this type of neurons that is typical of the disease (Kim et al., 2007). miR-433 has as well been linked to PD, as a risk conferring polymorphism in fibroblast growth factor 20 (*FGF20*) has been shown to disrupt a miR-433 target site, leading to increased *FGF20* translation; this in turn leads to an increased expression of alpha-synuclein, which ultimately causes PD (Wang et al., 2008a).

Tourette syndrome is a neurological disorder characterized by behavioral abnormalities and by motor and vocal tics. Sequence variants of a candidate gene on chromosome 13q31.1, named *SLITRK1* (Slit and Trk-like 1), were identified in Tourette syndrome patients, one of them being located in the 3'UTR of the gene within the binding site for miR-189 (Abelson et al., 2005); this mutation was shown to positively affect the interaction of the *SLITRK1* mRNA and miR-189, leading to a more stringent repression of the gene.

Finally, a common polymorphism in the serotonin receptor 1B (*HTR1B*) affecting the target site for miR-96 has been shown to be associated with aggressive human behaviors (Jensen et al., 2008).



## microRNA target prediction methods

Since the very first miRNAs *lin-4* and *let-7* were identified, researchers have developed numerous computational methods that can complement biological experiments to understand the diverse regulatory functions of miRNAs. Most computational methods can be classified into two broad categories, programs for miRNA gene identification and programs for miRNA target identification; in this chapter we are giving an overview of the second group.

The basic principle of many computational tools is that they are somehow constructed from experimental examples, which means they are based on machine-learning algorithms (Yoon and De Micheli, 2006); for example, a target detection algorithm can be trained using the properties of known miRNA-mRNA duplexes and can then be used for predicting new duplexes. However, since the mechanisms behind miRNAs and their actions are not completely revealed, the limited availability of precise and reliable experimental elucidation of miRNA targets remains a major bottleneck and a challenge for the effectiveness of computational methods. This problem is more evident in animal miRNA target prediction, due to the imperfect complementarity of miRNAs to their targets. The detection principles used by most approaches are relatively similar and rely on the previous knowledge on the pairing of *lin-4* and *let-7* in *C.elegans* as well as the bantam miRNA in *Drosophila* (Brennecke et al., 2003).

In general, prediction criteria include the following:

1. miRNA target sites are located in the 3'UTR sequence of potential target mRNAs. In particular, strong binding and perfect complementarity of the first eight nucleotides at the 5' end of the mature miRNA - the so-called *seed* region - is considered very important, whereas G:U wobbles reduce the silencing efficacy (Doench and Sharp, 2004). A limitation in this context is the acquirement of a correct set of potential target sequences: the annotation of UTRs is in fact not always accurate, also depending on the genome that is being considered. When there is no cDNA or EST sequence available to annotators, genes are normally annotated as ending with the stop codon; some target prediction methods like miRanda (Enright et al., 2003; John et al., 2004) have tried to circumvent this problem by taking a constant length of sequence downstream of the stop codon, even if the length of 3'UTRs is known to vary quite widely and this approach risks missing target sites or introducing false ones (Lindow and Gorodkin, 2007). With

respect to the requirement of perfect complementarity to the seed region, it improves the signal-to-noise ratio of predictions as it is actually estimated that seed sites may outnumber other sites by 10:1; however miRNAs target sites can tolerate G:U wobbles within the seed region (Miranda et al., 2006) and extensive base pairing with the remainder of the miRNA may compensate missing complementarity of the 5' seed (Brennecke et al., 2005).

**2.** The thermodynamics of miRNA-mRNA duplexes are considered important by most prediction algorithms; the variation of free energy associated with the duplexes can be calculated with RNA folding programs.

**3.** Conservation of target sites among related genomes is the most commonly used property for reducing the search space when predicting targets, based on the assumption that targets are under positive selection. Again, this requirement improves the general performance of prediction methods; nevertheless it can't be taken as an absolute truth. Most of the early discovered miRNAs – especially in their mature form - were in fact very well conserved over long evolutionary distances, suggesting that conservation should be a defining characteristic of miRNA genes and as a consequence of their target sequences (Ambros et al., 2003). In addition, a more recent study demonstrated that sequences complementary to seed regions are better conserved in 3'UTRs than random sequences of the same length (Xie et al., 2005). However, the idea that all miRNAs are deeply conserved has been challenged, and a large number of taxon-specific miRNAs have now been identified (Bentwich et al., 2005) or computationally predicted (Miranda et al., 2006).

**4.** Other aspects can also be taken into consideration as important features of miRNA targeting: the efficiency of RNA silencing can be increased by a combinatorial control of a single target by multiple miRNAs or similarly by having multiple binding sites for a given miRNA (Doench and Sharp, 2004); lack of a strong secondary structure at the miRNA-binding site on the target may be a favoring factor (Du and Zamore, 2005); miRNAs could also target other miRNAs for silencing (Lai et al., 2004).

The different predictions programs are basically combinations of these criteria, especially the first three; the most commonly used are described below; a summary of their main features is given in Table 3.

**miRanda** ([www.microrna.org](http://www.microrna.org)) was originally designed to identify miRNA targets in *Drosophila* and man. It selects target sites on the basis of sequence

complementarity, which is evaluated using an algorithm that does not consider the seed region but gives higher weight to matches at the 5' end of the mature miRNA. It also takes into account the free energy of the RNA–RNA duplex (calculated with RNAFold) and the extent of conservation of the miRNA target. It is estimated to have a 24-39% false positive rate (Bentwich, 2005).

**TargetScan** ([www.targetscan.org](http://www.targetscan.org)) was initially developed by Lewis et al. in 2003 to identify mammalian targets and was then improved two years later with the release of TargetScanS. TargetScan (Lewis et al., 2003) looked for perfect matches to a 7-nucleotide seed starting from the second nucleotide of the miRNA, used RNAFold to calculate the free energy of the binding and accounted for both single and multiple binding sites. With the improved algorithm TargetScanS (Lewis et al., 2005) some of the parameters of the previous versions were relaxed and new criteria were incorporated: it requires a shorter seed of 6 nucleotides that is preceded by an adenosine, does not consider anymore the conservation of sequences flanking the seed and it does not rely on free-energy calculations. Furthermore, TargetScanS scans sequence conservation on two more species (chicken and dog) in addition to the three previously examined genomes (mouse, rat and human). It is worth mentioning that since the July 2006 release (version 4.0) TargetScan has relaxed the conservation requirement, allowing searching also for poorly conserved miRNAs and target sequences. TargetScan is estimated to have a 22-31% false positive rate.

**PicTar** (<http://pictar.mdc-berlin.de>) predicts miRNA targets in vertebrates, *C.elegans* and *Drosophila* (Krek et al., 2005). The algorithm is trained to identify binding sites targeted by a single miRNA as well as those that are coregulated by several miRNAs. It finds perfect matches of 7 nucleotides starting at position 1 or 2 of the 5' end of the miRNA. Similar to miRanda the hybridization energy is then calculated and unstable duplexes are discarded. It is also able to calculate the likelihood - under a lot of assumptions - that a transcript is regulated by two or more miRNAs in combination, and is estimated to have ~30% false positive rate.

**DIANA-MicroT** ([http://diana.pcbi.upenn.edu/cgi-bin/micro\\_t.cgi](http://diana.pcbi.upenn.edu/cgi-bin/micro_t.cgi)) predicts human miRNA targets and takes a different approach: it focuses on single binding site targets and requires 3' binding besides the obligatory 5' seed, as well as a typical central bulge (Kiriakidou et al., 2004).

Finally, **RNAhybrid** (<http://bibiserv.techfak.uni-bielefeld.de/rnahybrid>) is an RNA folding algorithm improved over RNAFold or Mfold, which allows free-energy assessment of hybridizations of a short RNA to a long RNA (e.g. a miRNA to its

target) and identifies the most favorable ones. It can be used as a prediction tool by forcing a match with the seed region (Rehmsmeier et al., 2004).

| <i>Method name</i> | <i>Matching criteria</i>            | <i>Energy filter</i>                                                                 | <i>Search space reduction</i> | <i>Scoring scheme for selection of candidates</i>             | <i>Submit sequence for online search</i> |
|--------------------|-------------------------------------|--------------------------------------------------------------------------------------|-------------------------------|---------------------------------------------------------------|------------------------------------------|
| TargetScanS        | Seed variations only                | None                                                                                 | Whole genome alignments       | All equal                                                     | No                                       |
| miRanda            | Weighted alignment emphasizing seed | Hybridization energy threshold (RNAfold with linker)                                 | AVID alignment of UTRs        | <i>Ad hoc</i>                                                 | No                                       |
| PicTar             | Seedmatch or compensatory           | Hybridization energy threshold (RNAfold). > 33% of energy for perfect match of miRNA | Whole genome alignments       | Maximum likelihood, combined for all sites meeting thresholds | No                                       |
| RNAhybrid          | Integrated match and energy         | Guarantees to find lowest energy site                                                | Not implemented               | Extreme value distribution. BLAST-like e-value                | Yes                                      |
| Diana-microT       | Dynamic programming—dinucleotides   | Hybridization energy threshold + rules                                               | Not implemented               | All equal                                                     | Yes                                      |

**Table 3** Overview of miRNA target prediction programs and their computational principles. *Adapted from Lindow et al., 2007.*

## **2. Objectives**



The general aim of this work was to explore the role of miRNAs in the regulation of the human neurotrophin-3 receptor NTRK3, with particular emphasis on the contribution of miRNAs to the fine-tuning and balance between the two major NTRK3 isoforms (full-length and truncated).

More in detail, the research objectives were as follows:

- To set up a luciferase reporter-based system for a rapid and high throughput analysis and validation of predicted miRNA target sites in the 3'UTRs of full-length and truncated NTRK3. The assay was optimized with the aim of establishing a protocol applicable to the analysis of other genes of interest in the laboratory.
- To further validate whether miRNAs causing a significant reduction in luciferase activity are also able to regulate endogenous NTRK3, in a neuron-like context (SH-SY5Y neuroblastoma cells).
- To examine the effects of the repression of NTRK3 after overexpression of the corresponding miRNAs by analyzing possible alterations in downstream signaling pathways and in the general physiology of cells.
- To analyze the consequences of the overexpression of miRNAs of particular interest at the transcriptome level, in order to identify pathways and molecular networks in which these miRNAs could play a regulatory role.
- To investigate the possible function of miRNAs in the regulation of NTRK3 not only through direct targeting of the two isoforms, but also in the control of factors involved in their alternative splicing.





## **3. Materials and methods**



### 3'UTR cloning

The 3'UTRs of the full-length and truncated isoforms of *NTRK3* (FL-NTRK3 and TR-NTRK3) and *BDNF* were PCR-amplified from BACs CTD-2508H23 and RP11-587D21 respectively, using *PfuTurbo*<sup>®</sup> DNA polymerase (Stratagene). PCR reactions were performed according to the manufacturer's instructions, using ~100 ng of DNA template in 50 µL total volume. The following forward (For) and reverse (Rev) primers containing an *Xba* I restriction site at the 5' end (underlined) were used:

|          |     |                                                   |
|----------|-----|---------------------------------------------------|
| FL-NTRK3 | For | 5'-acacact <u>ctag</u> agtctgccccaaagaggtgta-3'   |
|          | Rev | 5'-acacact <u>ctag</u> accaaactgccttacagggttt-3'  |
| TR-NTRK3 | For | 5'-acacact <u>ctaga</u> aataagccttcccggacatt-3'   |
|          | Rev | 5'-acacact <u>ctag</u> atgcaaaatttccaaataagagg-3' |
| BDNF     | For | 5'-acacact <u>ctag</u> acattgaccattaaaaggggaag-3' |
|          | Rev | 5'-acacact <u>ctag</u> accagaacccccagatttta-3'    |

Annealing temperatures were 56 °C for FL-NTRK3 and 54 °C for TR-NTRK3 and BDNF. PCR fragments of 334, 2110 and 2969 bp respectively were purified using the QIAquick PCR Purification Kit (QIAGEN) and *Xba* I-digested (all restriction enzymes were obtained from New England BioLabs). The firefly luciferase reporter vector pGL4.13 (Promega, Fig.1) was as well digested with *Xba* I and dephosphorylated with calf intestine alkaline phosphatase (Roche). Plasmid DNA and PCR products were then purified and ligated over night (ON) with T4 DNA Ligase (Invitrogen), using ~100 ng of total DNA in 20 µL final volume and a 3:1 insert:vector molar ratio. One microliter of each ligation reaction was used to transform 25 µL of One Shot<sup>®</sup> TOP10 Chemically Competent E. Coli cells (Invitrogen), following a standard chemical transformation procedure. Transformed cells were plated onto LB agar plates containing ampicillin (100 mg/mL) and ampicillin-resistant colonies were analyzed. Plasmid DNA mini preparations were obtained using the QIAprep<sup>®</sup> Spin Miniprep Kit (QIAGEN) from 5 mL ON cultures grown in LB plus ampicillin; recombinant colonies were selected by *Hind* III digestion and the authenticity and orientation of the inserts were confirmed by sequencing, using the following primers flanking the *Xba* I restriction site on pGL4.13:

For 5'-agatccgagatttcatt-3'  
 Rev 5'-tggttgtccaaactcatcaa-3'

Sequencing reactions were performed using the ABI PRISM<sup>®</sup> BigDye Terminator Sequencing Kit (Applied Biosystems), purified with the Montage<sup>™</sup> SEQ<sub>96</sub> Sequencing Reaction Cleanup Kit (Millipore) and then run and analyzed with the ABI PRISM<sup>®</sup> 3730xl DNA Analyzer (Applied Biosystems). Plasmid DNA maxi preparations from positive clones were finally obtained using the QIAGEN<sup>®</sup> Plasmid Maxi Kit (QIAGEN), following the manufacturer's instructions. Constructs were named pGL4.13-FL, pGL4.13-TR and pGL4.13-BDNF.

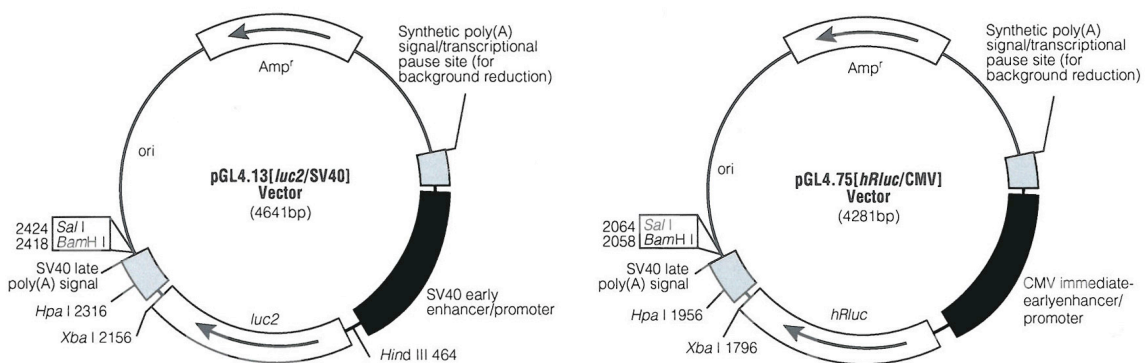


**Fig.1** pGL4.13 (*Photinus pyralis*) and pGL4.75 (*Renilla reniformis*) luciferase reporter vectors.

## Cell culture

Two human immortal cell lines were used in this work, HeLa and SH-SY5Y. HeLa are cervix adenocarcinoma cells; the name HeLa comes from the patient's name, Henrietta Lacksand, from whom cervical cancer cells were originally taken in the 1950s. SH-SY5Y are epithelial-like neuroblastoma cells; SH-SY5Y is a clonal subline of the neuroepithelioma cell line SK-N-SH, established in 1970 from the bone marrow biopsy of a 4-year-old girl with metastatic neuroblastoma.

Both cell lines are adherent and grow on tissue culture-treated polystyrene culture dishes (nunc<sup>™</sup>) at 37°C, 5% CO<sub>2</sub> and 70-80% relative humidity. Cells were maintained in Dulbecco's Modified Eagle's Medium (DMEM) supplemented with 10% fetal bovine serum (FBS), 2 mM L-glutamine, 100 units/ml penicillin and 100 µg/ml

Streptomycin (all from GIBCO™, Invitrogen). In the case of SH-SY5Y cells, FBS was heat inactivated for 45 minutes at 56°C prior to use.

### Optimization of transfection conditions

HeLa and SH-SY5Y cells were transiently transfected by lipofection using Lipofectamine™ 2000 (Invitrogen), following the transfection procedure indicated by the manufacturer.

While conditions for plasmid DNA transfection into HeLa cells are well established, little information was available about the cotransfection of plasmids and small RNAs; optimization was needed in order to obtain optimal efficiency in both plasmid DNA and small RNA delivery. Cotransfection of HeLa cells was therefore optimized using a GFP-containing plasmid (pEGFP-C1, Clontech) and a commercially available GFP-specific siRNA (Ambion). Different seeding densities, plasmid and siRNA concentrations were tested in 12-well plates; >80% transfection efficiency was obtained plating ~150000 cells per well and using 3 µL Lipofectamine™ 2000, 100-300 ng of plasmid DNA and 5-30 nM siRNA, which provided a complete inhibition of GFP activity as detected by observation under a fluorescence microscope. These starting conditions were scaled down proportionally to the surface area of 96-well plates (1:10 relative to 12-well plates) and then adjusted for the simultaneous transfection of a firefly luciferase reporter plasmid (pGL4.13), a renilla luciferase reporter plasmid (pGL4.75, Promega) and human miRNA mimics (miRIDIAN™ miRNA mimics, Dharmacon) - chemically modified double-stranded RNA oligonucleotides that mimic endogenous mature miRNA function. This second part of the optimization was accomplished using pGL4.13-BDNF, pGL4.75 and the miR-1 mimic, as BDNF had previously been validated as a target for this miRNA (also see Results). Finding the optimal firefly:renilla plasmid ratio was the most critical step; it was finally set to ~20:1 over 30 ng of total DNA, with subsequent small adjustments depending on the specific firefly construct. Different miRNA mimic concentrations were also tested (3, 10 and 30 nM) and mimics were ultimately used at 10 nM.

Transfection of SH-SY5Y cells with miRNA mimics was optimized in 6-well plates using a fluorescein-labeled double-stranded RNA oligomer (siGLO Green Transfection Indicator, Dharmacon); optimal efficiency was obtained at 50-200 nM

siGLO concentration. miRNA mimics were therefore tested at 50, 100 and 200 nM concentration and were ultimately used at 100 nM.

## Luciferase assay

Dual-luciferase assays rely on two different reporter genes, firefly (*Photinus pyralis*) and renilla (*Renilla reniformis*) luciferases, to evaluate regulated gene expression; the assay is performed by sequentially measuring the firefly and renilla luciferase activities of the same sample, with the results expressed as the ratio of firefly to renilla luciferase activity (FLuc/RLuc). In our case the firefly reporter plasmid (pGL4.13) was used to clone the 3'UTRs of interest, while the renilla reporter plasmid (pGL4.75) was used to control for transfection efficiency.

HeLa cells were seeded at  $1.3 \times 10^4$  cells per well in 96-well plates and cotransfected 24 hours after seeding with the firefly reporter constructs described above (pGL4.13-FL, 13.5 ng; pGL4.13-TR, 24 ng; pGL4.13-BDNF, 17 ng; pGL4.13 empty vector, 10 ng), the renilla reporter plasmid (pGL4.75, 3 ng), and the appropriate miRNA mimic (10nM), using 0.3  $\mu$ L Lipofectamine<sup>TM</sup> 2000 per well. Twenty-four hours after transfection the activity of firefly and renilla luciferases were determined using the Dual-Glo<sup>TM</sup> Luciferase Assay System (Promega), following the manufacturer's instructions, and an Orion Microplate Luminometer (Berthold).

The relative reporter activity was obtained by normalization of firefly luciferase activity to renilla luciferase activity. Furthermore, each relative reporter activity was additionally normalized to that of the empty vector transfected with the corresponding miRNA, in order to correct for vector-dependent unspecific effects. Results were then compared to the mean of two different negative controls (miRIDIAN<sup>TM</sup> miRNA Mimics Negative Controls #2 and #4, whose sequences are based on *C. elegans* miRNAs for use as negative experimental controls in human). Each experiment was done in triplicate and at least three independent experiments were performed for each miRNA. Data are reported as means  $\pm$  S.E and statistical significance was determined using Student's *t* test ( $p < 0.05$ ).

## Protein extraction

Total protein extracts from SH-SY5Y cells were prepared as follows; two different lysis buffers were used, depending on the analyzed protein.

For NTRK3 and PTBP1, cells were solubilized with RIPA (Radio-Immuno-Precipitation Assay) buffer: 50 mM Tris-HCl pH 7.4, 150 mM NaCl, 2mM EDTA, 0.1% SDS, 1% Nonidet P 40, 1% sodium deoxycholate, 1 mM Na<sub>3</sub>VO<sub>4</sub>, 1 mM PMSF, 50 mM NaF and 1x protease inhibitors (Complete Mini, EDTA-free, Roche).

For the analysis of ERK phosphorylation, cells were lysed in a buffer containing 50mM Tris-HCl pH 7.4, 50mM NaF, 10mM sodium pyrophosphate (PPiNa) and 0.005% Triton X-100, to better preserve phosphorylated proteins.

In both cases, cells were rapidly rinsed with ice-cold PBS; PBS was carefully removed and either cells were immediately processed or plates were frozen at -80°C and thawed on ice when needed. Cells were solubilized on ice with the appropriate lysis buffer and subsequently scraped off, incubated on ice for 15 minutes and centrifuged at 12000 rpm for 15 minutes at 4°C to remove nuclei and cellular debris. Supernatants were then collected and either immediately used or frozen at -80°C. Total protein concentration was determined using the Bradford protein assay, adding 2 µL of protein extract to 250 µL of ready-to-use Bradford Reagent (Sigma). Absorbance was measured at 595 nm using a Versamax Microplate Reader (Molecular Devices).

## Differentiation of SH-SY5Y cells

SH-SY5Y cells express high levels of retinoic acid (RA) receptor (Lovat et al., 1993); RA is a potent regulator of morphogenesis, growth and cell differentiation and plays a major role in neuronal cell differentiation. SH-SY5Y normally propagate via mitosis and divide continuously; upon exposure to RA they reduce their growth rate and differentiate by extending neurites to the surrounding area into cells that are biochemically, ultrastructurally and electrophysiologically similar to neurons (Kaplan et al., 1993).

At day 0,  $\sim 1.0 \times 10^6$  cells were plated on 100 mm cell culture plates in DMEM (supplement with FBS, glutamine and antibiotics as previously described) with the addition of 10 µM *all-trans*-RA (Sigma). Depending on the time point needed, at day 3 after the induction of differentiation cells were either harvested or trypsinized and

plated again at the desired density in fresh medium complemented with RA. In the case of the RA-differentiation time course (day 3, day 6 and day 10) at each step part of the cells was harvested and part was plated at  $\sim 1.5 \times 10^6$  cells per plate (day 3) or  $\sim 2.0 \times 10^6$  cells per plate (day 6) to provide material for the following time point. Given that RA progressively reduces the growth rate, seeding cells at increasing densities allowed cultures to reach a similar confluence ( $\sim 80-90\%$ ) before harvesting at each step.

### Transfection of SH-SY5Y cells

For miRNAs targeting the truncated isoform, undifferentiated SH-SY5Y cells were plated at  $2 \times 10^5$  cells per well in 6-well plates and transfected 24 hours later with the appropriate miRNA mimic at a concentration of 100 nM, following the standard transfection procedure indicated by the manufacturer. Briefly, transfection was performed using 1.5 mL of Opti-MEM<sup>®</sup> I Reduced Serum Medium (GIBCO, Invitrogen) as plating medium. Ten microliters of 20  $\mu$ M miRIDIAN<sup>™</sup> miRNA mimic and 5  $\mu$ L of Lipofectamine<sup>™</sup> 2000 were diluted in 250  $\mu$ L of Opti-MEM<sup>®</sup> each and incubated for 5 minutes; the two solutions (250+250  $\mu$ L) were then mixed together, incubated for 20-30 minutes and added to each well containing cells and 1.5 mL of plating medium. Three hours after transfection Opti-MEM<sup>®</sup> was removed and changed to normal culture medium (DMEM plus 10% FBS, glutamine and antibiotics). Cells were analyzed 24, 48 or 72 hours after transfection.

For miRNAs targeting the full-length isoform, SH-SY5Y cells were differentiated with 10  $\mu$ M *all-trans*-RA and plated in 6-well plates at a concentration of  $3 \times 10^5$  cells per well at day 3 of RA treatment; 24 hours later (day 4 of RA treatment) cells were transfected as described above with 100 nM miRNA miRIDIAN<sup>™</sup> miRNA mimic and analyzed 24, 48 or 72 hours after transfection (day 5, 6 or 7 of RA treatment).

For the analysis of ERK phosphorylation, differentiated cells were seeded and transfected as explained above; 72 hours after transfection cells were rinsed with PBS, incubated with serum-free medium for 5 hours and then acutely stimulated for 10 minutes with 30ng/mL neurotrophin-3 (Alomone Labs).



## Western blot optimization for NTRK3

Immunoblot analysis of NTRK3 presented a series of issues that had to be solved in order to be able to correctly detect and quantify the levels of the full-length and truncated isoforms.

### a. NTRK3 antibody

Even though a few anti-NTRK3 antibodies are available from different commercial sources they in general do not work well, at least for Western blotting (WB), and working conditions are far from being well defined. Given the high level of conservation among the three Trk receptors, the existence of different isoforms for each of them and the variety of post-translational modifications they are subject to, it was hard to find an antibody that undoubtedly detected the two human NTRK3 receptor variants. We tested a total of six antibodies (from Chemicon, Genetex, Neuromics, Upstate and two from Santa Cruz) on both nitrocellulose and polyvinylidene fluoride (PVDF) membranes, trying different dilutions, blocking and incubation conditions; we could finally obtain good results with an anti-TrkC goat polyclonal antibody from Upstate (Millipore), which could clearly detect the full-length isoform.

### b. Gel electrophoresis and transfer

To improve the detection of the truncated isoform, which remained unclear, we tried polyacrylamide gradient gels in order to obtain better band resolution. We decided to use the NuPAGE<sup>®</sup> electrophoresis system (NuPAGE<sup>®</sup> Bis-Tris Gels, 4-12%, Invitrogen) because, as compared to the traditional Laemmli SDS-PAGE system that operates at alkaline pH, it maintains a neutral pH 7.0 environment during electrophoresis, which improves protein stability and results in sharper band resolution. With this system we could detect a band corresponding to the truncated isoform; however, its expression was low with respect to the full-length isoform.

As far as protein transfer, we compared a conventional semi-wet blotting method with the iBlot<sup>™</sup> Dry Blotting System (Invitrogen). This system is composed of a gel transfer device and ready-made gel transfer stacks, and allows a quick and reliable transfer of proteins without using transfer buffers. Proteins transferred with this system normally exhibit higher immunodetection sensitivity when compared to proteins transferred using conventional methods. With this system we could further

improve the NTRK3 western blot, which showed lower background, sharper bands, higher reproducibility and, in particular, allowed to better detect the truncated isoform more clearly.

### c. Loading control

Given that changes in gene expression and protein accumulation induced by miRNAs can be very subtle and that the basal NTRK3 expression levels - especially the truncated isoform - in SH-SY5Y cells are not high, we wanted to make sure to be working in the best possible conditions for protein detection and quantification. We considered two aspects: the use of the appropriate loading control and the sensitivity of the detection method. We tested the reliability as loading controls of three proteins with relatively constant expression -  $\beta$ -actin,  $\alpha$ -tubulin and glyceraldehyde 3-phosphate dehydrogenase (GAPDH) - by analyzing by WB consecutive dilutions of a protein extract of SH-SY5Y cells containing from 2.5 to 60  $\mu$ g of total protein. Surprisingly, no or little protein load-dependent variation in band intensity was found when  $\beta$ -actin and tubulin antibodies were used, indicating that they were not suitable loading controls. On the other hand, with the anti-GAPDH antibody a clear gradual increase in band intensity along with the increasing protein load was observed, with a good correlation between the two; we therefore chose GAPDH to check for equal protein loading in WB analyses.

### d. Detection method

The low levels of the truncated isoform of NTRK3 made its quantification by enhanced chemiluminescent detection (ECL, Amersham) complicated. We therefore tested fluorescent detection using the ODYSSEY<sup>®</sup> infrared imaging system (LI-COR<sup>®</sup> Biosciences), which requires the use of fluorescently-labeled secondary antibodies that are detected with an infrared scanner. This system allows the quantification of low-abundance proteins that chemiluminescence can't, and in addition only one exposure is needed to image strong and weak bands on the same blot. To assess the accuracy and reproducibility of protein quantification with this system, we performed a WB analysis of NTRK3 in consecutive dilutions of a protein extract containing 2.5, 5, 10 and 20  $\mu$ g of total protein, which were loaded three times on the same gel in two independent immunoblots. The results were very satisfactory, showing a good correspondence between the amounts of loaded protein and the quantification; we therefore employed fluorescent detection for our analyses.

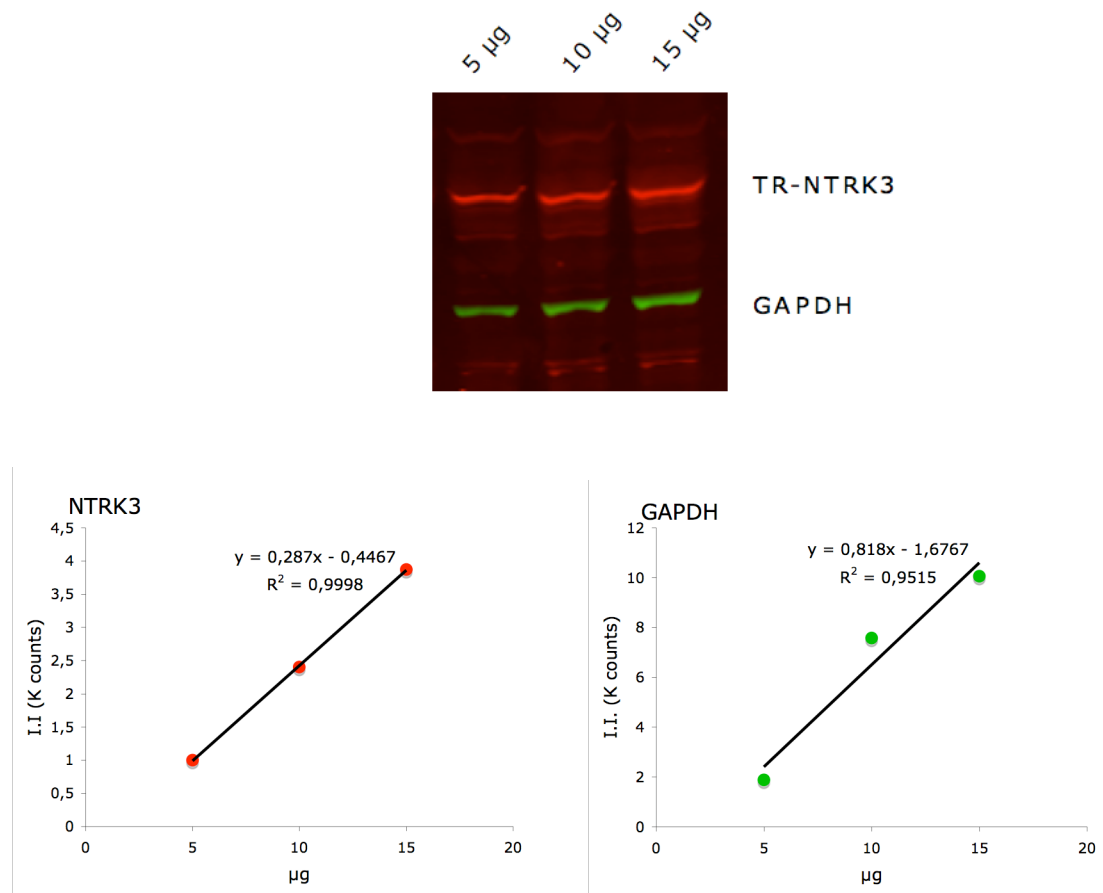


**Fig.2** WB of a protein gradient (up) with the corresponding standard curves (down) for TR-NTRK3 and GAPDH. 5, 10 and 15 µg protein gradients were loaded on each protein gel and standard curves were calculated for each immunoblot.

Furthermore, to increase the quantification accuracy, we decided to load on each gel a gradient of one of the control samples. Using a gradient in each WB, FL-NTRK3, TR-NTRK3 and GAPDH were quantified by densitometry and the corresponding standard curve equations were calculated; blots were considered reliable for quantification only if standard curves showed a correlation coefficient ( $R^2$ )>0.9 (Fig.2). Densitometry counts for each sample were then corrected using the calculated standard curve equations.

## Western blotting

Protein extracts were resolved in NuPAGE<sup>®</sup> 4-12% Bis-Tris polyacrylamide gels with NuPAGE<sup>®</sup> MES SDS Running Buffer and transferred to nitrocellulose membranes

using the iBlot™ Dry Blotting System (Invitrogen). Before blotting, gels were equilibrated in 100 ml equilibration buffer (2x NuPAGE® Transfer Buffer, 10% methanol and 1:1000 NuPAGE® Antioxidant) for 20 minutes at room temperature (RT, all NuPAGE® products are from Invitrogen).

Immunodetection was performed using the ODYSSEY® infrared imaging system, following the manufacturer's instructions for two-color WB. After transfer, membranes were rinsed with water, equilibrated in TBS for a few minutes and blocked in ODYSSEY® blocking buffer for 1 hour at RT. Blots were then incubated with the appropriate primary antibody diluted in 1:1 ODYSSEY® blocking buffer/TBST (TBS plus 0.1% Tween-20, Sigma). As a loading control, membranes were simultaneously incubated with a monoclonal anti-GAPDH antibody for 15 minutes at RT. After washing three times for 10 minutes with TBST, membranes were probed with the appropriate fluorophore-labeled secondary antibodies diluted in 1:1 ODYSSEY® blocking buffer/TBST for 45 minutes at RT, washed again three times, rinsed in TBS to remove residual Tween-20 and finally scanned on an ODYSSEY® infrared scanner. Fluorescent bands were quantified using the ODYSSEY® software.

For the analysis of ERK phosphorylation, pan-ERK was used as a loading control instead of GAPDH. In this case the anti-phospho-ERK and the anti-pan-ERK antibody were incubated separately to avoid interference, as they are directed against the same protein. Five independent experiments were performed; data are reported as means  $\pm$  S.E and statistical significance was determined using Student's *t* test.

Primary and secondary antibodies and their working conditions are listed below.

### Primary antibodies

Anti-TrkC goat polyclonal IgG, Upstate (catalog # 07-226)

1:1000, 1 hour at RT

Anti-PTBP1 goat polyclonal antibody, Abcam (catalog # ab5642)

1:500, 1 hour at RT

Anti-GAPDH mouse monoclonal antibody, Chemicon (catalog # MAB374)

1:4000, 15 minutes at RT

Anti-MAP Kinase, Activated (diphosphorylated ERK-1&2) mouse monoclonal antibody, Sigma (catalog # M9692)

1:3000, ON at 4°C

Anti-p44/42 MAP kinase rabbit polyclonal antibody, Cell Signaling (catalog # 9102)  
1:1000, 1 hour at RT

#### Secondary antibodies

Alexa Fluor® 680 rabbit anti-goat IgG, Invitrogen (catalog # A-21088) 1:6000, 45 minutes at RT

IRDye® 680 donkey anti-mouse IgG, LI-COR® (catalog # 926-32222)  
1:15000, 45 minutes at RT

IRDye® 800CW donkey anti-mouse IgG, LI-COR® (catalog # 926-32212) 1:15000,  
45 minutes at RT

IRDye® 800CW donkey anti-rabbit IgG, LI-COR® (catalog # 926-32213) 1:15000, 45 minutes at RT

### **Purification of total RNA**

Total RNA including short RNAs was extracted from HeLa and SH-SY5Y cells using the RNeasy® Mini Kit (QIAGEN). Cells grown on 100 mm or 6-well culture plates were lysed by adding 700 µL QIAzol Lysis Reagent directly to the culture dish, and further processed following the manufacturer's instructions. In particular, RNA was DNase-treated using the RNase-free DNase Set (also from QIAGEN), which allows on-column digestion of DNA during RNA purification. The elution of RNA from columns was performed in two steps (using 40+30 µL H<sub>2</sub>O) in the case of 100 mm plates and in a single step (40 µL H<sub>2</sub>O) in the case of 6-well plates. RNA was quantified with a NanoDrop™ 1000 Spectrophotometer (Thermo Scientific) and RNA quality was assessed using the Agilent 2100 Bioanalyzer (Agilent Technologies), obtaining rRNA ratios (28s/18s) of at least 1.8 and RNA integrity numbers (RIN) >9. The RNA yield was approximately 30 µg from 100 mm plates and 5-6 µg from 6-well plates.

### **miRNA expression analysis using custom oligonucleotide microarrays (Agilent, 11k)**

miRNA expression in HeLa and SH-SY5Y cells was analyzed using custom 11k oligonucleotide microarrays (Agilent Technologies). Microarrays included a set of probes for the mature and precursor forms of 326 known human miRNAs (Sanger miRBase release 7.2). Negative controls included probes for 20 *Bacillus subtilis*-specific sequences, 20 rare sequences not present in human genome and 100 mouse-specific sequences. Briefly, 2 µg of total RNA were labelled with the Hy5<sup>TM</sup> or Hy3<sup>TM</sup> fluorescent labels using the miRCURY<sup>TM</sup> LNA microRNA Labelling kit (Exiqon), following the manufacturer's instructions. Pairs of labelled samples were hybridized to dual-channel microarrays for 40 hours at 55°C using Agilent hybridization reagents. Microarray images were quantified using the GenePix 6.0 (Axon) software. Only spots with signal intensities twice above the local background, not saturated and not flagged by GenePix, were considered reliable and used for subsequent analysis. Extracted intensities were subtracted from the local background and the log<sub>2</sub> ratios were normalized in an intensity-dependent fashion by global lowness. All quantitative and statistical analyses were performed using the MMARGE tool.

### **Whole-genome expression analysis using beadchip microarrays (Illumina HumanRef-8 v3.0)**

HumanRef-8 BeadChips target approximately 24500 well-annotated RefSeq transcripts and enable the interrogation of eight samples in parallel; sixteen total RNA samples obtained from four independent experiments (each experiment including four samples: SH-SY5Y cells transfected with two negative controls, miR-128 and miR-509) were analyzed on two chips. Starting from 200 ng total RNA, biotin-labeled cRNA was synthesized and hybridized according to the manufacturer's instructions. Experiments were performed at the CRG Microarrays Unit; data were analyzed using the Array File Maker (AFM) 4.0 software package.

### Real-time quantitative RT-PCR (*NTRK3*)

RNA levels of the full-length and truncated isoforms of *NTRK3* after miRNA overexpression were analyzed by real-time quantitative RT-PCR using SYBR Green I (Roche); 1.5 µg of DNase-treated RNA extracted from transfected cells were retrotranscribed with the SuperScript™ III First-Strand Synthesis System for RT-PCR (Invitrogen) according to the manufacturer's instructions, using oligo(dT) primers (20µL reaction volume). The obtained cDNA was diluted 1:3 in water and 2.5 µL of the dilutions were used to prepare the real-time PCR reactions (10 µL total volume, in triplicate), which were performed with the LightCycler® 480 Instrument (Roche) in 384-multiwell plates. Specific primers were designed for the two *NTRK3* isoforms and for *GAPDH*, which was used as a housekeeping gene, and are listed below. All amplicons were ~100 bp in length and forward and reverse primers were located in different exons. The amplification efficiency was calculated analyzing seven consecutive 1:3 dilutions of a reference sample and was ~2 in all cases.

|          |     |                            |
|----------|-----|----------------------------|
| FL-NTRK3 | For | 5'-cagccatggtccaactctc-3'  |
|          | Rev | 5'-ccagcatgacatcgtaacc-3'  |
| TR-NTRK3 | For | 5'-tccagagtgggaagtgtct-3'  |
|          | Rev | 5'-ccatggttaagaggcttga-3'  |
| GAPDH    | For | 5'-ctgacttcaacagcgacacc-3' |
|          | Rev | 5'-ccctgtgctgtagcctaat-3'  |

Thermal cycling was performed as follows: one pre-incubation cycle at 95°C for 10 minutes (ramp rate: 4.8 °C/s); 45 amplification cycles at 95 °C for 10 seconds, 57 °C for 30 seconds and 72 °C for 5 seconds (ramp rates: 4.8, 2.2 and 4.8 °C/s). Melting curves were then recorded by heating to 95°C for 5 seconds and cooling slowly until 65 °C.

### miRNA quantitative RT-PCR

The expression levels of miR-128 and miR-509 in different human tissues and in SH-SY5Y cells were analyzed using TaqMan® MicroRNA Assays. This method allows real-time quantification of mature miRNAs in a two-step process. First, cDNA is reverse transcribed from total RNA samples using miRNA-specific primers; cDNA

samples are then PCR-amplified and quantified by means of TaqMan<sup>®</sup> MGB (minor groove binder) probes containing a reporter dye (FAM<sup>™</sup> dye). Reverse transcription was performed following the manufacturer's instructions, from 10 ng of starting total RNA. PCR reactions were performed in triplicate in 10 µL total volume, using 384-multiwell plates and the Applied Biosystems 7900HT Fast Real-Time PCR System (Applied Biosystems). Small nucleolar RNA RNU58B was used as an endogenous control.

### **Cell counting**

Cells cultured on 6-well plates and transfected with miR-128, miR-509 and the related negative controls were trypsinized and resuspended in 1 mL DMEM; 100 µL of each sample were then diluted in 10 mL of Coulter Isoton II diluent (Beckman Coulter) and counted using a Z2<sup>™</sup> Series Coulter Particle Count and Size Analyzer (Beckman Coulter). The counter detects changes in the electrical conductance of a small aperture as fluid containing cells is drawn through. Cells, being non-conducting particles, alter the effective cross-section of the conductive channel. Three independent experiments were performed and in each experiment each sample was counted three times.

### **MTT cell viability assay**

MTT assay is a colorimetric assay based on MTT (3-(4,5-Dimethylthiazol-2-yl)-2,5-diphenyltetrazolium bromide), a yellow compound that is reduced to formazan by respiratory chain enzymes in the mitochondria of living cells, giving a purple color; the assay is therefore largely a measure of mitochondrial activity.

Undifferentiated SH-SY5Y cells transfected with miR-128 and miR-509 and the related negative controls were analyzed 24, 48, 72 and 96 hours after transfection. MTT was added to cultured cells at a final concentration of 0.5 mg/mL of culture medium. Cells were incubated at 37 °C for 1 hour to allow the formation of formazan precipitates; culture medium was removed and formazan was solubilized with dimethyl sulfoxide (DMSO) by pipetting. After five minutes, the absorbance of the formazan solution was measured at 550 nm using a Versamax Microplate Reader (Molecular Devices).



## Flow cytometry

SH-SY5Y cells transfected with miR-128, miR-509 and the related negative controls were analyzed by flow cytometry to evaluate possible alterations in their volume and/or morphological complexity. Seventy-two hours after transfection, cells grown on 6-well plates were trypsinized and resuspended in 1 mL of PBS. Samples were examined using a BD FACSCanto Flow Cytometer and the BD FACSDiva software (both from BD Biosciences). A two-parameter forward/side scatter (FSC/SSC) analysis was performed; forward scatter correlates with the cell size and side scatter depends on the density of the cell (i.e. number of cytoplasmic granules, membrane size), and in this manner cell populations can be distinguished based on their difference in size and density. In each analysis 5000 events were recorded.

## Computational methods

The full-length and truncated isoforms of *NTRK3* and *BDNF* were searched for putative miRNA target sites using three web-based miRNA target prediction methods: miRanda ([www.microrna.org](http://www.microrna.org), 2005 release), TargetScan ([www.targetscan.org](http://www.targetscan.org), releases 2.0, 2.1, 3.0 and 3.1) and PicTar (<http://pictar.mdc-berlin.de>). The analysis of potential binding sites for miR-24 in the 3'UTR of FL-NTRK3 was performed using RNA hybrid (<http://bibiserv.techfak.uni-bielefeld.de/rnahybrid>).

Genomic coordinates are according to the human assembly release of March 2006 (H. sapiens hg18). Sequences were obtained from the University of California Santa Cruz (UCSC) Genome Browser (<http://www.genome.ucsc.edu>). Sequence analysis was performed using the 4peaks software (<http://mekentosj.com/4peaks/>) and Multalin (<http://prodes.toulouse.inra.fr/multalin/multalin.html>). Primers were designed using the Primer3 software (<http://frodo.wi.mit.edu/cgi-bin/primer3/primer3.cgi>) and PCR annealing temperatures were calculated with the Optimase ProtocolWriter™ (<http://mutationdiscovery.com>). Pathway analysis from microarray expression data was performed with the Ingenuity Pathway Analysis Software (IPA) version 6.3 ([www.ingenuity.com](http://www.ingenuity.com)).



## **4. Results**



## 1. Screening of *NTRK3*'s putative miRNA target sites using a luciferase reporter-based system

As mentioned in the introduction, the *NTRK3* (*TrkC*) gene undergoes alternative splicing, yielding three transcript variants in humans; two of them correspond to the full-length tyrosine kinase receptor (FL-*NTRK3*), with or without a 14 amino acid insert in the tyrosine kinase domain, and the third gives rise to a truncated kinase-deficient receptor (TR-*NTRK3*) (Shelton et al., 1995). Accordingly, two major protein isoforms with molecular weights of 150 kDa (full-length) and 50 kDa (truncated) have been described (Beltaifa et al., 2005). Interestingly, at the mRNA level the two isoforms present different 3'UTR regions: the two full-length transcripts have in fact a short 3'UTR sequence (178 bp) while the truncated transcript has a relatively long one (1981 bp).

First of all, we performed an *in silico* analysis of putative miRNA target sites in the 3'UTRs of the full-length and truncated isoforms of *NTRK3*; we then proceeded to the experimental validation of predicted target sites, analyzing the effects of miRNA mimic overexpression both on luciferase-3'UTR reporter constructs and on the endogenous full-length and truncated protein isoforms.

### Target predictions and tested miRNAs

Several computational tools have been developed for the prediction of miRNA targets since miRNAs were discovered. The full-length and the truncated isoform of *NTRK3* were searched for putative target sites with three widely used miRNA target prediction programs: miRanda, TargetScan and PicTar. A detailed description of the different methods is given in the introduction; briefly, miRanda (John et al., 2004) predicts miRNA targets based on sequence complementarity, giving higher weight to matches at the 5' end of the mature miRNA and taking into account the free energy of the RNA-RNA duplex as well as the extent of conservation of the miRNA target. TargetScan (Lewis et al., 2005) and PicTar (Krek et al., 2005) consider as well target conservation but, unlike miRanda, look for perfect matches between the mRNA target and the seed region of the miRNA; TargetScan requires 100% complementarity and does not conduct free energy calculations, while with PicTar mismatches are allowed provided that they do not result in increased free energy.

The false-positive rates are estimated at 24-39% for miRanda (Bentwich, 2005), at 22-31% for TargetScan (Lewis et al., 2003) and at approximately 30% for PicTar (Sethupathy et al., 2006).

The computational analysis that was the basis for our experimental work took into account the 326 human miRNAs annotated in version 7.1 of the miRbase database (<http://microrna.sanger.ac.uk>), released in October 2005; the output is shown in Table 1 (black). We could identify three miRNAs with one putative target site each in the 3'UTR of FL-NTRK3; two were predicted by miRanda and the other by both miRanda and PicTar. As for TR-NTRK3, we identified a total of thirty miRNAs, sixteen predicted by miRanda, nine by TargetScan and five by both; PicTar could not be used for this isoform as it does not consider this variant of *NTRK3*. Out of the thirty miRNAs, twenty-one had only one potential target site in the 3'UTR of *NTRK3*, whereas the remaining nine had two different target sequences each.

All the aforementioned target sites are highly conserved across genomes, as conservation across species is one of the requirements these computational methods are based on. However, since the July 2006 release (version 4.0)

**Table 1** miRNAs with predicted target sites in FL-NTRK3, TR-NTRK3 and *BDNF* according to miRanda (M), TargetScan (TS) and PicTar (P)

| miRNA          | FL-NTRK3 | TR-NTRK3    | BDNF               | miRNA          | FL-NTRK3    | TR-NTRK3    | BDNF               |
|----------------|----------|-------------|--------------------|----------------|-------------|-------------|--------------------|
| hsa-let-7b     |          | M(1)        |                    | hsa-miR-182    |             |             | M(1), TS(1), PT(1) |
| hsa-let-7e     | M(1)     |             |                    | hsa-miR-185    | M(1), PT(1) |             |                    |
| hsa-miR-1      |          |             | M(3), TS(3), PT(3) | hsa-miR-188    |             | M(1)        |                    |
| hsa-miR-9      |          | TS(1)       |                    | hsa-miR-198    |             | M(1)        | M(1)               |
| hsa-miR-10a    |          |             | M(1), TS(1), PT(1) | hsa-miR-200a   |             |             |                    |
| hsa-miR-15a    |          |             | M(2), TS(1), PT(1) | hsa-miR-200b   |             |             |                    |
| hsa-miR-16     |          |             | M(2), TS(1), PT(1) | hsa-miR-204    |             | M(1)        | TS(3)              |
| hsa-miR-17-3p  |          |             |                    | hsa-miR-206    |             |             | M(3), TS(3), PT(3) |
| hsa-miR-17-5p  |          | TS(2)       |                    | hsa-miR-211    |             | M(1)        | TS(3)              |
| hsa-miR-18a    |          | M(1)        |                    | hsa-miR-221    |             |             |                    |
| hsa-miR-18a*   |          |             |                    | hsa-miR-296    |             | M(1)        |                    |
| hsa-miR-20a    |          | TS(2)       |                    | hsa-miR-324-5p |             | M(1), TS(1) | M(1)               |
| hsa-miR-24     |          | TS(1)       |                    | hsa-miR-326    |             | M(2)        |                    |
| hsa-miR-30e-3p |          |             | TS(2), PT(1)       | hsa-miR-330-3p |             | M(2), TS(2) | M(1)               |
| hsa-miR-30e-5p |          |             | M(1), TS(1)        | hsa-miR-331    |             | M(2)        |                    |
| hsa-miR-93     |          | TS(1)       |                    | hsa-miR-340    |             | M(1)        |                    |
| hsa-miR-103    |          |             | M(1), TS(1), PT(1) | hsa-miR-345    |             | TS(1)       |                    |
| hsa-miR-106a   |          | TS(2)       |                    | hsa-miR-374    |             |             |                    |
| hsa-miR-106b   |          | TS(2)       |                    | hsa-miR-384    |             | TS(1)       |                    |
| hsa-miR-107    |          |             | M(1), TS(2), PT(1) | hsa-miR-412    |             | M(1)        | M(1), TS(1)        |
| hsa-miR-125a   |          | M(2)        | M(1)               | hsa-miR-422a   |             | M(1)        |                    |
| hsa-miR-125b   |          | M(2)        |                    | hsa-miR-449    |             | M(1)        | M(1)               |
| hsa-miR-128a   |          | M(1), TS(1) |                    | hsa-miR-485-3p |             | TS(1)       |                    |
| hsa-miR-128b   |          | M(1), TS(1) |                    | hsa-miR-509    |             | M(1), TS(2) |                    |
| hsa-miR-133a   |          | M(1)        |                    | hsa-miR-617    |             | TS(1)       |                    |
| hsa-miR-141    |          |             |                    | hsa-miR-625    |             | TS(2)       | TS(1)              |
| hsa-miR-149    |          | M(1), TS(1) |                    | hsa-miR-765    |             | TS(1)       |                    |
| hsa-miR-151-3p | M(1)     |             |                    | hsa-miR-768-5p |             | TS(1)       |                    |

The number of target sites predicted in each case is indicated in brackets. Black=miRNAs targeting *NTRK3*, based on miRBase 7.1; blue=later-added miRNAs; green=miRNAs targeting only *BDNF*; red=unrelated miRNAs. Note: later miRBase releases considered miR-128a and miR-128b as the same miRNA, miR-128.

TargetScan relaxed the conservation requirement and incorporated a new feature that also allowed searching for poorly conserved miRNAs and target sequences; predictions for the full-length isoform did not substantially change, but the new feature, together with the incessant discovery of new miRNAs, dramatically expanded the list of predicted target sites in the truncated isoform. Since it would have been very expensive to validate all of them, among the newly added miRNAs we chose six that were of particular interest because we found different allelic variants within their target sequences (Table 1, blue). We could actually identify a total of seven variants falling within the binding sites of eleven miRNAs predicted to target the truncated isoform, namely miR-128, miR-198, miR-330, miR-345, miR-384, miR-485-3p, miR-509, miR-617, miR-625, miR-765 and miR-768-5p. In particular, miR-128, miR-509 and miR-768-5p present overlapping target sequences (Fig.3), therefore a single allelic variant affects the three; the same applies also to miR-345, miR-485-3p and miR-617 (Muiños-Gimeno et al., 2008).

In addition, we tested for comparison seventeen more miRNAs with no putative binding sites in either *NTRK3* isoform; ten of them were predicted to target *BDNF* (Table 1, green) whereas the remaining seven were not related with either *NTRK3* or *BDNF* (Table 1, red). It is worth mentioning that besides these ten miRNAs, nine of those targeting TR-NTRK3 also had putative target sequences in the 3'UTR of *BDNF*.

### Optimization of the luciferase assay

In order to validate the computational predictions we set up a luciferase reporter-based system. The entire 3'UTRs of the full-length and truncated isoforms of *NTRK3* (178 and 1981 bp respectively) and of *BDNF* (2941 bp) were cloned immediately downstream of the firefly luciferase open reading frame in a pGL4.13 plasmid (Promega), and the resulting constructs were designated pGL4.13-FL, pGL4.13-TR and pGL4.13-BDNF.

Besides being of interest per se, in the perspective of this work *BDNF* was primarily used as a tool to establish the luciferase assay conditions. In fact, when we started setting up the assay *BDNF* had already been experimentally validated as a target for miRNA miR-1, in a study where a similar strategy was used (Lewis et al., 2003); we therefore employed the miR-1/*BDNF* pair as a positive control. After that, we did not engage into a comprehensive validation of putative targets as we

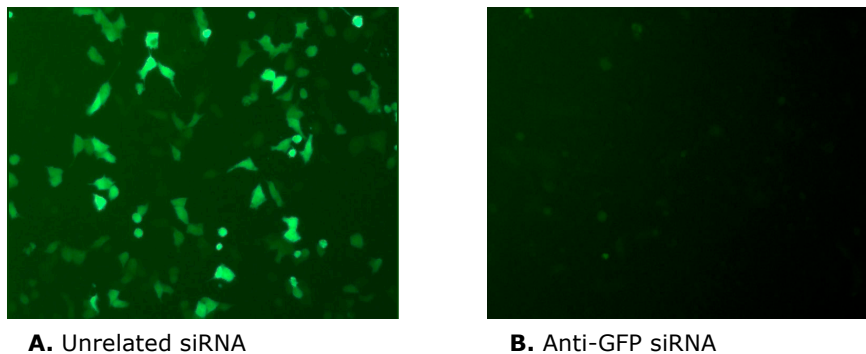


**Fig.1** Optimization of plasmid DNA/small RNA cotransfection. HeLa cells were cotransfected with pEGFP and a control siRNA (A) or an anti-GFP siRNA (B). The anti-GFP siRNA completely abolishes GFP expression. Similar results were obtained with siRNA concentrations ranging from 5 to 30 nM.

did with *NTRK3*; we just tested the miRNAs included in Table 1, only ten of which were specifically predicted to target *BDNF* by at least two computational methods. Dual-luciferase assays rely on two different reporter genes, renilla and firefly luciferase, to evaluate regulated gene expression; the assay is performed by sequentially measuring the firefly and renilla luciferase activities of the same sample, with the results expressed as the ratio of firefly to renilla luciferase activity (FLuc/RLuc). In our case the firefly reporter plasmid (pGL4.13) was used to clone the 3'UTRs of interest, whereas the renilla reporter plasmid (pGL4.75) was used to control for transfection efficiency.

HeLa and HEK (Human Embryonic Kidney) 293 are widely used cell lines for this kind of assay; after trying both we decided to use HeLa cells because they were easier to manipulate. Transfection of HeLa cells was optimized testing different seeding densities - and therefore different cell confluences at the moment of transfection - and different DNA and small RNA concentrations. A first approximation was carried out using a GFP containing plasmid and a GFP-specific siRNA (Fig.1); best results were obtained by transfecting at ~80% confluence with 10-30 ng of plasmid DNA and 5-30 nM siRNA (96-well plates); practically complete inhibition of GFP activity could be achieved 24 hours after transfection and remained constant for at least the following 48 hours.

Starting conditions established with GFP were then used as a basis to determine the optimal firefly/renilla plasmid ratio (approximately 20:1 over 30 ng of total DNA) and the appropriate miRNA mimic concentration (10 - 30 nM) for the luciferase assay; as mentioned before, this second part of the optimization was accomplished using the *BDNF* construct and miR-1.



## Validation of predicted target sites using luciferase reporter constructs

A total of fifty-six miRNAs (Table 1) and two non-targeting controls were tested on the three constructs pGL4.13-FL, pGL4.13-TR and pGL4.13-BDNF and the empty pGL4.13 vector, and luciferase activities were determined. All of the assays were performed in triplicate in at least three independent experiments (data are reported as means  $\pm$  SE relative to the mean of the two negative controls; statistical significance was determined using Student's *t* test ( $p < 0.05$ )).

The luciferase activity of the pGL4.13-FL construct (Fig.2a) was significantly decreased by three miRNAs: miR-24, miR-151-3p and miR-185. This was in agreement with computational methods only in part, as miR-151-3p and miR-185 were actually predicted to target the full-length isoform, whereas miR-24 was not. On the other hand let-7e, which was predicted by miRanda at the time the study was done, did not cause any reduction in luciferase activity. Interestingly, in the latest release of miRanda (January 2008) let-7e does not appear anymore as a potential regulator of the full-length isoform. Among the three miRNAs the strongest repression was observed with miR-185 (54% reduction), followed by miR-151-3p (20%) and miR-24 (10%).

Regarding pGL4.13-TR, the luciferase activity was significantly reduced by eight miRNAs (Fig.2b), all of which were predicted by at least one program: miR-128, miR-324-5p, miR-330, miR-485-3p, miR-509, miR-625, miR-765 and miR-768-5p. The most conspicuous inhibition was detected with miR-625 (62% reduction), miR-509 (47%) and miR-128 (32%), while with the other five miRNAs the percentage reduction ranged between 30% and 13%.

As for pGL4.13-BDNF, we could identify seven miRNAs that significantly inhibited the luciferase activity (Fig.2c): miR-1, miR-16, miR125b, miR-204, miR-206, miR-211 and miR-412; miR-125b was the only unpredicted one, however its homolog miR-125a, which shares the same seed region and only differs by having three extra nucleotides in the 3' moiety, was predicted by miRanda. The strongest reduction in luciferase activity was detected with miR-1 and miR-206 (31% and 38% respectively), while with the other miRNAs it ranged from 11% to 19%. Interestingly, miR-1 and miR-206 on the one hand and miR-204 and miR-211 on the other belong to the same miRNA families (i.e. share a common seed region), and the degrees of luciferase downregulation we observed indeed reflected their similarity.

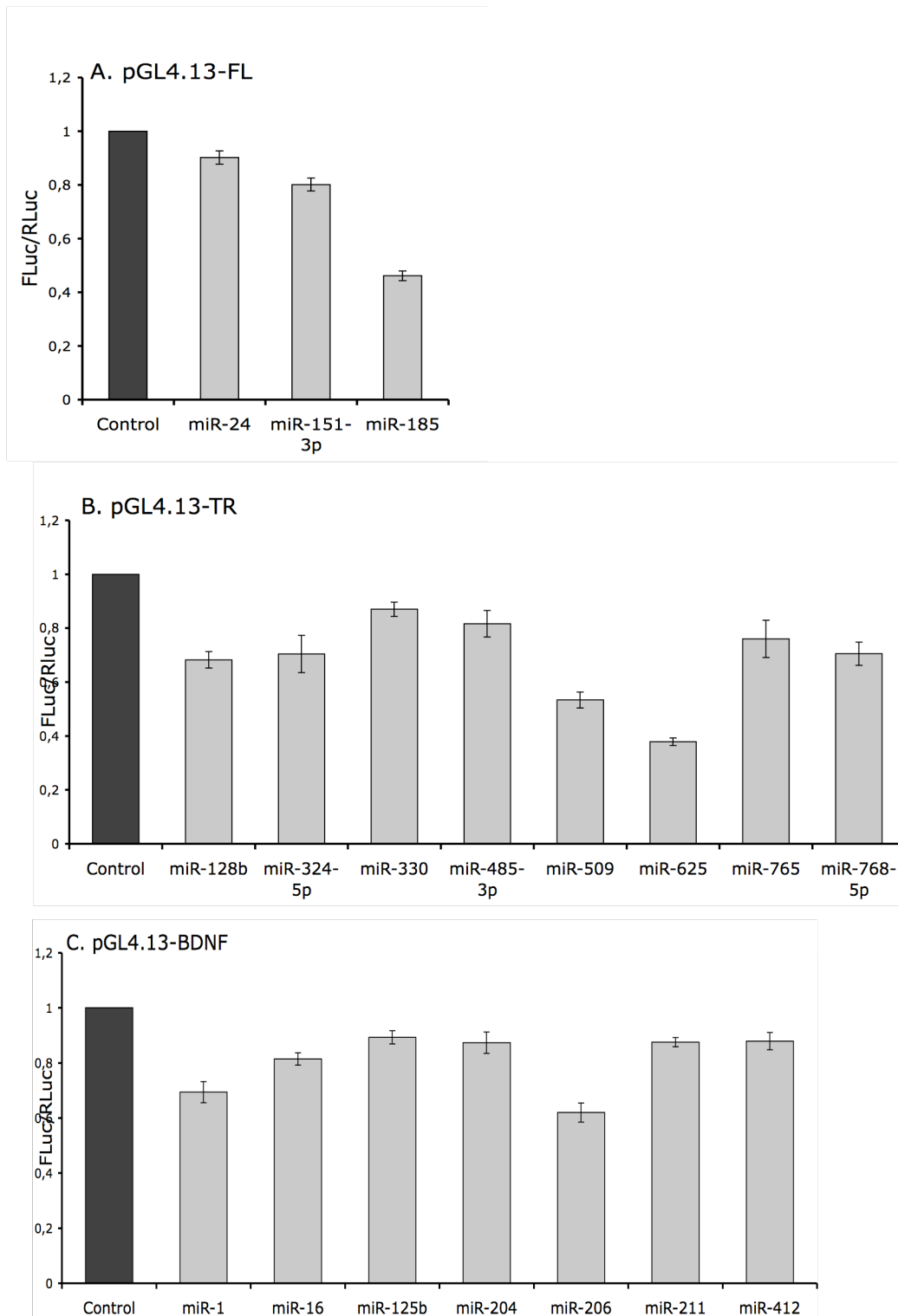


**Fig.2** Luciferase assay results. HeLa cells were cotransfected with pGL4.13-FL (A), pGL4.13-TR (B) or pGL4-BDNF (C) and the indicated miRNA mimics at a concentration of 10 nM. Luciferase activities were measured 24 hours after transfection; firefly luciferase activity was normalized to renilla luciferase activity, and results from at least three independent experiments are presented as means  $\pm$  SE ( $p < 0.05$ ).

The analysis of how many miRNAs were experimentally validated out of the predicted ones allowed us to evaluate the performance of the three computational methods; given that we are dealing with very small numbers, this can't be taken as an absolute estimation of the efficacy of each method, but can be useful as an indication of a tendency. The overall sensitivity (i.e. the rate of true positives) of the three programs, calculated over the two *NTRK3* isoforms and *BDNF* altogether, was 26% for miRanda, 41% for TargetScan and 40% for PicTar - having miRanda predicted a total of thirty-nine miRNAs, TargetScan thirty-four and PicTar only ten. The performance of the combination of the three algorithms was also assessed, taking into account only the miRNAs that were predicted by at least two programs (seventeen in total). As expected this restriction increased the sensitivity, which rose up to 53%. When considering only miRNAs that had more than one putative target site in the same 3'UTR, sensitivity resulted to be 44% with miRanda (four out of nine predicted miRNAs), 50% with TargetScan (six out of twelve) and 100% (two out of only two) with PicTar. Finally, for miRNAs predicted by at least two programs and with more than one putative target site (according to at least one program) sensitivity was 62% (five out of eight miRNAs in total).

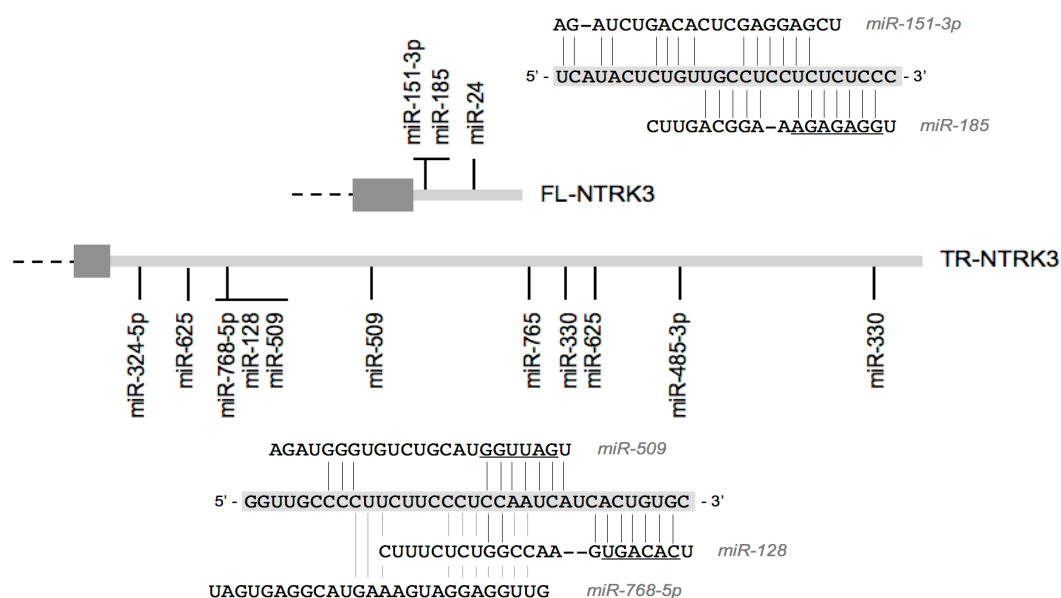


**Fig.3** Relative location of the target sequences of validated miRNAs in the 3'UTRs of FL-NTRK3 and TR-NTRK3. An enlargement of overlapping target sites is also shown, where sequence pairing to the 3'UTRs (lines) and miRNA seed regions (underlines) are indicated. The miR-24 target site corresponds to the minimum free energy hybridization according to RNAhybrid (see fig.4).

An overview of the relative positions of the validated miRNAs within the 3'UTRs of FL-NTRK3 and TR-NTRK3 is given in Fig.3. It is interesting to note that in the full-length isoform miR-151-3p and miR-185 have partially overlapping target sequences. Similarly, in the truncated isoform miR-128, miR-509 and miR-768-5p target the same region of the 3'UTR; in particular miR-509 and miR768-5p share part of seed region, while miR-128 has an independent seed but its 3' end overlaps with the seed regions of the other two miRNAs. This suggests that the binding of these miRNAs to their target sequences might be mutually exclusive.

Finding that miR-24 was able to downregulate the full-length isoform was particularly surprising and could appear contradictory, since miR-24 was not predicted to have putative target sites in this isoform by any of the interrogated computational methods. This is due to the lack of perfect complementarity between the 3'UTR of FL-NTRK3 and the seed region of miR-24. Perfect pairing to the seed is in fact the currently preferred method to predict and analyze miRNA targeting, but despite its importance and although it is actually estimated that seed sites may outnumber other sites by 10:1, a seed site is neither necessary nor sufficient for miRNA downregulation. miRNAs target sites can tolerate G:U wobbles within the seed region (Miranda et al., 2006) and extensive base pairing with the remainder of the miRNA may compensate missing complementarity of the 5' seed (Brennecke et al., 2005). We therefore looked for potential binding sites for miR-24 using RNAhybrid, a program that finds the energetically most favorable hybridizations of a small RNA to a large RNA (Rehmsmeier et al., 2004). RNAhybrid leaves perfect complementarity constraints in the 5' part of the miRNA as an option. As expected, if perfect match restrictions are applied no hybridizations can be found, but if the constraints are relieved the program indicates a number of potential target sites. The top hit of miR-24 is located at nucleotide position 78 to 101 of the 3'UTR of FL-NTRK3 and has a minimum free energy (mfe) of -28.1 kcal/mol (Fig.4).

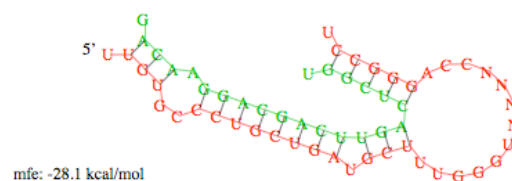


**Fig.4** Minimum free energy hybridization of miR-24 (green) and the 3'UTR of FL-NTRK3 (red, nucleotide positions 1726-1758 downstream of the stop codon). The computational modeling was done using the RNAhybrid software, without perfect complementarity constraints to the seed region of the miRNA.

## miRNAs targeting pGL4.13-TR do not act synergistically

Since multiple target sites in the same 3'UTR are thought to be cooperative and to increase the efficacy of miRNA inhibition (Doench et al., 2003), we analyzed whether the cotransfection of different miRNAs repressing pGL4-13-TR could lead to a more dramatic reduction in luciferase activity.

Thirteen combinations of two miRNAs (at equal concentration) were tested, and in no case we could detect a significant decrease in luciferase expression as compared to the corresponding miRNAs taken individually. The luciferase activity of cells transfected with miRNA pairs was in fact never lower than that observed with the miRNA causing the stronger reduction. As an example, some of the combinations tested are presented in Fig.5.

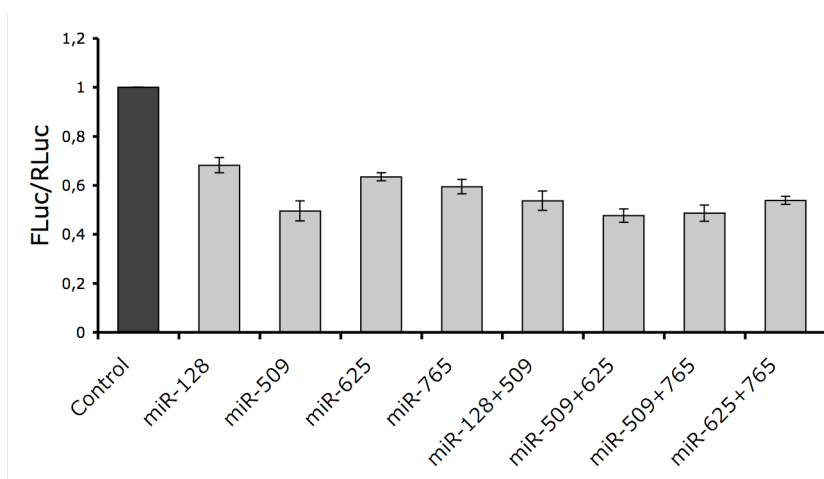


**Fig.5** pGL4.13-TR and miRNA combinations. Cells were cotransfected as explained in fig.2 with pGL4.13-TR and individual miRNA mimics (10 nM) or combinations of two different mimics (5 nM + 5 nM). Results from at least three independent experiments are presented as means  $\pm$  SE.

## 2. miRNA-mediated regulation of endogenous NTRK3

### Expression profile of FL-NTRK3 and TR-NTRK3 in SH-SY5Y cells

SH-SY5Y is a third generation neuroblastoma cell line; it is a subclone of the SK-N-SH line, which was originally established from a bone marrow biopsy of a neuroblastoma patient (Biedler et al., 1973), and has been widely used as a model to study neurodegenerative disorders such as Alzheimer and Parkinson's diseases.

SH-SY5Y cells express high levels of retinoic acid (RA) receptor (Lovat et al., 1993). RA is a potent regulator of morphogenesis, growth and cell differentiation and plays a major role in the nervous system. SH-SY5Y normally propagate via mitosis and divide continuously; upon exposure to RA they reduce their growth rate and differentiate by extending neurites into cells that are biochemically, ultrastructurally and electrophysiologically similar to neurons (Kaplan et al., 1993). RA treatment has as well been shown to induce the appearance of functional receptors of the Trk (NTRK) family in SH-SY5Y cells, including the full-length isoform of NTRK3 (Encinas et al., 1999); furthermore, a recent study has demonstrated that in another neuroblastoma cell line (SK-N-BE) the level of FL-NTRK3 increases during RA treatment while that of the truncated isoform decreases (Laneve et al., 2007). We therefore considered that SH-SY5Y cells could be a good system to study the regulation of NTRK3.

We characterized the expression of NTRK3 at different time points during RA exposure (untreated, day 3, day 6 and day 10) by Western blotting. Cells were treated with 10  $\mu$ M RA and, similarly to Laneve et al., we could observe an increase in the levels of the full-length isoform and conversely a decrease of the truncated isoform. The level of the full-length protein, almost undetectable in untreated cells, was  $\sim$ 2.5-fold higher after three days of RA treatment,  $\sim$ 4-fold higher after six days and reached up to  $\sim$ 8-fold after ten days. The expression of the truncated isoform on the other hand was reduced in the presence of RA by approximately 50% after three days of exposure, and kept decreasing very slightly through day 10 (Fig 6).

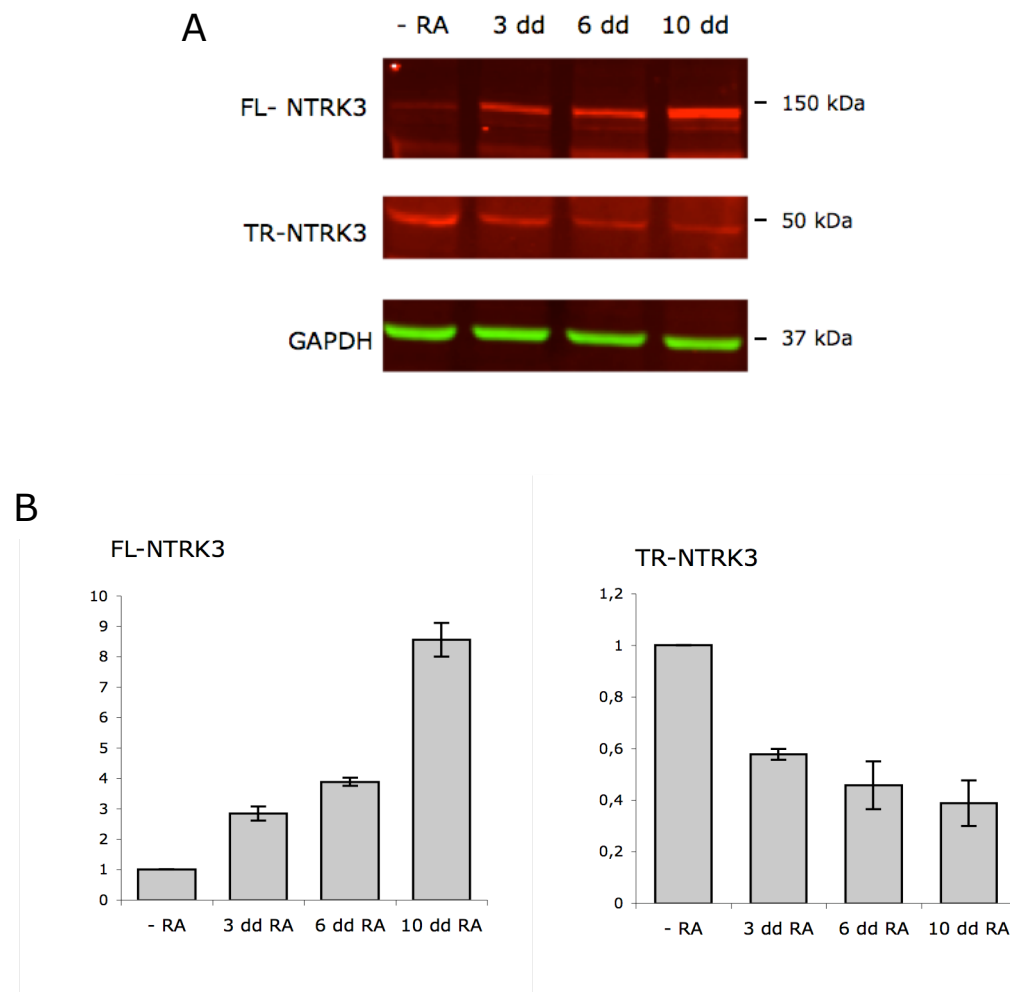


**Fig.6** Characterization of the expression of NTRK3 in RA-differentiated SH-SY5Y cells. A: Immunoblotting of the full-length and truncated isoforms of NTRK3 in SH-SY5Y cells treated with RA for the times indicated. GAPDH was used as a loading control. B: Protein levels were quantified by densitometry and are reported as arbitrary units relative to untreated cells.

## miRNA expression in HeLa and SH-SY5Y cells

miRNA expression in HeLa and SH-SY5Y cells was analyzed using custom 11k oligonucleotide microarrays (Agilent) including the 326 human miRNAs annotated in the miRbase sequence database release 7.1. The results for eight miRNAs regulating *NTRK3* according to the luciferase assays are shown in Fig.7, as a scale ranging from undetectable to strongly expressed estimated based on the hybridization signal intensity relative to background. miR-625, miR-765 miR-768-5p are not included as they had not yet been discovered at the time the experiment was performed. The expression levels of miR-9, miR-125a and b and miR-124a are also presented; the relevance of these miRNAs will be discussed later and the Discussion section.

**Table 2** miRNA expression in HeLa cells, untreated SH-SY5Y cells and differentiated SH-SY5Y cells (6 days RA exposure)

|            | HeLa | SH-SY5Y | SH-SY5Y (RA day 6) |
|------------|------|---------|--------------------|
| miR-9      | -    | -       | -                  |
| miR-24     | ++++ | +++++   | +++++              |
| miR-124    | -    | -       | -                  |
| miR-125a   | +    | +++     | ++++               |
| miR-125b   | ++   | +++     | ++++               |
| miR-128    | -    | +       | +                  |
| miR-151-3p | -    | -       | -                  |
| miR-185    | -    | -       | -                  |
| miR-324-5p | -    | -       | -                  |
| miR-330    | -    | +       | +                  |
| miR-485-3p | -    | +       | +                  |
| miR-509    | -    | -       | -                  |

Expression levels are indicated as a scale from undetectable (-) to strongly expressed (+++++)

## Validation of miRNA target predictions on endogenous NTRK3 by miRNA mimic overexpression

SH-SY5Y cells were used to investigate whether miRNAs causing a significant decrease in luciferase activity were also able to downregulate endogenous NTRK3. Given the expression profiles of the two protein variants in this cell line, we chose untreated cells to study the truncated isoform and RA-differentiated cells for the full-length isoform. miR-128, miR-324-5p, miR-330, miR-485-3p, miR-509, miR-625, miR-765 and miR-768-5p were therefore transfected into undifferentiated cells



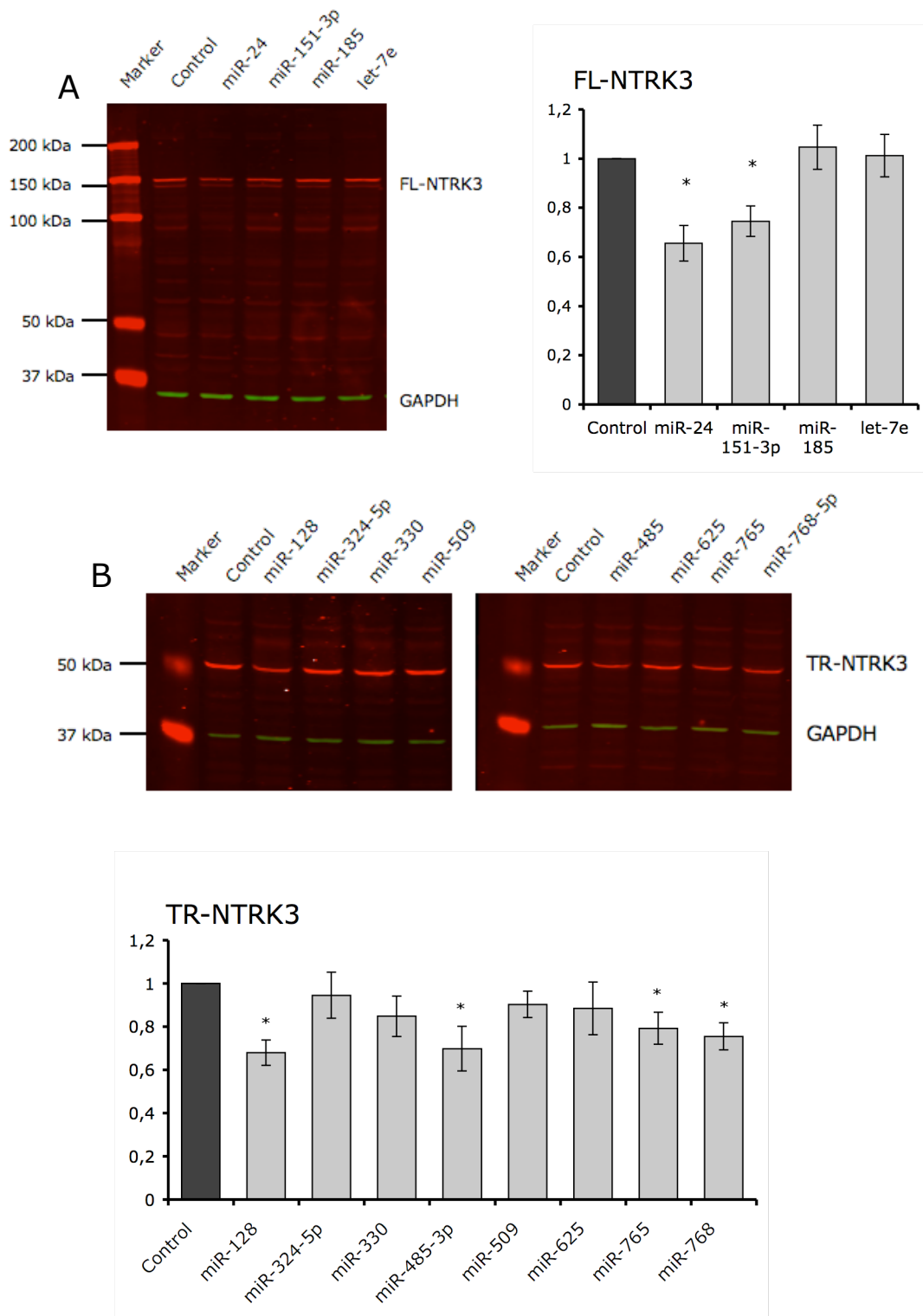


**Fig.7.** Western blot analysis of NTRK3 levels in cells transfected with the indicated miRNA mimics. RA-differentiated cells were transfected with miRNA mimics (100 nM) targeting FL-NTRK3 (A) and undifferentiated cells were transfected with mimics targeting TR-NTRK3 (B). In both cases protein levels were analyzed 72h after transfection and are reported relative to control cells. Data from four independent experiments are presented as means  $\pm$  SE (\* $p$ <0.05).

whereas miR-24, miR-151-3p and miR-185 were transfected into differentiated cells; let-7e, which was predicted to target the full-length isoform but caused no appreciable change in luciferase activity, was also tested in differentiated cells. Protein levels were assessed by Western blotting 72 hours after transfection (Fig.7). In agreement with the luciferase assay data, FL-NTRK3 levels were significantly reduced by miR-24 and miR-151-3p; a slight inhibition was also observed with miR-185, but it did not reach statistical significance. On the other hand no reduction was detected with let-7e, again in accordance with our previous results. The degrees of reduction varied compared to those observed in the luciferase assay: the strongest down-regulation was in fact obtained with miR-24 (41%), followed by miR-151-3p (34%).

With respect to the truncated isoform, a significant down-regulation ranging approximately between 20% and 30% was observed with miR-128, miR-485-3p, miR-765 and miR-768-5p; the strongest repression was observed with miR-128 (32% reduction) and with miR-485-3p (30%). The remaining four miRNAs (miR-324-5p, miR-330-3p, miR-509 and miR-625) caused a slighter reduction in the expression levels (maximum 15%), but none of them reached statistical significance.

In summary, these results confirm that endogenous FL-NTRK3 is regulated by miR-24 and miR-151-3p (two out of three miRNAs regulating the luciferase construct) whereas endogenous TR-NTRK3 is regulated by miR-128, miR-485-3p, miR-765 and miR-768-5p (four out of eight).

Although as previously mentioned the expression of these miRNAs is in general low in SH-SY5Y cells, we did a couple of pilot experiments using LNA<sup>TM</sup>-based antisense probes to inhibit endogenous miR-151-3p and miR-128 and see if this could cause an increase in NTRK3 levels. We could not detect changes in NTRK3 expression, probably due to the low endogenous levels.

Finally, in order to determine whether the regulation observed after overexpression of the six miRNAs occurs through mRNA cleavage or translational repression, we quantified the full-length and truncated *NTRK3* transcripts by real-time quantitative RT-PCR, using specific primers for the two isoforms. The mRNA levels were not affected by any of the six miRNAs, indicating that they may act by way of translational repression.

## miRNA-mediated repression of FL-NTRK3 affects downstream NT3-induced signaling

In order to investigate the possible physiological relevance of miRNA-mediated down-regulation of FL-NTRK3 we examined the effects of miRNA overexpression on NTRK3-induced signaling. We analyzed ERK1/2 phosphorylation as a readout for Ras/MAPK pathway activation; the Ras/MAPK pathway has been long known to be relevant for neuronal survival and differentiation and is activated upon stimulation of full-length NTRK (Trk) receptors having tyrosine kinase activity (Kaplan and Miller, 1997). In particular, NT3 has been shown to promote tyrosine phosphorylation of ERK1 and 2 in SH-SY5Y cells (Encinas et al., 1999).

RA-differentiated cells were transfected as previously described, serum-starved for 5 hours and then acutely stimulated with NT3; ERK1/2 phosphorylation was assessed by Western blotting using an anti-phospho-erk specific antibody. The total amount of ERK1 and 2 (phosphorylated and dephosphorylated) was probed with an anti-pan-ERK antibody and used as a loading control.

We could detect a reduction of ERK phosphorylation with miR-24 and miR-151-3p but not with miR-185, consistently with our previous results. The reduction was not very strong (10-15% approximately), but the basal phosphorylation in

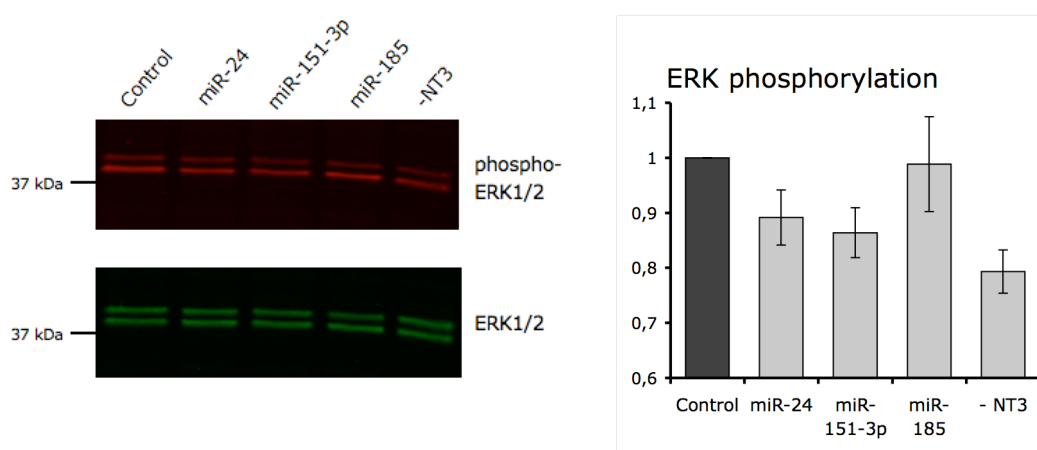


**Fig.8** Analysis of ERK1/2 phosphorylation after NT3 stimulation of cells transfected with the indicated miRNAs. Differentiated SH-SY5Y cells were transfected as explained before; 72 hours after transfection cells were serum-starved for 5 hours and stimulated with NT3 (30ng/mL) for 10 minutes. Phosphorylated ERK 1 and 2 were detected with a specific antibody and the membrane was then reprobbed with an anti-pan-ERK antibody; total ERK was used as a loading control. Phosphorylation levels are reported relative to control cells as means  $\pm$  SE (three independent experiments). The basal phosphorylation level in unstimulated cells is also shown (-NT3).

unstimulated cells level was already considerable (Fig.8, -NT3): this is probably the reason why we could not detect a broader difference. If we consider the miRNA-induced decrease in phosphorylation relative to the overall span between control and unstimulated cells, and take unstimulated cells as our virtual zero, the observed changes become substantial as with both miR-24 and miR-151-3p ERK phosphorylation decreases by over 50%. These experiments demonstrate that transfection of miR-24 and miR-151-3p in SH-SY5Y cells not only inhibits the expression of the full-length isoform of NTRK3 but also affects downstream NT3-induced signaling.

### **Effects of miR-128 and miR-509 overexpression in undifferentiated SH-SY5Y cells**

After transfection, cells were routinely examined under a phase-contrast microscope to check for possible alterations induced by the overexpression of the different miRNAs. While in most cases there was no appreciable alteration, considerable changes in the appearance of SH-SY5Y cells were observed after transfection with miR-128 and miR-509. Although in different ways, both miRNAs seemed to affect cell morphology and/or distribution as well as the total number of cells (Fig.9). In the case of miR-128 cells were evenly scattered over the culture plate and acquired rounded bodies with short neurites; the overall cell size looked smaller than control cells and the culture confluence appeared to be higher, suggesting a possible increase in the total number of cells. On the other hand, cells transfected with miR-509 tended to form aggregates and gather in clusters, which resulted in an uneven distribution over the plate; furthermore, by simple observation the number of cells seemed to be remarkably lower compared to the control, even if we could not detect an abnormal amount of dead cells in any of the manipulation steps.

Given that miR-128 considerably downregulated TR-NTRK3, it was reasonable to speculate that the repression of this variant could be responsible for at least part of the observed effects. To test this hypothesis we used an siRNA directed against TR-NTRK3 (designed and provided by Gene Link), which targeted an isoform-specific sequence located within the 3'UTR region (starting at nucleotide position 3433 of the mRNA sequence). We transfected undifferentiated cells with the siRNA and a non-silencing negative control and confirmed by Western blotting that the siRNA was able to effectively silence TR-NTRK3; the protein level decreased by

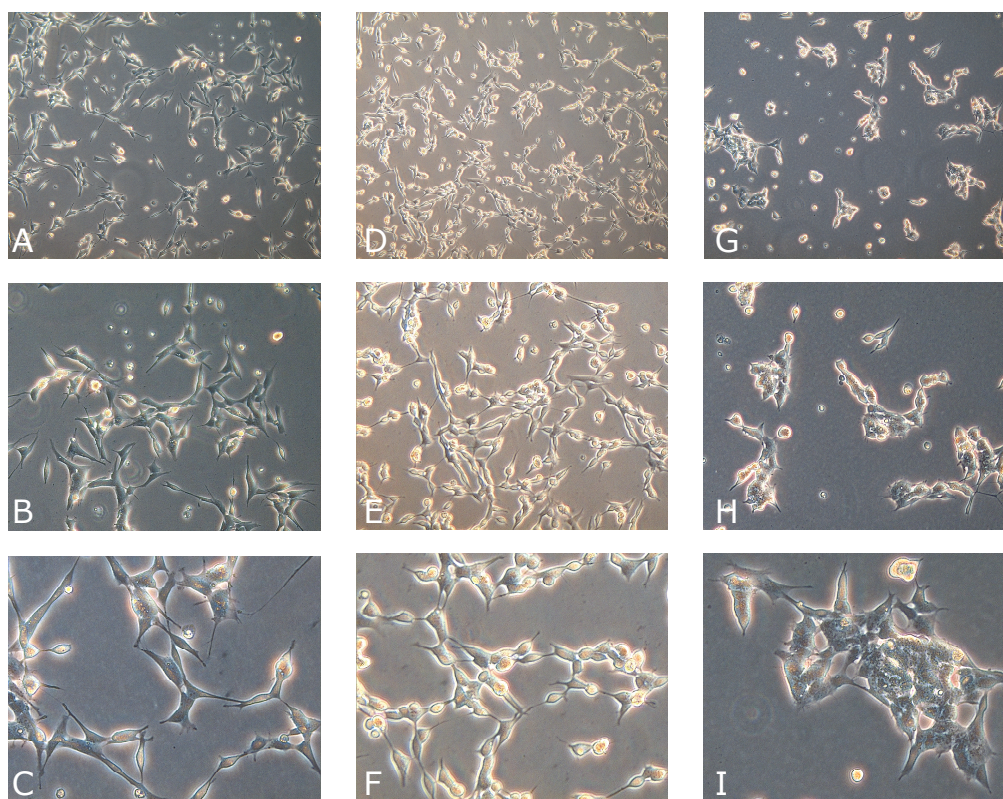


**Fig.9** Phase-contrast micrographs of undifferentiated SH-SY5Y cells transfected with miR-128 and miR-509, at increasing magnifications. Cells were transfected as described before with 100 nM non-targeting control (A,B,C), miR-128 (D,E,F) and miR-509 (G,H,I). Images were taken 72 hours after transfection.

approximately 25% relative to the negative control (data not shown), a degree of reduction comparable to that observed with miR-128. Interestingly, the morphology of cells 72 hours after transfection was similar to that described for miR-128 (Fig.10). These results support the hypothesis that the miR-128-mediated repression of TR-NTRK3 may contribute to the altered morphological phenotype; however, as each miRNA can have hundreds of different targets, this does not exclude the contribution of other genes whose expression is regulated by miR-128 and which may play a role in the observed changes.

Although less clearly, cells transfected with miR-485-3p as well seemed to be in the process of acquiring a rounded shape, but the effect was less evident than with miR-128; it is interesting that these two miRNAs are exactly the ones that cause the strongest repression of the truncated isoform in SH-SY5Y undifferentiated cells.

In order to quantify the changes in cell numbers, cells were counted using a Coulter cell and particle counter 72 hours after transfection with miR-128, miR-509,



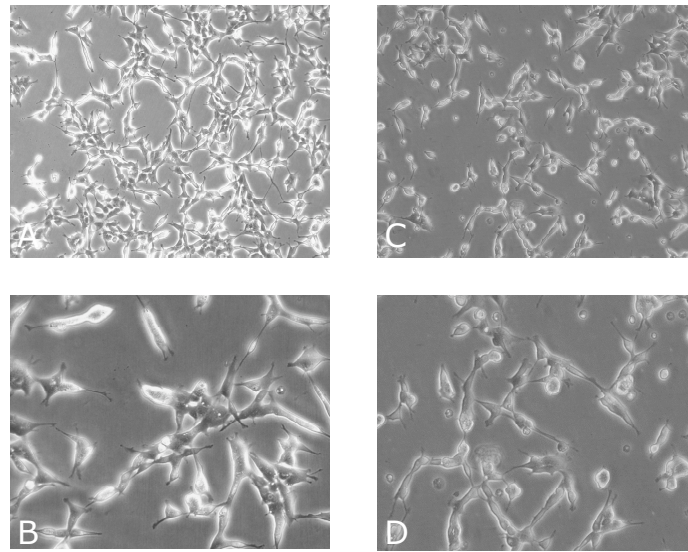


**Fig. 10** Phase-contrast micrographs of undifferentiated SH-SY5Y cells transfected with a non-silencing siRNA (A,B) and with an siRNA directed against the truncated isoform of NTRK3 (C,D), at increasing magnifications. Cells were transfected as previously described with 100 nM small RNA and images were taken 72 hours after transfection.

the TR-NTRK3-specific siRNA and the respective negative controls (Fig.11): with miR-128 the total number of cells was 27% higher compared to the control, whereas the siRNA caused a reduction of approximately 20% in total cell number. This suggests that the morphological changes observed with miR-128 may indeed be a consequence of the repression of the truncated isoform of NTRK3, whereas the variation in cell number could be due to some off-target effect of the miRNA. On the other hand, no significant change could be detected with miR-509, indicating that the apparent decrease in cell number is due to their agglomerating together, rather than to a real reduction.

Cells transfected with miR-128 and with miR-509 were also analyzed by flow cytometry to evaluate whether the visible changes in the morphology of cells were accompanied by a variation of their actual volume and/or if the complexity of the cytoplasm was altered. A two-parameter forward/side scatter (FSC/SSC) flow cytometry was performed, revealing no shift of the population with either miR-128 or miR-509. This indicates that there is no variation of the actual size or complexity of cells and that the observed morphological changes are due to other factors, as could be for example an alteration of the adhesive and motility properties of the cell. Fig.12 shows the forward-scatter parameter (FSC, proportional to the cell size) plotted against the side-scatter parameter (SSC, which relates to the granularity of the cell).

Finally, we performed an MTT assay to check whether miR-128 and miR-509 overexpression could affect mitochondrial activity or cell viability. Cells were analyzed 24, 48, 72 and 96 hours after transfection revealing no appreciable alteration.

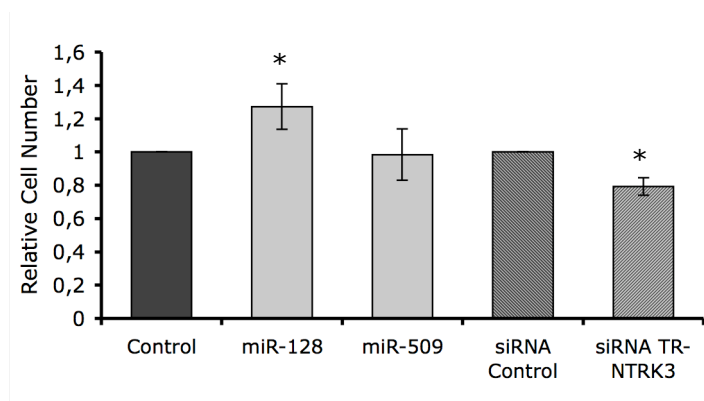


**Fig.11** Cell counting. Undifferentiated SH-SY5Y cells were transfected with miR-128, miR-509, a TR-NTRK3-specific siRNA and the corresponding negative controls; 72 hours after transfection cells were trypsinized, resuspended in the appropriate buffer and passed through a Coulter cell counter. Results from three independent experiments are reported as means  $\pm$  SE, relative to the respective controls (\* $p < 0.05$ ).

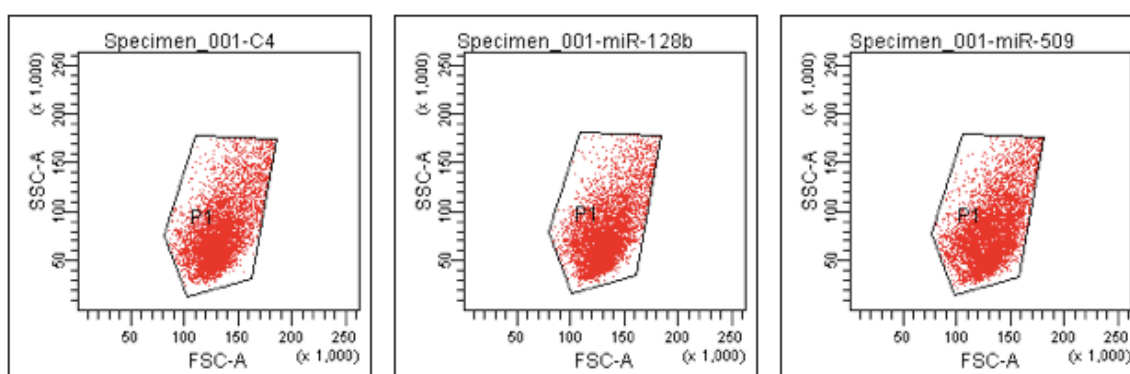


**Fig.12** Two-parameter forward/side scatter (FSC/SSC) flow cytometry analysis of SH-SY5Y cells transfected with a non-targeting control, miR-128 and miR-509.control. No profile shift was observed.

## Expression profiles of miR-128 and miR-509 in different human tissues and in SH-SY5Y cells

miR-128 is a brain-enriched miRNA, whose expression has been shown to correlate and increase with neuronal differentiation (Sempere et al., 2004) (Smirnova et al., 2005). Furthermore, accumulation of miR-128 has been detected in the hippocampus of Alzheimer's disease brains (Lukiw, 2007). On the other hand very little is known about miR-509; as of this writing, the only published information available reports that it is expressed in testis (Novotny et al., 2007). We analyzed the expression of miR-128 and miR-509 in different human organs by real-time quantitative RT-PCR using TaqMan<sup>®</sup> miRNA assays (Fig.13); total RNAs from adult brain, colon, heart, kidney, liver, lung, ovary, skeletal muscle, spleen, testis, thymus and from placenta were obtained from Stratagene. The analysis showed that, as expected, miR-128 is highly expressed in brain; high levels - comparable to that of the endogenous control - were also detected in skeletal muscle, followed by thymus and kidney. On the other hand miR-509 resulted to be highly expressed in

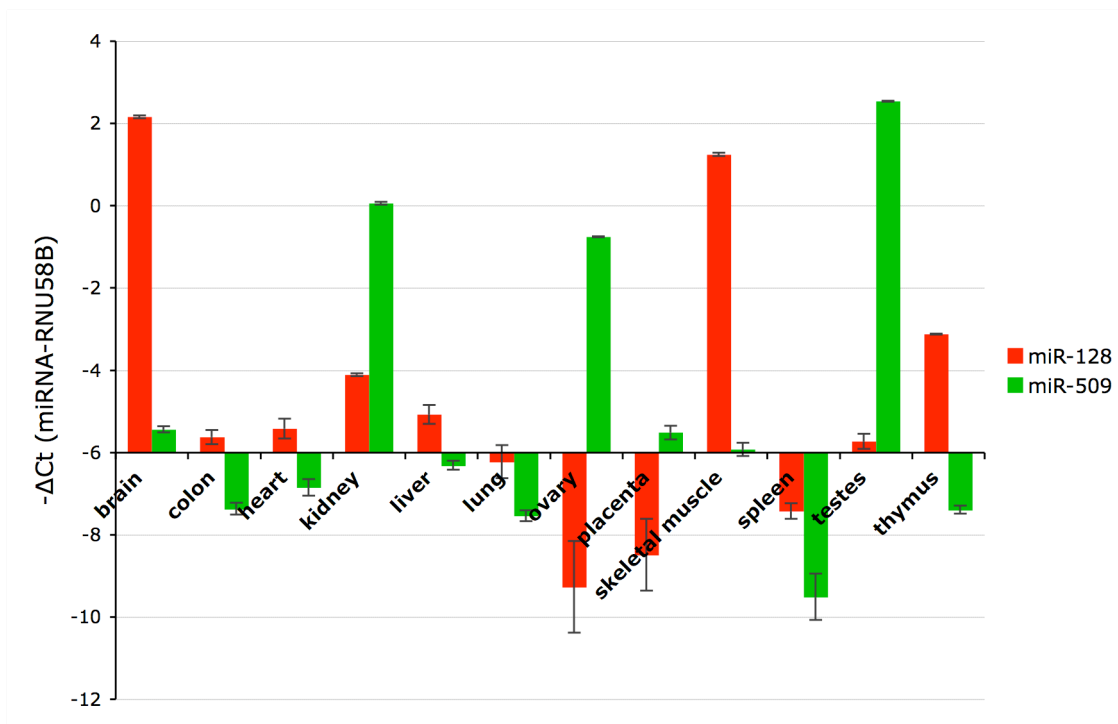


**Fig.13** Real-time RT-PCR analysis of miR-128 and miR-509 in different human tissues, (TaqMan<sup>®</sup> miRNA assays). Small nucleolar RNA RNU58B was used as an endogenous control for normalization. Results are reported as  $-\Delta C_t$ s between each miRNA and the endogenous control ( $\Delta C_t$ s are shown with a minus sign as lower  $\Delta C_t$ s indicate higher miRNA expression).  $\Delta C_t=0$  corresponds to the expression level of RNU58B in each sample.



testis, which is consistent with the available information; furthermore, its levels are also high in kidney and ovary.

We also examined the expression of miR-128 and miR-509 in SH-SY5Y cells at different stages of RA treatment. Both miRNAs showed low levels of expression in this system, with crossing point (Ct) values of approximately 34 in undifferentiated cells (as opposed to the Ct~25 observed for miR-128 in brain). However, although the overall levels remained low, we could detect an increase of miR-128 expression and a decrease of miR-509 during RA-mediated differentiation (Fig.14).

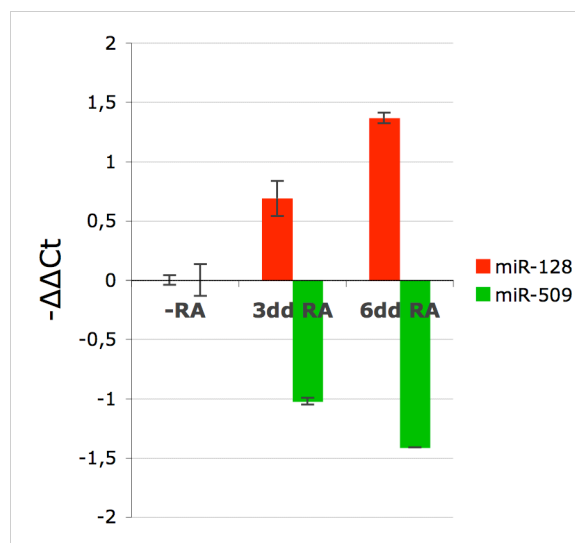


**Fig.14** Real-time RT-PCR analysis of miR-128 and miR-509 in SH-SY5Y cells during RA-mediated differentiation. In this case results are reported as  $-\Delta\Delta C_t$ s relative to untreated cells:  $\Delta\Delta C_t$ s represent the difference between the  $\Delta C_t$  of each sample and the  $\Delta C_t$  of the reference sample (-RA).

### 3. Effects of miR-128 and miR-509 overexpression on the transcriptome of SH-SY5Y cells

To further characterize the consequences of miR-128 and miR-509 overexpression in SH-SY5Y cells we performed a whole-genome expression analysis using microarrays. Total RNA was extracted from undifferentiated cells transfected with miR-128, miR-509 and two negative controls, 72 hours after transfection. Four independent experiments were hybridized using Illumina's HumanRef-8 v3.0 expression beadchips, which target approximately 24500 well-annotated RefSeq transcripts; hybridization data were then analyzed using the Array File Maker (AFM) 4.0 software package (Breitkreutz et al., 2001). Considering a fold-change (FC) cutoff of 1.2 and a q-value <5, we could identify a total of 183 deregulated genes upon miR-128 overexpression, 116 of which were down-regulated and 67 up-regulated, and a total of 751 deregulated genes upon miR-509 overexpression, 480 of which were down-regulated and 271 up-regulated. In the case of miR-128 the

maximum fold-change was approximately 1.8 for up-regulated genes and -2 for down-regulated genes, whereas in the case of miR-509 genes were deregulated by up to 3-fold in both directions. The top ten upregulated and downregulated genes for the two miRNAs are listed in Tables 3 and 4. The differences in the total number of deregulated genes as well as in the overall degree of deregulation are consistent with the expression patterns of the two miRNAs: miR-128 is in fact a brain-enriched miRNA; it is thus reasonable that its overexpression can have less dramatic consequences than the overexpression of miR-509, which is not normally expressed in the nervous system.

### **Overlapping between miRNA target predictions and deregulated genes**

Microarray results were compared to target predictions for miR-128 and miR-509, in order to check whether some of the deregulated genes could be potential direct targets of the two miRNAs; such genes would probably undergo miRNA-mediated regulation through mRNA cleavage rather than translational repression.

We analyzed the intersection of the genes deregulated according to the array experiment and the putative target genes predicted by miRanda and TargetScan. In the case of miR-128, 31 genes predicted by miRanda were deregulated (2.7% out of a total of 1144 predicted genes) and 38 genes predicted by TargetScan (5.7% out of 669); as expectable, in both cases there was a huge predominance of downregulation, with only 4 upregulated and 27 downregulated genes out of 31 predicted by miRanda, and just one upregulated gene and 37 downregulated out of 38 predicted by TargetScan. For miR-509, the overlap was 83 genes out of 1221 (6.8%) predicted by miRanda and 28 out of 106 (26.4%) predicted by TargetScan. In this case as well, only 10 out of 83 miRanda genes and none of the TargetScan genes were upregulated. The overlap with TargetScan predictions is shown in Table 5.

**Table 3** Top ten upregulated and downregulated genes upon overexpression of miR-128 in SH-SY5Y cells.

| GENE SYMBOL     | GENE NAME                                                                                | FC     | FUNCTION                                                                                                                                                                                                                  |
|-----------------|------------------------------------------------------------------------------------------|--------|---------------------------------------------------------------------------------------------------------------------------------------------------------------------------------------------------------------------------|
| <i>DYNC1I1</i>  | Dynein, Cytoplasmic 1, Intermediate chain 1                                              | 1.781  | microtubule-based vesicular trafficking; retrograde axonal transport of signaling endosomes containing neurotrophins and associated downstream kinases                                                                    |
| <i>HMGCS1</i>   | 3-hydroxy-3-methylglutaryl-Coenzyme A Synthase 1                                         | 1.728  | lipogenesis and biosynthesis of cholesterol                                                                                                                                                                               |
| <i>BCL2</i>     | B-cell CLL/Lymphoma 2                                                                    | 1.689  | regulation of cell death and caspase activity; antiapoptotic                                                                                                                                                              |
| <i>CREB3L2</i>  | cAMP Responsive Element Binding protein 3-like 2                                         | 1.652  | transcription factor of the CREB3 family; astrocyte proliferation in response to inflammation and trauma (gliosis)                                                                                                        |
| <i>TRAF3IP2</i> | TRAF3 Interacting Protein 2 (AKT1)                                                       | 1.558  | activation of the transcription factor NFkB; implicated in malignant processes and in the regulation of the apoptotic response; mediates the antiapoptotic effect of TGF-beta and TNF-alpha                               |
| <i>ISLR2</i>    | Immunoglobulin Superfamily containing Leucine-rich Repeat 2                              | 1.544  | integral membrane protein                                                                                                                                                                                                 |
| <i>KLF6</i>     | Krüppel-like Factor 6                                                                    | 1.544  | zinc finger transcription factor; adipogenesis and inhibition of cellular growth                                                                                                                                          |
| <i>PRICKLE1</i> | Prickle homolog 1, Drosophila                                                            | 1.508  | may regulate neurite formation during brain development                                                                                                                                                                   |
| <i>ADIPOR1</i>  | Adiponectin Receptor 1                                                                   | 1.504  | component of the energy homeostatic mechanism; increases fatty acid oxidation and glucose uptake; may participate in the control of food intake and higher brain functions                                                |
| <i>PRSS3</i>    | Protease, Serine 3                                                                       | 1.498  | encodes mesotrypsin, a brain-specific trypsin form thought to protect neural cells from apoptotic cell death                                                                                                              |
| <i>TMSB10</i>   | Thymosin Beta 10                                                                         | -1.583 | organization of the cytoskeleton, cell motility and spreading: binds to actin monomers and inhibits actin polymerization; anti-apoptotic action in chick embryo motoneurons                                               |
| <i>TRAPPC4</i>  | Trafficking Protein Particle Complex 4 (synbindin)                                       | -1.589 | vesicular transport from endoplasmic reticulum to golgi; possible role in postsynaptic membrane trafficking                                                                                                               |
| <i>G6PC3</i>    | Glucose 6 Phosphatase Catalytic 3                                                        | -1.595 | regulation of glucose homeostasis: catalyzes hydrolysis of G6P to glucose and phosphate                                                                                                                                   |
| <i>VPB1</i>     | Von Hippel-Lindau Binding Protein 1                                                      | -1.617 | chaperone protein; maturation of the cytoskeleton and morphogenesis; possible role in the transport and correct localization of the tumor suppressor von Hippel-Lindau (VHL) protein                                      |
| <i>NGFRAP1</i>  | Nerve Growth Factor Receptor Associated Protein 1                                        | -1.637 | p75NTR-associated protein; mediates apoptosis in response to NGF                                                                                                                                                          |
| <i>PKIA</i>     | Protein Kinase (cAMP-dependent, catalytic) Inhibitor Alpha                               | -1.699 | PKA inhibition                                                                                                                                                                                                            |
| <i>YWHAB</i>    | Tyrosine 3-monooxygenase/tryptophan 5-monooxygenase activation protein, beta polypeptide | -1.713 | member of the brain-abundant 14-3-3 protein family; may play a role in linking mitogenic signaling and the cell cycle machinery                                                                                           |
| <i>PAIP2</i>    | PABP-interacting protein 2                                                               | -2.034 | translational repressor; acts on VEGF (Vascular Endothelial Growth Factor)                                                                                                                                                |
| <i>CHGB</i>     | Chromogranin B                                                                           | -2.050 | secretory protein expressed in neuronal cells; guides and sorts the secretion of neuropeptides                                                                                                                            |
| <i>TROVE2</i>   | TROVE domain family, member 2                                                            | -2.069 | RNA-binding protein; major autoantigen in patients suffering from autoimmune diseases; binds small RNAs of unknown function (Y RNAs) and misfolded noncoding RNAs; possible function in the degradation of defective RNAs |

**Table 4** Top ten upregulated and downregulated genes upon overexpression of miR-509 in SH-SY5Y cells.

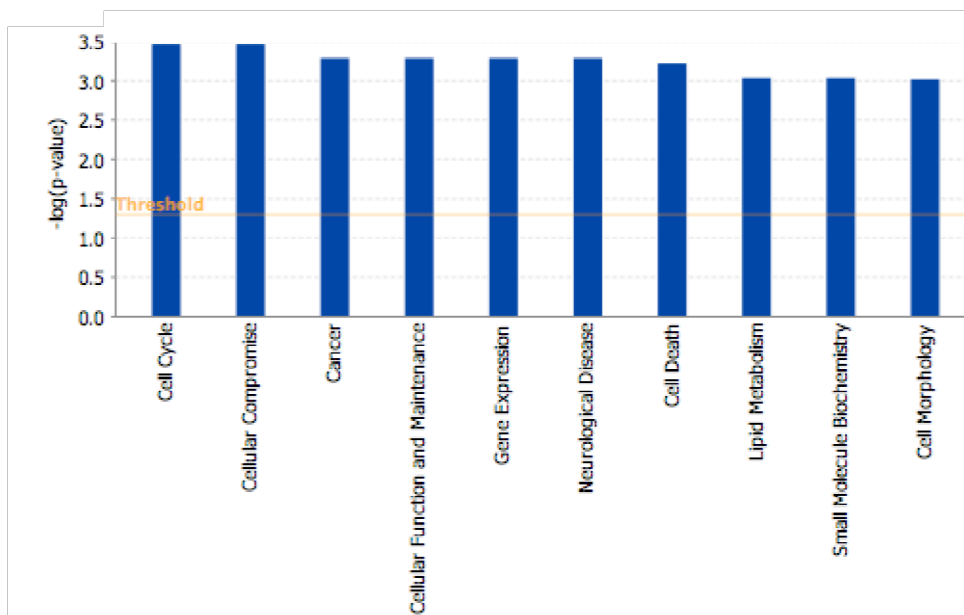
| GENE SYMBOL    | GENE NAME                                                          | FC     | FUNCTION                                                                                                                                                                                                                                    |
|----------------|--------------------------------------------------------------------|--------|---------------------------------------------------------------------------------------------------------------------------------------------------------------------------------------------------------------------------------------------|
| <i>H19</i>     | H19, imprinted maternally expressed transcript, non-protein coding | 3.165  | maternally expressed non-coding mRNA; strongly expressed during embryogenesis; influences cell growth; putative tumor suppressor gene                                                                                                       |
| <i>CDKN1C</i>  | Cyclin-dependent Kinase Inhibitor 1C                               | 3.100  | strong inhibitor of several G1 cyclin/CDK complexes; negative regulator of cell proliferation                                                                                                                                               |
| <i>DOK4</i>    | Docking protein 4                                                  | 2.546  | adaptor protein; associates with the GDNF receptor RET and mediates signal transduction, critical for neuronal differentiation                                                                                                              |
| <i>CDKN1A</i>  | Cyclin-dependent Kinase Inhibitor 1A                               | 2.495  | inhibitor of cyclin-CDK2 or -CDK4 complexes; regulator of cell cycle progression at G1; mediates p53-dependent G1 phase arrest in response to a variety of stress stimuli; regulatory role in S phase DNA replication and DNA damage repair |
| <i>EEF1A2</i>  | Eukaryotic translation Elongation Factor 1 Alpha 2                 | 2.289  | monomeric GTPase involved in protein synthesis; possible role in actin bundling, cell cycle regulation and apoptosis                                                                                                                        |
| <i>NRP1</i>    | Neuropilin 1                                                       | 2.007  | membrane-bound receptor; mediates the response to VEGF and semaphorins; role in angiogenesis, axon guidance, cell survival, migration and invasion                                                                                          |
| <i>PFKFB4</i>  | 6-phosphofructo-2-kinase/fructose-2,6-biphosphatase 4              | 1.921  | glycolytic regulator; synthesis and degradation of fructose 2,6-bisphosphate                                                                                                                                                                |
| <i>BCAR3</i>   | Breast Cancer anti-estrogen Resistance 3 (AND-34)                  | 1.900  | guanyl-nucleotide exchange (GEF) factor; causes estrogen-independent proliferation in human breast cancer cells                                                                                                                             |
| <i>CALCA</i>   | Calcitonin-related polypeptide Alpha                               | 1.857  | peptide hormone synthesized by the parafollicular cells of the thyroid; causes reduction in serum calcium                                                                                                                                   |
| <i>GPR64</i>   | G protein-coupled receptor 64                                      | 1.835  | adhesion G protein-coupled receptor; specifically expressed in the epididymis ductal systems involved in spermatozoon maturation                                                                                                            |
| <i>NAV2</i>    | Neuron navigator 2                                                 | -2.197 | RA-responsive gene; role in neurite outgrowth and axonal elongation possibly by facilitating interactions between microtubules and neurofilaments                                                                                           |
| <i>ADAMTS9</i> | ADAM metalloproteinase with Thrombospondin type 1 motif, 9         | -2.208 | member of the ADAMTS protein family; implicated in the cleavage of proteoglycans, control of organ shape during development, and inhibition of angiogenesis                                                                                 |
| <i>POPDC2</i>  | Popeye Domain Containing 2                                         | -2.230 | membrane associated protein; predominantly expressed in skeletal and cardiac muscle                                                                                                                                                         |
| <i>NCALD</i>   | Neurocalcin Delta                                                  | -2.233 | calcium-binding protein; possible regulator of G protein-coupled receptor signal transduction; binds to clathrin, tubulin and actin following Ca <sup>++</sup> elevation                                                                    |
| <i>NETO2</i>   | Neuropilin and Tolloid-like 2                                      | -2.242 | predicted transmembrane protein; contains a motif that in other proteins is essential for the internalization of clathrin coated pits during endocytosis                                                                                    |
| <i>RAB5C</i>   | Ras-associated protein 5C                                          | -2.261 | small GTPase involved in the early endocytic pathway; upregulated in postmortem hippocampal tissue of AD patients                                                                                                                           |
| <i>CTSC</i>    | Cathepsin C                                                        | -2.272 | lysosomal cysteine proteinase; activation of many serine proteinases in immune/inflammatory cells                                                                                                                                           |
| <i>SYT4</i>    | Synaptotagmin IV                                                   | -2.705 | calcium-dependent exocytosis, including neurotransmitter release                                                                                                                                                                            |
| <i>FAM62B</i>  | Family with sequence similarity 62 member B                        | -2.801 | NA                                                                                                                                                                                                                                          |
| <i>DDAH1</i>   | dimethylarginine dimethylaminohydrolase 1                          | -3.073 | nitric oxide generation                                                                                                                                                                                                                     |

**Table 5** Overlapping between target predictions (TargetScan) for miR-128 (left) and miR-509 (right) and deregulated genes.

| miR-128         |       |                 |       | miR-509         |       |
|-----------------|-------|-----------------|-------|-----------------|-------|
| GENE            | FC    | GENE            | FC    | GENE            | FC    |
| <i>TROVE2</i>   | -2,07 | <i>PHB</i>      | -1,27 | <i>RAB5C</i>    | -2,26 |
| <i>PAIP2</i>    | -2,03 | <i>PPAP2B</i>   | -1,26 | <i>ESRRG</i>    | -1,99 |
| <i>YWHAB</i>    | -1,71 | <i>ATP6V1A</i>  | -1,25 | <i>TWIST1</i>   | -1,96 |
| <i>PKIA</i>     | -1,70 | <i>STAG1</i>    | -1,21 | <i>PBX3</i>     | -1,90 |
| <i>NGFRAP1</i>  | -1,64 | <i>PRKX</i>     | -1,21 | <i>ARHGAP1</i>  | -1,89 |
| <i>C1orf144</i> | -1,62 | <i>RPS6KB1</i>  | -1,16 | <i>XPR1</i>     | -1,89 |
| <i>NGFRAP1</i>  | -1,61 | <i>CABLES2</i>  | -1,14 | <i>SYNE2</i>    | -1,79 |
| <i>TMSB10</i>   | -1,58 | <i>EIF2S2</i>   | -1,13 | <i>SF3B4</i>    | -1,72 |
| <i>UBE2E2</i>   | -1,58 | <i>RGL2</i>     | -1,10 | <i>RKHD2</i>    | -1,66 |
| <i>SEC61A1</i>  | -1,56 | <i>SH3BGRL2</i> | 1,34  | <i>RYBP</i>     | -1,66 |
| <i>GLTP</i>     | -1,53 |                 |       | <i>PTEN</i>     | -1,64 |
| <i>VANGL2</i>   | -1,52 |                 |       | <i>GTF3C2</i>   | -1,53 |
| <i>C12orf34</i> | -1,51 |                 |       | <i>ZNF423</i>   | -1,50 |
| <i>UBE2N</i>    | -1,50 |                 |       | <i>RAP2A</i>    | -1,47 |
| <i>CASC3</i>    | -1,49 |                 |       | <i>SNAP91</i>   | -1,46 |
| <i>DCUN1D4</i>  | -1,48 |                 |       | <i>OSBP</i>     | -1,43 |
| <i>WDR68</i>    | -1,46 |                 |       | <i>DEDD</i>     | -1,42 |
| <i>RNF144</i>   | -1,46 |                 |       | <i>VKORC1L1</i> | -1,39 |
| <i>PPP1CC</i>   | -1,44 |                 |       | <i>ZFAND3</i>   | -1,35 |
| <i>DAZAP2</i>   | -1,43 |                 |       | <i>BCAR1</i>    | -1,25 |
| <i>FBXO33</i>   | -1,43 |                 |       | <i>ARID1A</i>   | -1,23 |
| <i>VPS4B</i>    | -1,43 |                 |       | <i>ST3GAL2</i>  | -1,19 |
| <i>PDHX</i>     | -1,41 |                 |       | <i>USP47</i>    | -1,15 |
| <i>SLC39A11</i> | -1,41 |                 |       | <i>PHLPP1</i>   | -1,15 |
| <i>ZZZ3</i>     | -1,30 |                 |       | <i>RAD9A</i>    | -1,14 |
| <i>E2F7</i>     | -1,28 |                 |       | <i>ENPP2</i>    | -1,12 |
| <i>GPAM</i>     | -1,28 |                 |       | <i>COLEC12</i>  | -1,08 |
| <i>PDIA5</i>    | -1,28 |                 |       | <i>DEDD</i>     | -1,07 |

## Analysis of deregulated pathways

The two sets of genes deregulated by the overexpression of miR-128 and miR-509 and the corresponding expression values were uploaded into the Ingenuity Pathway Analysis software (IPA 6.3, Ingenuity Systems, Redwood City, CA); the IPA software allows to analyze the association of a set of genes with a given biological process or pathway, according to the Ingenuity Pathways Knowledge Base. The program was interrogated about the biological functions, canonical pathways and molecular networks that could be affected by the deregulation induced by miR-128 and miR-509; the statistical significance of the associations was calculated with the right-tailed Fisher's Exact Test (p-value threshold = 0.05).



| ID | Molecules in Network                                                                                                                                                                                                                                                                                                 | Top Functions                                                      |
|----|----------------------------------------------------------------------------------------------------------------------------------------------------------------------------------------------------------------------------------------------------------------------------------------------------------------------|--------------------------------------------------------------------|
| 1  | ↑AKAP13, ↑BAG3, ↑BCL2, ↓BMI1, ↓CBFB, ↑CDKN2D, ↓CHGB, ↓CYB561*,<br>↓DAZAP2 (includes EG:9802), ↓E2F7, ↑ETS1, ↑ETV4*, ↑GNA12, ↑GOT2, ↑GPAM, Hsp70, IFN Beta,<br>IKK, Interferon alpha, Jnk, ↑MAP4K2, NFkB, P38 MAPK, ↓PAIP2, ↓PHB, ↓PHC2, ↑PLAUR, Proteasome,<br>Rb, ↑SNAP91, ↓TBK1, ↑TRAF3IP2, ↓UBE2N, ↓VANGL2, Vegf  | Cancer, Gene Expression, Neurological Disease                      |
| 2  | ↑ADIPOR1, Afar, ↓AKR7A2, ↓AKR7A3, Akt, Ap1, ↓APEX1*, APPL1, ↑CBLB, ↓CHRNA3, ↑CYP2J2,<br>↓DAP3, ↑FASN, ↓GPAM, ↑HK1, ↑HMGC51, Hsp90, Insulin, ↑KLF6, mannose, Mapk, NEU3,<br>Oxidoreductase, PDGF BB, ↓PDIA5, ↑PPAP2B, SCAP, ↑SECISBP2, ↑SEPW1, SH2B2, ↑STX6, ↓TXNIP,<br>TXNRD1, VAMP4, WWOX                           | Lipid Metabolism, Molecular Transport, Small Molecule Biochemistry |
| 3  | ↓ATP6V1A, BRF1, ↑CALM1, CHRN81, ↑CLDN15, ↑DEXI, EMP3, ERBB2, ↓GPAM, IL15,<br>↑IRX3 (includes EG:79191), MXI1, MYBL1, MYC, MYCBP2, MYO9B, NFYB, ↑NGFRAP1*, ↓NME4, NOSIP,<br>↑P4HA2, ↓PAICS*, PFDN4, PFDN5, POLD1, PPP2R5A, ↑PRSS3 (includes EG:5646), ↓SEC61A1, ↑SIPA1,<br>↓SPINK4, TJP2, ↓VBP1, VCAM1, ↓VPS4B, ZAP70 | Cancer, Reproductive System Disease, Tumor Morphology              |

**Fig.15** Most significant biological functions (top) and molecular networks (bottom) associated with the overexpression of miR-128, according to the Ingenuity Pathways Knowledge Base. Statistical significance of the associations was calculated using Fisher's Exact Test ( $p < 0.05$ ); the threshold line in the bar chart represents a p-value of 0.05.

### Pathways deregulated by mir-128 mimic overexpression

Genes deregulated upon overexpression of miR-128 were found associated with a number of biological functions, annotated pathways and molecular networks (Fig. 15). Some of the most significant associations with biological functions were found with cell cycle, cancer, neurological disease and cell death ( $-\log(p\text{-value}) > 3$ ). As far as canonical pathways, significant associations were found with pathways involved in metabolism, such as glycerolipid, pyruvate and botanoate metabolism, amino acid degradation and glycolysis/gluconeogenesis ( $-\log(p\text{-value}) > 3$ ). The deregulated molecules involved are basically enzymes, with a marked predominance of downregulation over upregulation, suggesting that these pathways may be to some extent inhibited or less efficient in miR-128-transfected cells.

On the other hand, no significant association was found with any annotated signaling pathway. In order to get a better idea of what cellular processes could be altered we therefore focused our analysis on molecular networks: the IPA software allows in fact to view how the significant molecules in a given dataset are known to interact with one another and with other closely related molecules. Fig.15 shows an overview of the three highest scored gene networks, which are exhaustively explained below and illustrated in fig.16.

**Network 1** (IPA score = 49) is associated with cancer, gene expression and neurological disease. Among the most deregulated genes in this network we can find *BCL2*, *TRAF3IP2*, *PAIP2* and *CHGB*. *BCL2* (B-cell CLL/Lymphoma 2, FC = 1.689) constitutes one of the central nodes of this network and is a well-known antiapoptotic gene; it codes for an outer mitochondrial membrane protein that suppresses apoptosis in a variety of cell systems, including neural cells. It regulates cell death by controlling the mitochondrial membrane permeability, blocking cytochrome *c* release from mitochondria and thus inhibiting caspase activity. *BCL2* upregulation in miR-128-transfected cells could explain the observed increase in cell number, which could be due to an enhanced inhibition of apoptosis. The other central nodes of network 1 (JNK, HSP70, IKK, P38 MAPK, IFN alpha and beta, proteasome complex) are as well related to apoptosis, cell death/survival and proliferation. We could not detect any changes in their mRNA levels, but rather than at the transcriptional level the activity of these proteins is controlled by post-translational mechanisms, such as phosphorylation/dephosphorylation, proteolytic cleavage or association with activators/inhibitors. Interestingly, the molecules surrounding these nodes, whose functions are mainly regulatory, are indeed altered at the mRNA levels, which could in turn influence the activation state of the nodes. *TRAF3IP2* (TRAF3 Interacting Protein 2, also known as AKT1, FC = 1.558) is also deregulated and is an activator of the transcription factor NFκB, another important node in this network. It has been implicated in malignant processes and in the regulation of the apoptotic response (Rayet and Gelin, 1999), and in particular it is thought to mediate the antiapoptotic effect of TGF-beta and TNF-alpha (Saile et al., 2001). *PAIP2* (PABP-interacting protein 2, FC = -2.034) is a translational repressor which acts on *VEGF* (Vascular Endothelial Growth Factor); VEGF, although most well studied for its role in tumor angiogenesis, is a potent mitogen and survival factor, which has more recently been demonstrated to have neuroprotective functions in the brain and is now considered a true neurotrophic factor. It has a role in a variety of conditions like amyotrophic lateral sclerosis, Parkinson's disease and Alzheimer's

disease and its expression is induced by multiple classes of antidepressants. The downregulation of *PAIP2* could lead to an augmented translation of VEGF, which is again consistent with the increase in cell number observed with miR-128. Finally, *CHGB* (Chromogranin B, FC = -2.050) is a secretory protein ubiquitously expressed in endocrine, neuroendocrine and neuronal cells whose function is guiding and sorting the secretion of neuropeptides and whose expression is low in patients with schizophrenia and Alzheimer's disease (Zhang et al., 2002).

**Network 2** (IPA score = 34) is associated with lipid metabolism, molecular transport and small molecule biochemistry, and among the upregulated genes it includes *HMGCS1*, *KLF6*, and *ADIPOR1*. *HMGCS1* (3-hydroxy-3-methylglutaryl-Coenzyme A Synthase 1, FC = 1.728) is an enzyme involved in lipogenesis and in particular in the biosynthesis of cholesterol, which is an essential component of myelin and is important for synapse formation; it is upregulated by several antipsychotic drugs used in schizophrenia therapy (Ferno et al., 2006). *KLF6* (Krüppel-like Factor 6, FC = 1.544) is a zinc finger transcription factor that has as well a role in adipogenesis and inhibits cellular growth; its function is abrogated in human cancers owing to increased alternative splicing, which yields a dominant-negative isoform that displays a markedly opposite effect on cell proliferation (Narla et al., 2005). Another downregulated gene is *ADIPOR1* (Adiponectin Receptor 1, FC = 1.504), a component of the energy homeostatic mechanism increasing fatty acid oxidation and glucose uptake; adiponectin and its receptors have recently been suggested as participating in the control of food intake and higher brain functions (Psilopanagioti et al., 2008). Downregulated genes of particular interest in this network are *DAP3* (Death Associated Protein 3, FC = -1.362), a mitochondrial ribosomal protein again involved in apoptosis (it mediates the induction of apoptosis by extracellular signals such as TNF-alpha, Fas ligand and gamma interferon, activating Caspase-8); *CHRNA3* (Cholinergic Receptor, Nicotinic Alpha 3, FC = -1.496), a subunit of the neuronal acetylcholine receptor implicated in nicotine addiction and alcohol dependence and related to the pathogenesis of sporadic Alzheimer's disease (Kawamata and Shimohama, 2002); *TXNIP* (Thioredoxin Interacting Protein, FC = -1.381), another pro-apoptotic factor which promotes vulnerability to oxidative damage by inhibiting thioredoxin and has recently been shown to be downregulated by synaptic NMDA receptor activity in rat (Papadia et al., 2008) and *APEX1* (Apurinic/Apyrimidinic Exonuclease 1, FC = -1.440), a multifunctional DNA repair enzyme involved in cell death and survival.



**Network 3** (IPA score = 24) is associated with cancer, reproductive system disease and tumor morphology and includes *PRSS3*, *VBP1*, *NGFRAP1* and *PAICS*. *PRSS3* (Protease, Serine 3, FC = 1.498) encodes mesotrypsin, a brain-specific trypsin form that according to studies conducted in rat astrocytes is thought to protect neural cells from apoptotic cell death through activation of a specific proteinase-activated receptor, *PAR1* (Wang et al., 2006b). *VBP1* (Von Hippel-Lindau Binding Protein 1, FC = -1.617) is a chaperone protein that is thought to play a role in the transport and correct localization of the von Hippel-Lindau (VHL) protein – a tumor suppressor – and is also important in the maturation of the cytoskeleton and in morphogenesis (Wang et al., 2006a). *NGFRAP1* (Nerve Growth Factor Receptor Associated Protein 1, FC = -1.637), a member of the Bex (Brain Expressed X-linked) family, is a p75NTR-associated protein that mediates apoptosis in response to NGF (whose signaling goes through NFkB) by interacting with the cell death domain of p75NTR (Mukai et al., 2003), pointing again to a miR-128-induced inhibition of apoptosis. Another strongly downregulated gene in network 3 is *PAICS* (Phosphoribosylaminoimidazole Carboxylase, FC= -1.554), an enzyme of the purine biosynthesis pathway.

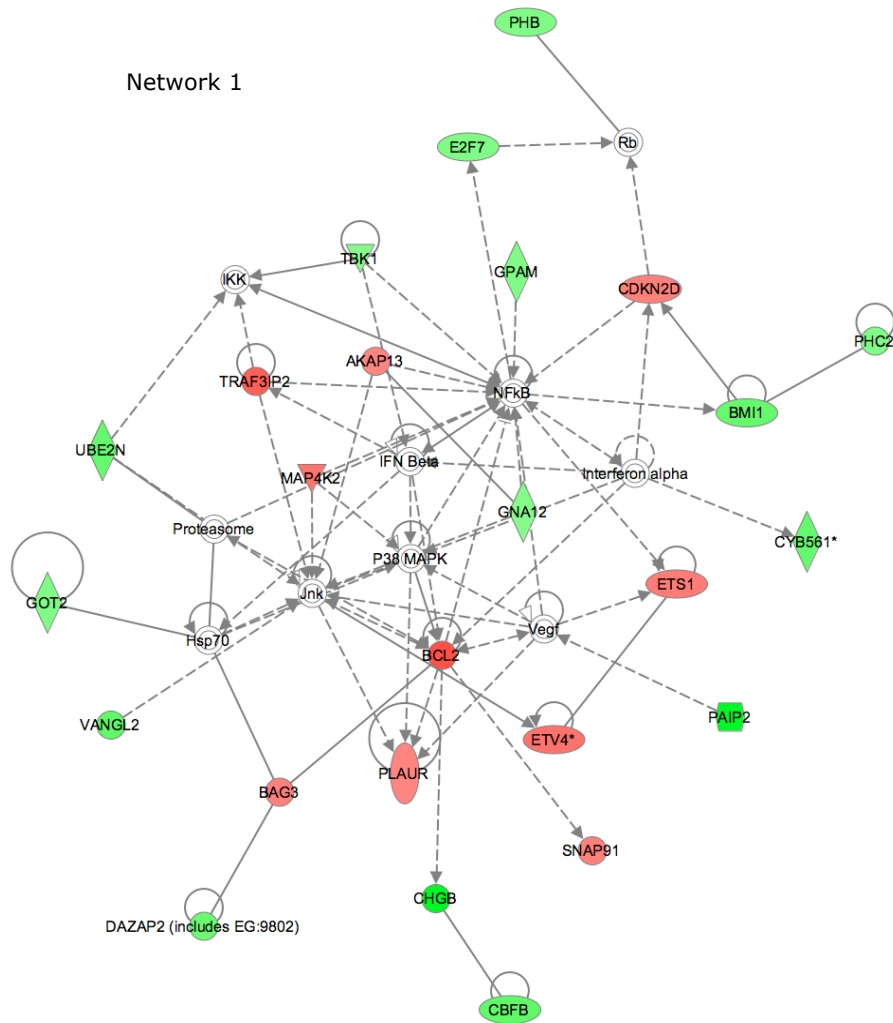
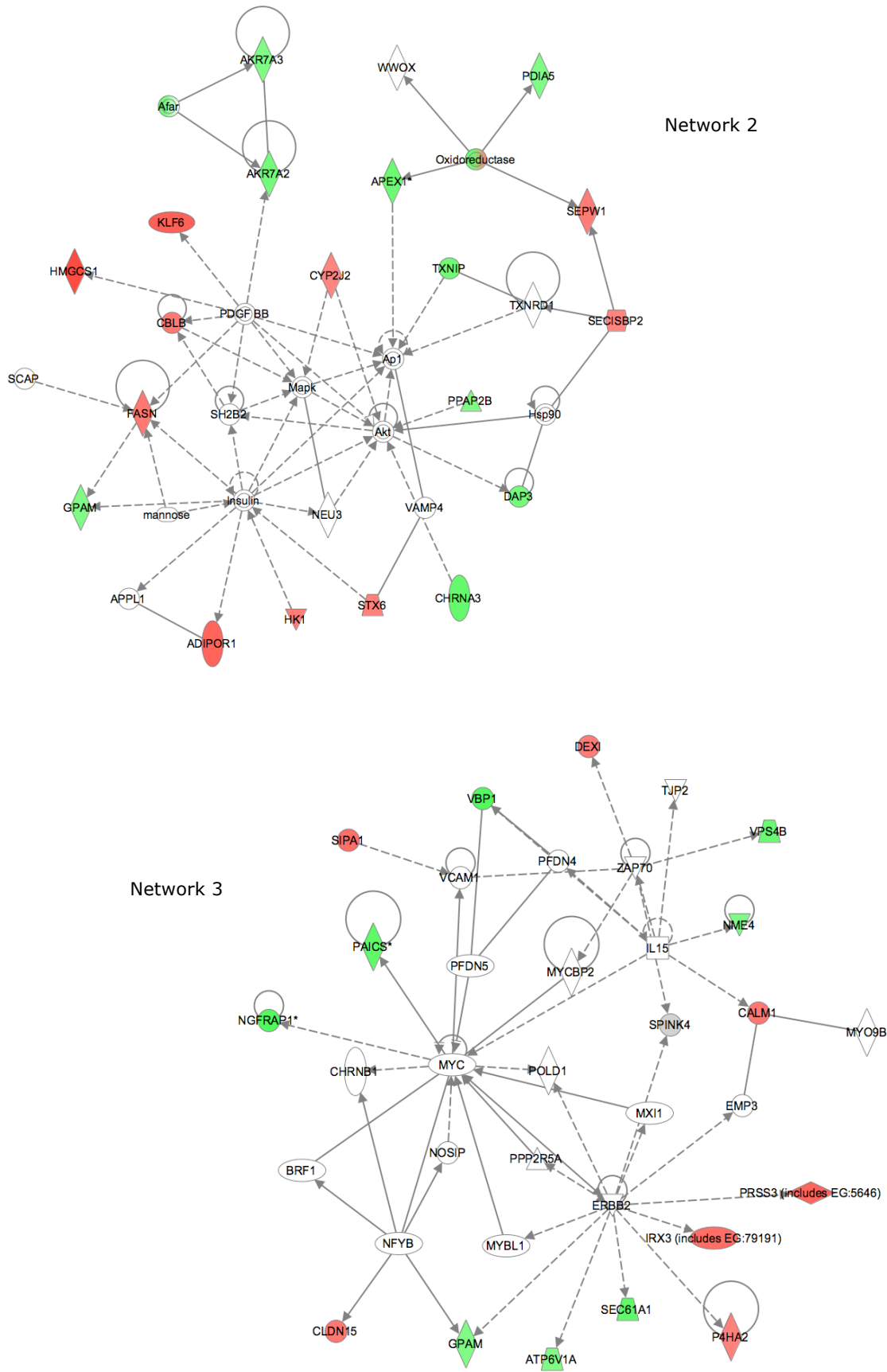


**Fig. 16** Top three molecular networks associated with the overexpression of miR-128 (current and next page).



### Pathways deregulated upon miR-509 mimic overexpression

As mentioned before, we could identify more than three times as many deregulated genes with miR-509 as with miR-128, with an overall degree of deregulation that was also higher. As a consequence, the significance of the associations with functions and pathways was very high, and the calculated p-values were extremely low ( $-\log(p\text{-value}) > 5$  for biological functions, Fig.17). The most significant associated biological function was by far cell cycle, followed by cancer, reproductive

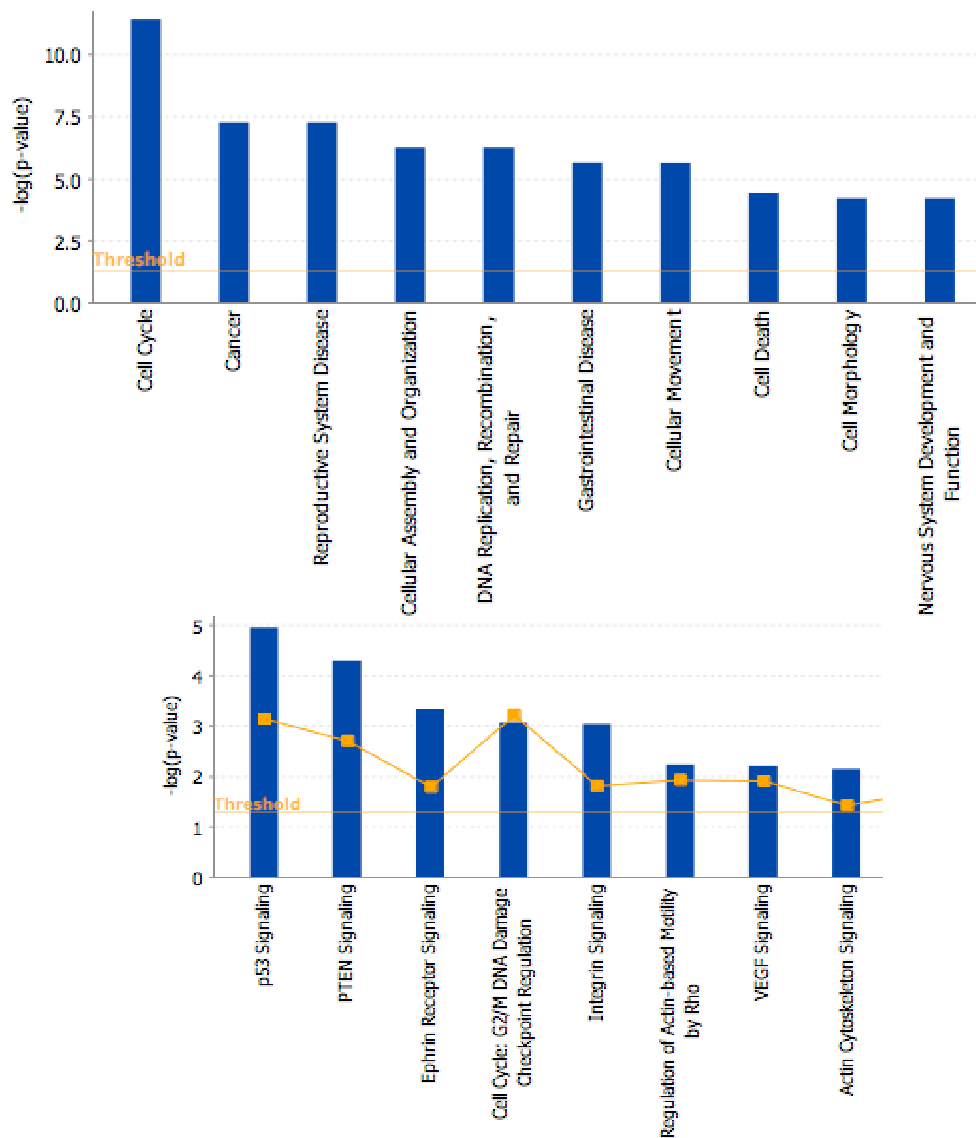


**Fig. 17** Most significant biological functions (top) and canonical pathways (bottom) associated with the overexpression of miR-509, according to the Ingenuity Pathway Knowledge Base. Statistical significance of the associations was calculated using Fisher's Exact Test ( $p < 0.05$ ). The threshold line represents a p-value of 0.05; the stacked line in canonical pathways indicates the ratio of deregulated genes divided by the total number of genes in that pathway.

system disease, cellular assembly and organization, DNA replication, recombination and repair, gastrointestinal disease, cellular movement, death and morphology among others.

In the case of miR-509 the analysis of annotated pathways was of particular interest because, as reflected by the high statistical significance, the number of deregulated molecules within the same pathway was in general pretty high: in the top seven pathways the ratio of molecules that met the FC cutoff requirements ranged in fact between 9% and 16%, indicating that these pathways were likely to be affected by the overexpression. The most significant pathways are described more extensively below and diagrams are shown in fig.18.

The two highest scored canonical pathways were **p53 and PTEN signaling**, two well-known tumor suppressor pathways. The former acts mainly through the regulation of the cell cycle, cell survival, cell death and apoptosis, while the latter is also related to actin organization, cell adhesion, migration and motility; they share some deregulated molecules, like PTEN itself, BCL2 and CDKN1A (a.k.a. p21Cip1). *PTEN* (Phosphatase and Tensin homolog, FC = -1.643) is a tumor suppressor that is mutated in a large number of cancers at high frequency and encodes a phosphatidylinositol-3,4,5-trisphosphate 3-phosphatase. It negatively regulates intracellular levels of phosphatidylinositol-3,4,5-trisphosphate in cells and functions as a tumor suppressor by negatively regulating AKT/PKB signaling pathway. *BCL2* (B-cell CLL/Lymphoma 2, FC = -1.599) is an antiapoptotic gene that was also deregulated by miR-128 (see previous section). *CDKN1A* (Cyclin-dependent kinase inhibitor 1A, FC = 2.495) encodes a potent cyclin-dependent kinase inhibitor, which binds to and inhibits the activity of cyclin-CDK2 or -CDK4 complexes and functions as a regulator of cell cycle progression at G1. It mediates p53-dependent cell cycle G1 phase arrest in response to a variety of stress stimuli; it also plays a regulatory role in S phase DNA replication and DNA damage repair. It was reported to be specifically cleaved by CASP3-like caspases and may be instrumental in the execution of apoptosis following caspase activation and ephrin receptor signaling. Even if they do not belong to this pathway, it is worth of mention that other CDK are on the contrary upregulated by miR-509: *CDKN3* (cyclin-dependent kinase inhibitor 3, FC = -1.568), a specific inhibitor of CDK2, and *CDKN2C* (cyclin-dependent kinase inhibitor 2C, FC = -1.363), an inhibitor of CDK4 and CDK6 that regulates G1 progression.

Other remarkably deregulated genes of the p53 pathway are *CDK2*, *BAX* and *BIRC5* (a.k.a. survivin). *CDK2* (Cyclin-Dependent Kinase 2, FC = -1.953) is a

catalytic subunit of the cyclin-dependent protein kinase complex whose activity is restricted to the G1-S phase and is essential for cell cycle G1/S phase transition; its downregulation is clearly consistent with the upregulation of its inhibitor *CDKN1A*. *BAX* (BCL2-Associated X protein, FC = 1.637) belongs to the BCL2 protein family; it forms a heterodimer with BCL2 and functions as an apoptotic activator. Whereas BCL2 is antiapoptotic and antiproliferative, BAX is proapoptotic and proliferative hence again its upregulation is consistent with the downregulation of its counterpart. *BIRC5* (Baculoviral IAP Repeat-Containing 5, FC = -1.551) is a member of the inhibitor of apoptosis (IAP) gene family, which encode negative regulatory proteins that prevent apoptotic cell death and whose expression is high during fetal development and in most tumors yet low in adult tissues.

The PTEN signaling pathway includes *SHC1* (Src Homology 2 domain Containing 1, FC = -1.451), the signaling adapter that couples activated receptor tyrosine kinases to Ras via the recruitment of the Grb2/SOS complex and is implicated in the cytoplasmic propagation of mitogenic signals; *GRB2* (growth factor receptor-bound protein 2, FC = 1.238) is also deregulated, even if in the opposite direction than *SHC1*. The Shc1-Grb2 complex is also involved in integrin signaling, where it transduces the signal to molecules implicated in actin cytoskeleton organization, cell adhesion and migration, like *PTK2* (PTK2 protein tyrosine kinase 2, a.k.a FAK, FC = -1.237) and *BCAR1* (breast cancer anti-estrogen resistance 1, a.k.a. CAS, FC = -1.253), which are interestingly both downregulated. *RAC1* (Ras-related C3 botulinum toxin substrate 1, FC = -1.732) belongs to the Ras superfamily of small GTP-binding proteins and is involved in cytoskeletal reorganization, cell motility and migration is as well downregulated.

As for the other pathways affected by the overexpression of miR-509 it is worth mentioning **ephrin receptor signaling**, G2/M DNA damage checkpoint regulation and integrin signaling. Ephrin receptors (EPHs) have multiple activities including widespread effects on the actin cytoskeleton, cell-substrate adhesion, intercellular junctions, cell shape and movement, and have been shown to be implicated as diverse functions as neural development, plasticity and regeneration, immune processes, glucose homeostasis and diabetes, bone maintenance, intestinal homeostasis as well as cancer (Pasquale, 2008). A distinctive feature of Eph-ephrin complexes is their ability to generate bidirectional signals that affect both the receptor-expressing and the ephrin-expressing cells. In cells transfected with miR-509 two of the eight known ephrin genes are upregulated (*EFNA4* and *EFNB1* , FC = 1.275 and 1.319 respectively) while the ephrin receptor *EPHB4* is downregulated

(FC = -1.242). Previously described altered genes like *SHC1*, *GRB2*, *BCAR1* and *PTK2* are also part of this pathway. Interestingly, all the genes altered in this pathway, with the only exception of the two ephrins, *GRB2* and *ARPC4*, are repressed, indicating a possible general impairment of processes like cell adhesion, migration and cytoskeletal organization, which would be coherent with the observed aggregation of miR-509-transfected cells.

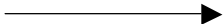
The fourth pathway entails the **G2/M DNA damage checkpoint** and is characterized by the downregulation of key genes for cell cycle progression and DNA replication, like *TOP2A* (topoisomerase II alpha, FC = -1.698), *CCNB2* (cyclin B2, FC = -1.581), and *CDC25B* and *C* (cell division cycle 25 homolog B and C, FC = -1.261 and -1.405 respectively); both cyclin Bs and Cdc25s are positive regulators of the cyclin-dependent kinase Cdc2, and are required for entry into mitosis. The upregulated genes are inhibitors of the Cdc2-cyclin B complex like the previously mentioned *CDKN1A*, *GADD45A* (growth arrest and DNA-damage-inducible alpha, FC = 1.307) as well as *YWHAB* (FC = 1.353), which conversely was downregulated by miR-128.

**Integrin signaling** is also affected by miR-509, and includes genes that are for the most part downregulated, many of which have already been described. Integrins play a direct role in cell adhesion and also activate a series of signaling pathways mediating transcriptional activation, cell mobility, cellular shape definition and regulation of the cell cycle. Of particular interest is the downregulation of *ACTB* (actin beta, FC = -1.390), *MYLK* (myosin light chain kinase, a.k.a. MLCK, FC = -1.231), a calcium/calmodulin dependent enzyme that phosphorylates myosin regulatory light chains and facilitates myosin interaction with actin filaments to produce contractile activity, *ARHGEF7* (rho guanine nucleotide exchange factor 7, a.k.a. PIX, FC = -1.614) an activator of Rac1, and *RAC1* itself, which as previously mentioned is responsible for actin rearrangements and membrane ruffling. A remarkable upregulation is seen with *BCAR3* (breast cancer anti-estrogen resistance 3, a.k.a *AND-34*, FC = 1.900), another guanyl-nucleotide exchange (GEF) factor known for causing estrogen-independent proliferation in human breast cancer cells. However the prevalence of downregulated molecules especially in the pathway leading to cytoskeletal rearrangements and motility points again to a decreased efficiency of these processes, which could explain the observed phenotype. Two more pathways go in a similar direction and are regulation of actin-based motility and actin cytoskeleton signaling. Both basically contain the relevant molecules described before and are clearly downregulated as pathways since all the genes

## Results

---

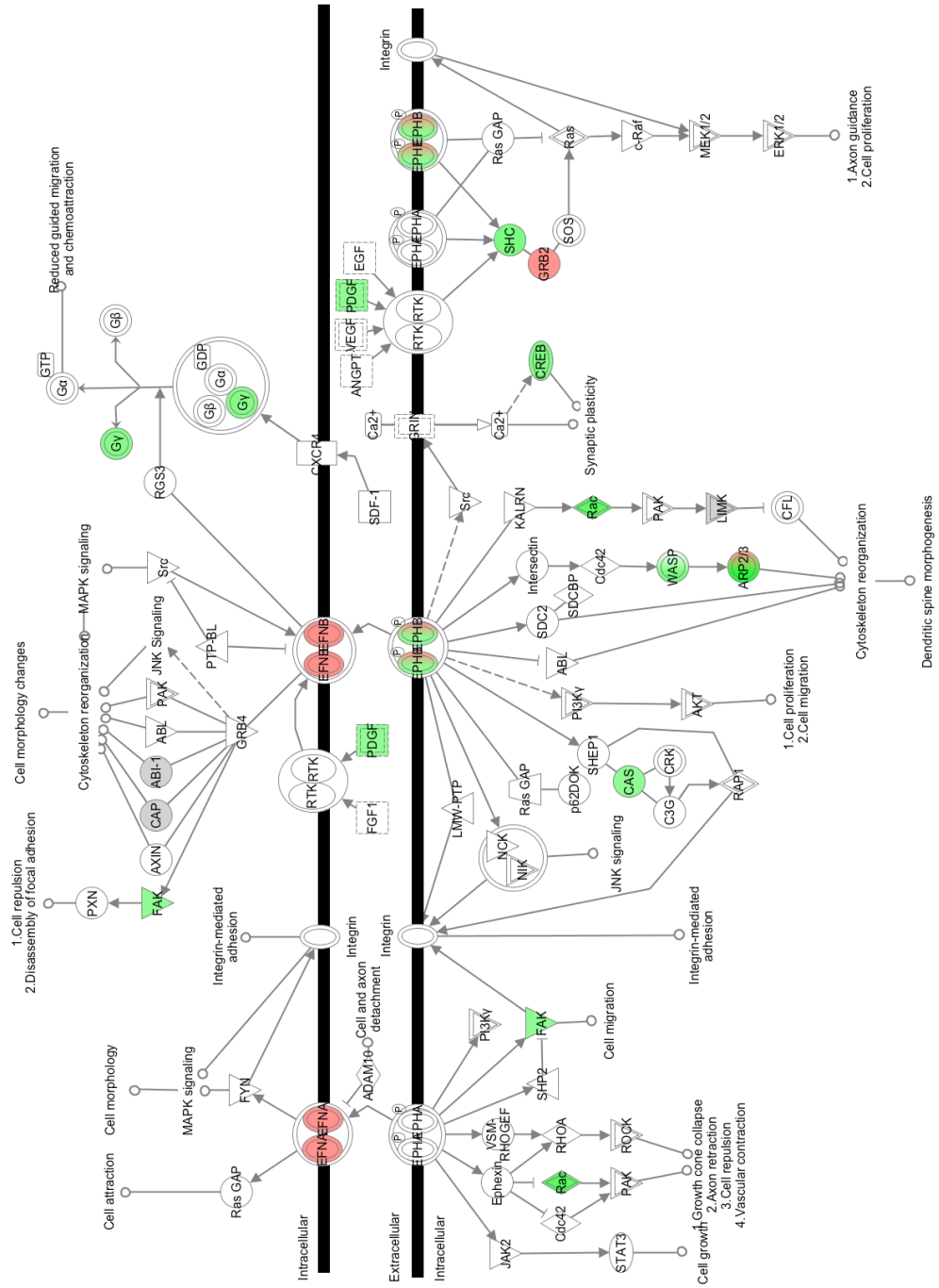
they involve (except *GRB2*) have negative fold changes. It is remarkable that besides the repression of actin beta and of actin-related signaling pathways, members of the tubulin family are as well downregulated: *TUBB* (tubulin beta), *TUBB2B* (tubulin beta 2B) and *TUBB2C* (tubulin beta 2C) have in fact a fold ranging between -1.35 and -1.40, indicating a possible general alteration of the cytoskeleton, which doesn't involve only actin-related structures but also tubulin.

**Fig.18** Diagrams of four annotated pathways altered by the overexpression of miR-509: PTEN signaling, ephrin receptor signaling, integrin signaling and regulation of actin-based motility by Rho. 



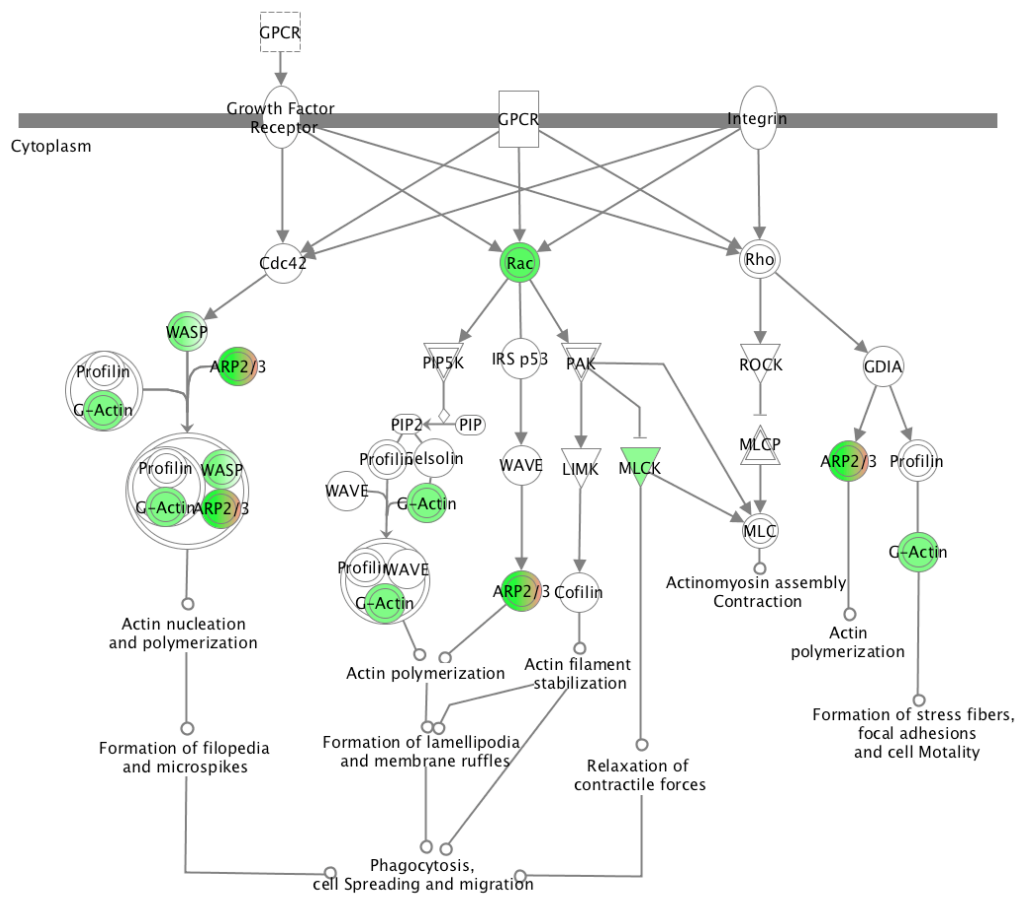


Ephrin Receptor Signaling





Regulation of Actin-based Motility by Rho



#### **4. miR-124a regulates the expression of the two NTRK3 isoforms through the splicing repressor PTBP1**

Alternative pre-mRNA splicing is a post-transcriptional regulation mechanism that allows rapid changes in the cellular proteome and is widely used during the development of the mammalian nervous system (Licatalosi and Darnell, 2006). PTBP1 (polypyrimidine tract binding protein 1) is a global repressor of alternative splicing in non-neuronal cells; it binds to pyrimidine-rich sequences in pre-mRNAs and inhibits the splicing of nearby neuron-specific alternative exons. It is expressed at high levels in non-neuronal cells but it is downregulated in the nervous system, allowing the inclusion of neuron-specific exons in mature mRNAs (Lillevall et al., 2001).

miR-124a is one of the most conserved and abundantly expressed nervous system-specific miRNAs (Lagos-Quintana et al., 2002); a recent study (Makeyev et al., 2007) has demonstrated that miR-124a directly targets the mRNA of PTBP1 and promotes nervous system development at least in part by repressing PTBP1 and triggering a downstream switch to neuron-specific alternative splicing.

To explore whether the alternative splicing of *NTRK3* could be affected by miR-124a through PTBP1 we overexpressed miR-124a in RA-differentiated SH-SY5Y cells and analyzed NTRK3 and PTBP1 levels by Western blotting at different time points after transfection. As expected, we could observe a significant reduction in PTBP1 expression, which interestingly was accompanied by a clear decrease in the full-length isoform of NTRK3 (Fig.19). With respect to the truncated isoform, it was not possible to quantify it precisely by WB: the levels of this variant are in fact very low in differentiated cells, which makes it almost undetectable using this technique. Nevertheless, densitometric analysis of the immunoblot revealed an increase in TF-NTRK3, at least 72 hours after transfection, but measurement variation was very high. We therefore analyzed the expression of the truncated isoform at the RNA level by real-time PCR, detecting a considerable increase in the TR-NTRK3 mRNA (~1.8-fold at 48 hours after transfection and ~3-fold at 72 hours, Fig.20).

These results show that overexpression of miR-124a and the consequent inhibition of PTBP1 cause discordant changes in the expression levels of the full-length and truncated isoforms of NTRK3, which are downregulated and upregulated respectively. The observed increase in the TR-NTRK3 mRNA suggests that miR-124a-mediated inhibition of PTBP1 could induce a switch in the alternative splicing

of *NTRK3*, favoring the formation of the truncated transcript over the full-length transcript.

We also analyzed the expression of PTBP1 during RA-induced differentiation (Fig.21) and could detect a ~20% decrease in PTBP1 levels after 3, 6 and 10 days of RA treatment, a reduction much less dramatic than that observed after transfection with miR-124a. This suggests that the regulation that PTBP1 may exert on *NTRK3* might not be physiologically during the differentiation of SH-SY5Y cells. It would be interesting to evaluate the role of such regulation in different contexts.

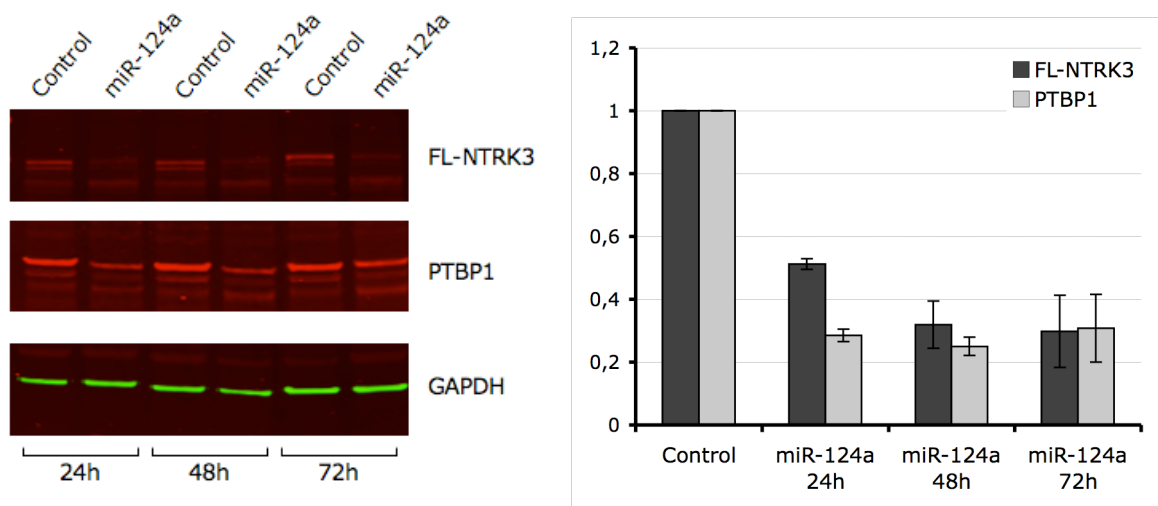


**Fig.19** Western blot analysis of RA-differentiated SH-SY5Y cells overexpressing miR-124a. Cells were transfected as described before; NTRK3 and PTBP1 expression was analyzed 24 hours, 48 hours and 72 hours after transfection. GAPDH was used as a loading control ( $p < 0.05$ ).

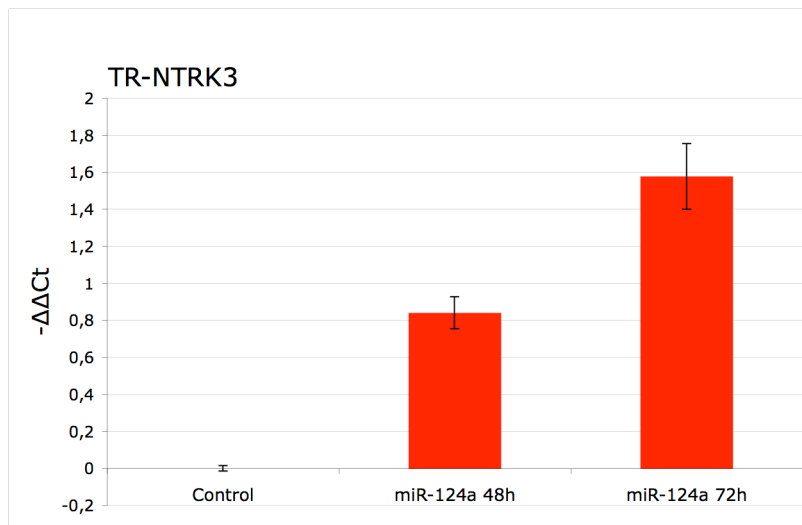


**Fig.20** Real-time RT-PCR analysis of TR-NTRK3 after transfection with miR-124a. Data are reported as  $-\Delta\Delta C_t$ s relative to control cells, which correspond to a 1.79-fold increase in expression at 48h and 2.98-fold at 72 hours ( $p < 0.05$ ).

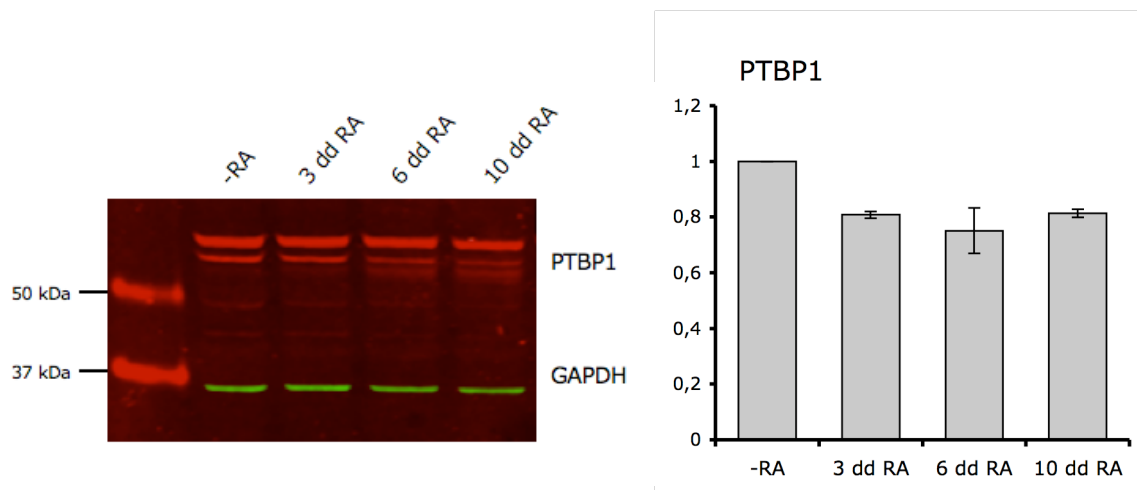


**Fig.21** Characterization of the expression of PTBP1 in RA-differentiated SH-SY5Y cells ( $p < 0.05$ ). GAPDH was used as a loading control.





## **5. Discussion**



In this work we have explored how miRNAs take part in the regulation of two different isoforms of the neurotrophin-3 receptor NTRK3. It is the first time that a study on miRNA-mediated regulation focuses on the possible contribution of miRNAs in determining the balance between two variants of the same gene. This is of particular interest in the case of *NTRK3* because full-length (catalytic) and truncated (non-catalytic) receptors not only exert a reciprocal regulatory activity through dominant-negative and ligand-sequestering mechanisms, but also trigger distinct downstream signaling pathways (Esteban et al., 2006). Catalytic and non-catalytic NTRK3 receptors are differentially expressed during the development of the nervous system (Menn et al., 1998) and the ratio between the two varies throughout neural development. The catalytic isoform is the only variant detected in proliferating neural stem cells, where it is thought to mediate cell survival; the non-catalytic isoform, conversely, appears as neurons begin to differentiate, suggesting that it may play a role in the maintenance of the differentiated state. Furthermore, the subcellular localization of the two isoforms is as well different, both in differentiating and mature neurons. Full-length receptors are in fact mainly expressed in the axonal compartment - raising the hypothesis that they may mediate axon guidance - while truncated receptors are in general predominant in the dendritic compartment and may be involved in synaptic plasticity (Menn et al., 2000).

miRNAs are important players in gene regulation in the nervous system, and in particular they are thought to contribute to the fine-tuning of neuronal gene expression during development and differentiation. Furthermore, a study published few years ago showed that mRNA and protein levels of NTRK3 change discordantly throughout the human lifespan (Beltaifa et al., 2005), indicating that NTRK3 expression is affected by some post-transcriptional regulation mechanism. These observations, together with the fact that the full-length and truncated transcripts of *NTRK3* present completely different 3'UTR regions, made the two receptor variants good candidates for being regulated by different sets of miRNAs.

Starting from an *in silico* analysis performed with miRNA target prediction programs such as miRanda, TargetScan and PicTar, we identified a group of miRNAs with putative target sites in the 3'UTRs of FL-NTRK3 (three miRNAs) or TR-NTRK3

(thirty-six). It is worth remarking that the study of miRNAs is complicated by the continuous discovery of new ones as well as by frequent corrections and modifications in their annotation (as far as sequences, nomenclature, etc). The Sanger miRbase miRNA database is in fact subject to an often problematic variability, which requires constant adjustments of experimental plans in order to keep up with the rapid evolution of the field. In our case the first analysis was carried out in 2005 when the use of target prediction methods was beginning to become popular, and was based on the 326 human miRNAs annotated in miRbase release 7.1. Even though as time went by we kept our list of miRNAs of interest as up-to-date as possible, for obvious practical reasons this study does not encompass all the miRNAs that appear in predictions at the present time.

With respect to the three prediction methods we used, they all predict miRNA targets based on sequence complementarity. miRanda gives higher weight to matches at the 5' end of the mature miRNA and takes into account the free energy of the RNA-RNA duplex as well as the extent of conservation of the miRNA target. TargetScan and PicTar consider as well target conservation but, unlike miRanda, look for perfect matches between the mRNA target and the seed region of the miRNA. TargetScan requires 100% complementarity and does not conduct free energy calculations, while with PicTar mismatches are allowed provided that they do not result in increased free energy. False-positive rate estimations are 24-39% for miRanda (Bentwich, 2005), 22-31% for TargetScan (Lewis et al., 2003) and approximately 30% for PicTar (Sethupathy et al., 2006). According to the luciferase assay results, in our hands the performance of the three programs was lower than estimated, TargetScan being the method showing the highest sensitivity (i.e. rate of true positives, ~40%).

A total of fifty-six, including the three thirty-nine predicted to target *NTRK3* plus seventeen unrelated miRNAs were tested experimentally on both isoforms using a luciferase-based reporter system. This first screening was performed by overexpressing miRNA mimics in HeLa cells and allowed us to validate three miRNAs for the full-length isoform and eight for the truncated isoform. Curiously, of the three miRNAs validated for FL-NTRK3 only two were in accordance with predictions (miR-151-3p and miR-185), while the third one, miR-24, was not predicted to target this isoform by any of the interrogated methods. There is actually no site of perfect complementarity between the 3'UTR of the full-length isoform and the 5' end of miR-24 (the so-called miRNA *seed* region), which is one of the basic requirements of most prediction programs. This points out one limitation of prediction methods:

even if target sites with perfect complementarity to the seed are definitely more common than other sites, giving such higher weight to perfect matches at the 5' end of the miRNA can lead to underestimate cases in which other factors, such as extensive base pairing with the remainder of the miRNA, may compensate missing complementarity of the 5' seed (Brennecke et al., 2005). In fact, the analysis of energetically favorable hybridizations of miR-24 to the 3'UTR of FL-NTRK3, using RNAhybrid, identified a few possible target sequences with low hybridization free energies, where only some nucleotides of the seed show perfect pairing to the mRNA.

Another well-accepted feature of miRNA-mediated repression is that multiple target sites in the same 3'UTR can act cooperatively and increase the efficacy of the inhibition (Doench and Sharp, 2004). As a matter of fact, among the miRNAs validated for the truncated isoform the two causing the strongest repression (miR-509 and miR-625, 47% and 62% reduction in luciferase activity respectively) have two predicted target sites each in the 3'UTR of TR-NTRK3, suggesting that the strong downregulation could be due to the synergism between the double target sites. On the other hand, miR-330 as well has two predicted binding sites, but only caused a very slight inhibition (13%). We also explored whether the combination of different miRNAs repressing the truncated isoform could lead to a more dramatic reduction; we tested thirteen sets of two miRNAs, and in no case could we observe any additive effect. This indicates a lack of synergism between the examined target sites; however, it has to be considered that the experimental miRNA concentrations may mask a possible cooperative effect, which might be important in physiological conditions, where miRNA levels are lower and the amount of available miRNA complexes is subject to subtle regulation. Furthermore, the fact that in the truncated isoform the same functional target sequence is recognized by different miRNAs with different patterns of expression, as is the case for miR-128 and miR-509, suggests that miRNAs with overlapping binding sites could be important for the regulation of *NTRK3* in a tissue-specific manner.

As the following step, we wanted to confirm if miRNAs validated on luciferase constructs were also able to regulate endogenous NTRK3. This part of the study was carried out in SH-SY5Y neuroblastoma cells, which predominantly express the truncated receptor in their undifferentiated state and the full-length receptor when treated with RA. miRNA mimics were transfected in this cell system and we could show that miR-24 and miR-151-3p (two out of three luciferase-validated miRNAs) repress the endogenous full-length isoform while miR-128, miR-485-3p, miR-765

and miR-768-5p (four out of eight) repress the truncated isoform. The total number of regulating miRNAs was therefore reduced compared to the results obtained in HeLa cells; in order to exclude a possible interference of endogenously expressed miRNAs on the outcome of these experiments we examined miRNA expression in the two cell lines. Information was gathered from a miRNA microarray analysis performed in our lab in both HeLa and SH-SY5Y cells. With the exception of miR-24, whose levels are high in both HeLa and SH-SY5Y, the expression of the other luciferase-validated miRNAs was in general low and comparable between the two cell lines. This rules out the possibility that high levels of endogenous miRNAs in SH-SY5Y cells could bias the results of the validation, making the overexpression of miRNA mimics less effective. We could therefore conclude that miRNAs identified through the luciferase assay and not confirmed on the endogenous protein were false-positives most likely due to the artificial context in which the 3'UTRs were inserted. Having the 3'UTRs cloned downstream of the luciferase ORF is in fact very likely to result in a spurious secondary mRNA structure, which could expose target sites for miRNA binding that are normally not accessible. In addition, luciferase assays are a very convenient and useful tool to rapidly and easily screen many miRNAs in a high throughput fashion, but they create an environment where the encounters between miRNA and target mRNA are extremely forced, as both are overexpressed, increasing the likelihood of false positives.

These observations could explain the discrepancies between our results and a work published in 2007 (Laneve et al., 2007), in which three miRNAs (miR-9, miR-125a and miR-125b) upregulated upon retinoic acid treatment in the neuroblastoma cell line SK-N-BE were identified as regulators of the truncated isoform of *NTRK3*; the downregulation of TR-*NTRK3* induced by these miRNAs was linked to a decrease in cell proliferation. Similarly to our strategy, in this study the validation of TR-*NTRK3* as a target of miR-9 and miR-125a/b was performed with a luciferase reporter assay and double-checked by Western blotting on the endogenous protein. miR-9 and miR-125a/b are predicted to target *NTRK3* by TargetScan and miRanda respectively, and as such they were included from the beginning in the list of miRNAs tested in our screening. In our hands, none of the three miRNAs caused a significant reduction in *NTRK3* expression - either in luciferase activity or in endogenous protein levels. At least for the luciferase part, a possible justification is that Laneve et al. did not clone the whole 3'UTR of the truncated isoform for their analysis, but only the portion containing the target sites for miR-9 and miR-125a/b, located at approximately 300 bp from one another; using such a short segment of

the 3'UTR may have prevented the formation of some secondary structure of the RNA, leaving the two predicted target sites artificially exposed. In contrast, we considered the whole 3'UTR, which is 1981 bp in length. As far as endogenous TR-NTRK3, a factor that could explain the divergence between Laneve et al. and our results is that experiments were performed in different cell lines (SK-N-BE versus SH-SY5Y), though both are derived from neuroblastoma.

Finding that neither miR-509 nor miR-625 regulate the endogenous truncated isoform was also surprising, given that as mentioned above these two miRNAs, with two predicted target sites each, caused a remarkable inhibition of luciferase activity in HeLa cells. A possible hypothesis to explain this result is that the activity of miRNAs causing such a dramatic inhibition of *NTRK3* expression might be physiologically relevant in tissues or cell types where the gene needs to be completely shut off, whereas miRNAs whose effects are milder may be needed for the fine-tuning of the expression in contexts where NTRK3 receptors are present. This could also apply to miR-185, the miRNA causing the strongest reduction in luciferase activity in the case of the full-length isoform (54%), which was not validated on the endogenous protein.

Regarding the physiological consequences of miRNA overexpression and NTRK3 downregulation, we showed that the repression of the full-length receptor mediated by miR-24 and miR-151-3p reduces ERK phosphorylation. ERK 1 and 2 (i.e. MAPK3 and MAPK1 respectively) are key components of the Ras/Raf/MEK/MAPK pathway, one of the signal transduction pathways triggered by Trk receptors upon neurotrophin binding, which activates the transcription of genes promoting neuronal differentiation. After NT3 stimulation, cells transfected with miR-24 and miR-151-3p showed a decrease in ERK1/2 phosphorylation, indicating that these two miRNAs not only have an effect on NTRK3 levels but also on the activation of at least one of the downstream signaling pathways induced by its ligand NT3; it would be interesting to analyze whether other pathways such as PI3K and PLC- $\gamma$  are as well affected.

On the other hand, we observed striking morphological changes in undifferentiated SH-SY5Y cells transfected with miR-128, a brain-enriched miRNA that regulates the truncated isoform. Cells showed rounded bodies and shorter neurites than control, the overall cell size looked smaller and we could detect a 27% increase in total cell number. The morphological phenotype was very similar to that obtained after transfection with an siRNA specific for TR-NTRK3; conversely, the siRNA caused a reduction in cell number (~20%) instead of an increase. This

indicates that the morphological alterations caused by miR-128 may indeed be a consequence of the repression of the truncated isoform, whereas the variation in cell number is probably due to some off-target effect of this miRNA. Furthermore, cells transfected with miR-485-3p as well acquired similar morphological features, although less evident than with miR-128. Interestingly, miR-128 and miR-485-3p are the miRNAs causing the strongest reductions in TR-NTRK3 levels (32% and 30% respectively) in our model system.

As described before, miR-509 had been identified as a potential regulator of the truncated isoform in the luciferase assay, but failed to regulate the endogenous protein. Although it did not downregulate TR-NTRK3 in SH-SY5Y cells, the overexpression of miR-509 was as well accompanied by striking modifications in cell appearance: cells in fact tended to form aggregates and gather in clusters, resulting in an uneven distribution over the plate.

Flow cytometry analysis and MTT assays performed on cells transfected with miR-128 and miR-509 revealed no alterations in the actual size and complexity of cells, nor in their mitochondrial activity. Therefore, in order to have a general idea of which pathways could be affected by these two miRNAs, we decided to analyze the consequences of their overexpression at the transcriptome level, using whole-genome microarrays. As previously mentioned, miR-128 is a well-known brain-enriched miRNA, which accumulates in parallel with neuronal differentiation (Smirnova et al., 2005) and whose expression is increased in Alzheimer's disease (Lukiw, 2007), but very little is known about miR-509. We analyzed the levels of these two miRNAs by real-time quantitative RT-PCR in different human tissues and in SH-SY5Y cells, confirming that miR-128 is highly expressed in brain, as well as in skeletal muscle and to a lower extent in thymus, while miR-509 is highly expressed in testis, kidney and ovary. On the contrary, in agreement with the miRNA microarray experiment mentioned before, both miRNAs resulted to be poorly expressed in SH-SY5Y cells.

Whole genome microarray results after miR-128 and miR-509 overexpression indicated a large number of deregulated genes in both cases; however, the total number of altered genes as well as the overall degree of deregulation was higher with miR-509 than with miR-128. Although the two miRNAs are expressed at comparably low levels in our model system, these differences can be a consequence of their tissue-specific patterns of expression, miR-128 being endogenously expressed in neurons, which are more closely related to SH-SY5Y cells than tissues expressing miR-509.



In the case of miR-128, among the most deregulated genes we could find a few that are involved in apoptosis (for example BCL2), with a general tendency for antiapoptotic genes to be upregulated and for proapoptotic genes to be downregulated; this could explain the increase in cell number detected after transfection with miR-128. Other classes of deregulated genes include several involved in lipid and sugar metabolism. A downregulation of some genes implicated in the organization of the cytoskeleton was also observed, which could be related with the tendency of transfected cells to acquire rounded bodies with short neurites. It would be interesting at this point to analyze caspase activation to confirm the possible alteration of apoptosis as well as downstream molecules belonging to the pathway activated by TR-NTRK3 (such as actin and Arf6), which could also account for the observed morphological changes.

As far as miR-509, gene deregulation was more extreme and involved well-known annotated pathways implicated in tumor suppression (p53 and PTEN), regulation of actin cytoskeleton, cell shape, adhesion and movement (ephrin receptor signaling and integrin signaling among others) - which could explain the observed aggregation of transfected cells - and cell cycle progression. In particular, many of the downregulated molecules in the ephrin receptor pathway are involved in neuronal morphogenesis, suggesting that miR-509 could play a role in repressing neuron-specific pathways in the non-neuronal tissues where it is endogenously expressed.

It is also interesting to notice that among the genes downregulated upon miR-509 overexpression we could find PTBP1 (FC = -1.37), a splicing repressor whose inhibition results in increased TR-NTRK3 levels, as explained hereafter. This is just an example of how complex networks and feedbacks taking part in miRNA-mediated regulation can be, and could explain why miR-509, which reduced the luciferase activity of the TR-NTRK3 construct by almost 50% in HeLa cells, was not able to cause a significant repression of endogenous TR-NTRK3 in SH-SY5Y cells: a possible decrease in TR-NTRK3 levels caused by the overexpression of miR-509 might in fact have been compensated by the downregulation of PTBP1, which results in increased TR-NTRK3 expression. Moreover, as explained before miR-128 and miR-509 have overlapping binding sequences in the 3'UTR of TR-NTRK3, suggesting that the two miRNAs may be important for the regulation of this isoform in different tissues. Exploring whether the overexpression/inhibition of miR-509 can affect NTRK3 levels in cell lines derived from ovary, kidney or testis where miR-509 is naturally present could be a way to address this question.

One possible application of the microarray analysis of cells overexpressing a specific miRNA is the identification of potential targets: combining microarray results and target predictions it is in fact possible to identify genes that are repressed by the overexpression and are likely to contain functional target sites. As compared to other strategies of recent application, such as the biochemical identification of miRNA targets by co-immunoprecipitation of members of the Ago protein family with Ago-bound mRNAs (Beitzinger et al., 2007), this approach can be useful to discriminate targets regulated through mRNA cleavage rather than translational repression, as the inhibition of targets undergoing translational repression cannot be detected at the mRNA level. Interestingly, with both miR-128 and miR-509, predicted targets that resulted to be deregulated showed a clear predominance of downregulation over upregulation, supporting the hypothesis that those genes could be targeted by the two miRNAs. However, target validation is needed for each gene in order to confirm that such repression is directly caused by the miRNAs and not by some kind of negative feedback.

An intriguing example of predicted target that is downregulated is E2F7, a member of the E2F family of transcription factors that acts as a transcriptional repressor and inhibits cell cycle progression (de Bruin et al., 2003). The E2F family includes nine members, all of them involved in cell cycle regulation, DNA replication, DNA repair and mitosis, but some of them act as cell cycle promoters and others as inhibitors. E2F7 is a predicted target for miR-128 according to TargetScan and is downregulated upon miR-128 overexpression (FC = -1.28); being an inhibitor of cell cycle progression, its repression could be consistent with the increase in cell number observed with miR-128. Curiously, a very recent study has shown that in glioma cells miR-128 targets E2F3a, another member of the family that conversely promotes cell cycle progression; in glioma cells the overexpression of miR-128 in fact inhibits cell proliferation (Zhang et al., 2008). This suggests that miR-128 may exert opposite effects on the cell cycle depending on the cellular context in which it is expressed, by regulating different members of the same family of transcription factors with proproliferative or antiproliferative function.

The final part of our study was meant to explore if miRNAs could affect the levels of full-length and truncated NTRK3 not only through direct targeting, but also by controlling a previous stage of gene regulation, such as pre-mRNA splicing. The splicing regulator PTBP1 (polypyrimidine tract-binding protein 1) was a good candidate to mediate this kind of regulation; PTBP1 is in fact known to act as a repressor of alternative splicing in non-neuronal cells, inhibiting the splicing of

neuron-specific alternative exons (Lillevali et al., 2001). It is expressed at high levels in non-neuronal cells but is downregulated in the nervous system, allowing the inclusion of neuron-specific exons in mature mRNAs. miR-124 is a brain-specific miRNA (Sempere et al., 2004), which is expressed in neurons but not in astrocytes and whose levels increase over time in the developing nervous system. Furthermore, miR-124 stimulates neuronal differentiation and inhibits glial differentiation of embryonic stem cells in vitro (Krichevsky et al., 2006). PTBP1 has recently been validated as a target of miR-124, demonstrating that miR-124 promotes nervous system development at least in part by repressing PTBP1 (Makeyev et al., 2007). We checked whether the miRNA-mediated repression of PTBP1 could affect the ratio of the two NTRK3 receptor variants. After transfecting miR-124a into differentiated SH-SY5Y cells we could detect a dramatic decrease in PTBP1 levels (70% approximately), which was accompanied by a comparable reduction in FL-NTRK3 protein levels; at the same time, the truncated *NTRK3* transcript was upregulated by approximately 3-fold.

Taken together, these results indicate that NTRK3 may undergo miRNA-mediated regulation at two different levels. On the one hand, we show that distinct sets of miRNAs are able to repress each isoform by direct targeting; the degree of inhibition in this case varies depending on the miRNA but is in general relatively mild, the maximum reduction observed reaching approximately 30%. On the other hand, another miRNA with no target sites in the 3'UTRs of either isoform alters the relative expression of full-length and truncated receptors possibly by acting upon alternative splicing, through the splicing regulator PTBP1. The changes in NTRK3 levels detected in this case are definitely more dramatic and go in opposite directions, with a decrease in the expression of the full-length isoform and an increase of the truncated isoform. Further investigation is needed in order to understand what the physiological role of this second type of regulation may be. Little is known about the expression of NTRK3 receptors outside the nervous system, and in particular no isoform-specific information is available. The high levels of PTBP1 in this context could contribute to promote the expression of the full-length isoform versus the truncated isoform. Within the nervous system, as miR-124 plays a key role in the differentiation of progenitor cells to mature neurons, we can speculate that the miR-124-mediated downregulation of PTBP1 during neuronal differentiation could play a role in activating the expression of the truncated isoform, which as previously mentioned appears as neurons begin to differentiate. On top of this mechanism, the intervention of miRNAs acting through direct

targeting could add a further step of regulation facilitating the fine-tuning of the two receptor variants, as an additional factor in a complex regulatory network.

We also analyzed the expression profile of PTBP1 during RA-mediated differentiation in SH-SY5Y cells. Considering that PTBP1 is downregulated during neuronal differentiation, we expected it to decrease upon RA-treatment. On the other hand, considering the described effects of PTBP1 repression on NTRK3 (decrease of the full-length isoform and increase of the truncated isoform), a reduction in PTBP1 levels after RA exposure would have been in contradiction with the expression profile of NTRK3 during RA differentiation (increase of the full-length isoform and decrease of the truncated isoform). We could actually detect a decrease in PTBP1 levels, which were reduced by 20% at day 3 of RA treatment and remained constant through day 10. Such reduction is mild compared to what happens *in vivo*: PTBP1 is in fact undetectable in adult brain neurons (Lillevall *et al.*, 2001). Furthermore, the reduction is also mild relative to the repression induced by the overexpression of miR-124 in our experiment. These observations suggest that the regulation of PTBP1 is not as strict in SH-SY5Y cells as it is *in vivo*; therefore, the 20% reduction might not be sufficient to cause a notable effect on NTRK3 levels, or the regulatory function of PTBP1 might not play an important role in the biology of these cells, at least when differentiation is induced with RA. Moreover, the NTRK3 expression profile during RA-mediated differentiation in SH-SY5Y cells (and similarly in other neuroblastoma cell lines) is somehow in contradiction with what is known about the expression of the two isoforms in neural stem cells, where FL-NTRK3 is the only isoform present in proliferating neurons while TR-NTRK3 starts to be detected as they differentiate. Neural stem cells or neuronal primary cultures, given their faithfulness to physiological conditions, could actually be a good system to further confirm these results and see how/if the expression profiles of miR-124 and PTBP1 change relative to those of NTRK3.

It is worth remarking that the data presented here were obtained through an overexpression strategy, which was chosen as the miRNAs we were studying were in general poorly expressed in our model system, SH-SY5Y cells. We in fact tested the opposite approach - repressing miRNA activity through miRNA inhibitors - for miR-128 and miR-151-3p, but could not detect any effect on the expression of NTRK3, most likely due to the fact that the endogenous expression of the corresponding miRNAs is very low. As mentioned above a different cell system with higher endogenous miRNA levels, possibly neural stem cells or neuronal primary cultures as well as other cells of different origin, could be useful to accomplish an

adequate inhibition of miRNA activity and analyze the consequences on NTRK3 levels.

In summary, in this study we demonstrate that the full-length and truncated isoforms of NTRK3 are regulated by different miRNAs. We could identify two miRNAs (miR-24 and miR-151-3p) that repress the full-length isoform of NTRK3 and inhibit downstream signaling when overexpressed in SH-SY5Y neuroblastoma cells, and four miRNAs (miR-128, miR-485-3p, miR-625 and miR-768) that repress the truncated isoform. In particular, the overexpression of miR-128, a brain-enriched miRNA, causes morphological changes as well as an increase in cell number. miR-509, a miRNA that is not expressed in brain but is present at high levels in testis, kidney and ovary also caused important alterations in cell appearance. Whole-genome microarray analysis of cells transfected with the two miRNAs revealed interesting deregulations of important pathways such as apoptosis and cell survival/proliferation in the case of miR-128 and regulation of the actin cytoskeleton, cell shape, adhesion and movement in the case of miR-509. Furthermore, we could demonstrate that miR-124, another brain-enriched miRNA with no predicted target sites in either NTRK3 isoform, is able to influence the balance of the two isoforms, in association with the regulation of the splicing repressor PTBP1.



## **6. Conclusions**





In this study we demonstrate that the full-length and truncated isoforms of NTRK3 are regulated by different sets of miRNAs, which can act either by direct targeting of the two NTRK3 variants or by regulating their alternative splicing.

- Two miRNAs (miR-24 and miR-151-3p) repress the full-length isoform of NTRK3 and inhibit downstream signaling induced by NT3 stimulation when overexpressed in retinoic acid-differentiated SH-SY5Y neuroblastoma cells.
- Four miRNAs (miR-128, miR-485-3p, miR-625 and miR-768) cause a significant downregulation of the truncated isoform of NTRK3 when overexpressed in undifferentiated SH-SY5Y cells.
- The overexpression of the brain-enriched miR-128 in neuroblastoma cells causes morphological changes as well as an increase in cell number. Whole-genome microarray analysis of cells transfected with this miRNA reveals that it is involved in the regulation of important pathways such as apoptosis and cell survival/proliferation.
- The overexpression of miR-509, a miRNA that is not expressed in the brain but is present at high levels in testis, kidney and ovary causes an aggregation of neuroblastoma cells, which tend to form clusters. Whole-genome microarray analysis of cells transfected with this miRNA reveals a deregulation of pathways related with actin cytoskeleton organization, cell shape, adhesion and movement.
- miR-124, another brain-enriched miRNA with no predicted target sites in either NTRK3 isoform, is able to influence the balance of the two isoforms when overexpressed in SH-SY5Y cells, probably through the downregulation of the splicing repressor PTBP1.



## **7. References**



- Abelson, J. F., Kwan, K. Y., O'Roak, B. J., Baek, D. Y., Stillman, A. A., Morgan, T. M., Mathews, C. A., Pauls, D. L., Rasin, M. R., Gunel, M., Davis, N. R., Ercan-Sencicek, A. G., Guez, D. H., Spertus, J. A., Leckman, J. F., Dure, L. S. t., Kurlan, R., Singer, H. S., Gilbert, D. L., Farhi, A., Louvi, A., Lifton, R. P., Sestan, N., and State, M. W. (2005). Sequence variants in SLITRK1 are associated with Tourette's syndrome. *Science* **310**, 317-20.
- Alonso, P., Gratacos, M., Menchon, J. M., Saiz-Ruiz, J., Segalas, C., Baca-Garcia, E., Labad, J., Fernandez-Piqueras, J., Real, E., Vaquero, C., Perez, M., Dolengevich, H., Gonzalez, J. R., Bayes, M., de Cid, R., Vallejo, J., and Estivill, X. (2008). Extensive genotyping of the BDNF and NTRK2 genes define protective haplotypes against obsessive-compulsive disorder. *Biol Psychiatry* **63**, 619-28.
- Ambros, V., Bartel, B., Bartel, D. P., Burge, C. B., Carrington, J. C., Chen, X., Dreyfuss, G., Eddy, S. R., Griffiths-Jones, S., Marshall, M., Matzke, M., Ruvkun, G., and Tuschl, T. (2003). A uniform system for microRNA annotation. *Rna* **9**, 277-9.
- Anderson, C., Catoe, H., and Werner, R. (2006). MIR-206 regulates connexin43 expression during skeletal muscle development. *Nucleic Acids Res* **34**, 5863-71.
- Anderson, P., and Kedersha, N. (2006). RNA granules. *J Cell Biol* **172**, 803-8.
- Ashraf, S. I., and Kunes, S. (2006). A trace of silence: memory and microRNA at the synapse. *Curr Opin Neurobiol* **16**, 535-9.
- Aumiller, V., and Forstemann, K. (2008). Roles of microRNAs beyond development - Metabolism and neural plasticity. *Biochim Biophys Acta*.
- Barbacid, M. (1994). The Trk family of neurotrophin receptors. *J Neurobiol* **25**, 1386-403.
- Barbacid, M., Lamballe, F., Pulido, D., and Klein, R. (1991). The trk family of tyrosine protein kinase receptors. *Biochim Biophys Acta* **1072**, 115-27.
- Barbato, C., Ciotti, M. T., Serafino, A., Calissano, P., and Cogoni, C. (2007). Dicer expression and localization in post-mitotic neurons. *Brain Res* **1175**, 17-27.
- Barbato, C., Giorgi, C., Catalanotto, C., and Cogoni, C. (2008). Thinking about RNA? MicroRNAs in the brain. *Mamm Genome*.
- Baroukh, N., Ravier, M. A., Loder, M. K., Hill, E. V., Bounacer, A., Scharfmann, R., Rutter, G. A., and Van Obberghen, E. (2007). MicroRNA-124a regulates Foxa2 expression and intracellular signaling in pancreatic beta-cell lines. *J Biol Chem* **282**, 19575-88.
- Beitzinger, M., Peters, L., Zhu, J. Y., Kremmer, E., and Meister, G. (2007). Identification of human microRNA targets from isolated argonaute protein complexes. *RNA Biol* **4**, 76-84.

## References

---

- Beltaifa, S., Webster, M. J., Ligons, D. L., Fatula, R. J., Herman, M. M., Kleinman, J. E., and Weickert, C. S. (2005). Discordant changes in cortical TrkC mRNA and protein during the human lifespan. *Eur J Neurosci* **21**, 2433-44.
- Bentwich, I. (2005). Prediction and validation of microRNAs and their targets. *FEBS Lett* **579**, 5904-10.
- Bentwich, I., Avniel, A., Karov, Y., Aharonov, R., Gilad, S., Barad, O., Barzilai, A., Einat, P., Einav, U., Meiri, E., Sharon, E., Spector, Y., and Bentwich, Z. (2005). Identification of hundreds of conserved and nonconserved human microRNAs. *Nat Genet* **37**, 766-70.
- Bernstein, E., Kim, S. Y., Carmell, M. A., Murchison, E. P., Alcorn, H., Li, M. Z., Mills, A. A., Elledge, S. J., Anderson, K. V., and Hannon, G. J. (2003). Dicer is essential for mouse development. *Nat Genet* **35**, 215-7.
- Bhattacharyya, S. N., Habermacher, R., Martine, U., Closs, E. I., and Filipowicz, W. (2006). Stress-induced reversal of microRNA repression and mRNA P-body localization in human cells. *Cold Spring Harb Symp Quant Biol* **71**, 513-21.
- Biedler, J. L., Helson, L., and Spengler, B. A. (1973). Morphology and growth, tumorigenicity, and cytogenetics of human neuroblastoma cells in continuous culture. *Cancer Res* **33**, 2643-52.
- Boutz, P. L., Chawla, G., Stoilov, P., and Black, D. L. (2007). MicroRNAs regulate the expression of the alternative splicing factor nPTB during muscle development. *Genes Dev* **21**, 71-84.
- Breitkreutz, B. J., Jorgensen, P., Breitkreutz, A., and Tyers, M. (2001). AFM 4.0: a toolbox for DNA microarray analysis. *Genome Biol* **2**, SOFTWARE0001.
- Brennecke, J., Hipfner, D. R., Stark, A., Russell, R. B., and Cohen, S. M. (2003). bantam encodes a developmentally regulated microRNA that controls cell proliferation and regulates the proapoptotic gene hid in Drosophila. *Cell* **113**, 25-36.
- Brennecke, J., Stark, A., Russell, R. B., and Cohen, S. M. (2005). Principles of microRNA-target recognition. *PLoS Biol* **3**, e85.
- Cai, X., Hagedorn, C. H., and Cullen, B. R. (2004). Human microRNAs are processed from capped, polyadenylated transcripts that can also function as mRNAs. *Rna* **10**, 1957-66.
- Calin, G. A., and Croce, C. M. (2007). Investigation of microRNA alterations in leukemias and lymphomas. *Methods Enzymol* **427**, 193-213.
- Calin, G. A., Dumitru, C. D., Shimizu, M., Bichi, R., Zupo, S., Noch, E., Aldler, H., Rattan, S., Keating, M., Rai, K., Rassenti, L., Kipps, T., Negrini, M., Bullrich, F., and Croce, C. M. (2002). Frequent deletions and down-regulation of micro-RNA genes miR15 and miR16 at 13q14 in chronic lymphocytic leukemia. *Proc Natl Acad Sci U S A* **99**, 15524-9.

- Canossa, M., Griesbeck, O., Berninger, B., Campana, G., Kolbeck, R., and Thoenen, H. (1997). Neurotrophin release by neurotrophins: implications for activity-dependent neuronal plasticity. *Proc Natl Acad Sci U S A* **94**, 13279-86.
- Carleton, M., Cleary, M. A., and Linsley, P. S. (2007). MicroRNAs and cell cycle regulation. *Cell Cycle* **6**, 2127-32.
- Castren, E. (2004). Neurotrophins as mediators of drug effects on mood, addiction, and neuroprotection. *Mol Neurobiol* **29**, 289-302.
- Castren, E., Voikar, V., and Rantamaki, T. (2007). Role of neurotrophic factors in depression. *Curr Opin Pharmacol* **7**, 18-21.
- Chan, J. A., Krichevsky, A. M., and Kosik, K. S. (2005). MicroRNA-21 is an antiapoptotic factor in human glioblastoma cells. *Cancer Res* **65**, 6029-33.
- Chen, J. F., Mandel, E. M., Thomson, J. M., Wu, Q., Callis, T. E., Hammond, S. M., Conlon, F. L., and Wang, D. Z. (2006a). The role of microRNA-1 and microRNA-133 in skeletal muscle proliferation and differentiation. *Nat Genet* **38**, 228-33.
- Chen, Z. Y., Ieraci, A., Teng, H., Dall, H., Meng, C. X., Herrera, D. G., Nykjaer, A., Hempstead, B. L., and Lee, F. S. (2005). Sortilin controls intracellular sorting of brain-derived neurotrophic factor to the regulated secretory pathway. *J Neurosci* **25**, 6156-66.
- Chen, Z. Y., Jing, D., Bath, K. G., Ieraci, A., Khan, T., Siao, C. J., Herrera, D. G., Toth, M., Yang, C., McEwen, B. S., Hempstead, B. L., and Lee, F. S. (2006b). Genetic variant BDNF (Val66Met) polymorphism alters anxiety-related behavior. *Science* **314**, 140-3.
- Ciafre, S. A., Galardi, S., Mangiola, A., Ferracin, M., Liu, C. G., Sabatino, G., Negrini, M., Maira, G., Croce, C. M., and Farace, M. G. (2005). Extensive modulation of a set of microRNAs in primary glioblastoma. *Biochem Biophys Res Commun* **334**, 1351-8.
- Cimmino, A., Calin, G. A., Fabbri, M., Iorio, M. V., Ferracin, M., Shimizu, M., Wojcik, S. E., Aqeilan, R. I., Zupo, S., Dono, M., Rassenti, L., Alder, H., Volinia, S., Liu, C. G., Kipps, T. J., Negrini, M., and Croce, C. M. (2005). miR-15 and miR-16 induce apoptosis by targeting BCL2. *Proc Natl Acad Sci U S A* **102**, 13944-9.
- Clary, D. O., and Reichardt, L. F. (1994). An alternatively spliced form of the nerve growth factor receptor TrkA confers an enhanced response to neurotrophin 3. *Proc Natl Acad Sci U S A* **91**, 11133-7.
- Conaco, C., Otto, S., Han, J. J., and Mandel, G. (2006). Reciprocal actions of REST and a microRNA promote neuronal identity. *Proc Natl Acad Sci U S A* **103**, 2422-7.
- Coppola, V., Barrick, C. A., Southon, E. A., Celeste, A., Wang, K., Chen, B., Haddad el, B., Yin, J., Nussenzweig, A., Subramaniam, A., and Tessarollo, L. (2004). Ablation of TrkA function in the immune system causes B cell abnormalities. *Development* **131**, 5185-95.

- Dalmay, T. (2008). MicroRNAs and cancer. *J Intern Med* **263**, 366-75.
- Datta, S. R., Dudek, H., Tao, X., Masters, S., Fu, H., Gotoh, Y., and Greenberg, M. E. (1997). Akt phosphorylation of BAD couples survival signals to the cell-intrinsic death machinery. *Cell* **91**, 231-41.
- de Bruin, A., Maiti, B., Jakoi, L., Timmers, C., Buerki, R., and Leone, G. (2003). Identification and characterization of E2F7, a novel mammalian E2F family member capable of blocking cellular proliferation. *J Biol Chem* **278**, 42041-9.
- Dews, M., Homayouni, A., Yu, D., Murphy, D., Sevignani, C., Wentzel, E., Furth, E. E., Lee, W. M., Enders, G. H., Mendell, J. T., and Thomas-Tikhonenko, A. (2006). Augmentation of tumor angiogenesis by a Myc-activated microRNA cluster. *Nat Genet* **38**, 1060-5.
- Dierssen, M., Gratacos, M., Sahun, I., Martin, M., Gallego, X., Amador-Arjona, A., Martinez de Lagran, M., Murtra, P., Marti, E., Pujana, M. A., Ferrer, I., Dalfo, E., Martinez-Cue, C., Florez, J., Torres-Peraza, J. F., Alberch, J., Maldonado, R., Fillat, C., and Estivill, X. (2006). Transgenic mice overexpressing the full-length neurotrophin receptor TrkC exhibit increased catecholaminergic neuron density in specific brain areas and increased anxiety-like behavior and panic reaction. *Neurobiol Dis* **24**, 403-18.
- Doench, J. G., Petersen, C. P., and Sharp, P. A. (2003). siRNAs can function as miRNAs. *Genes Dev* **17**, 438-42.
- Doench, J. G., and Sharp, P. A. (2004). Specificity of microRNA target selection in translational repression. *Genes Dev* **18**, 504-11.
- Du, T., and Zamore, P. D. (2005). microPrimer: the biogenesis and function of microRNA. *Development* **132**, 4645-52.
- Eguchi, M., Eguchi-Ishimae, M., Tojo, A., Morishita, K., Suzuki, K., Sato, Y., Kudoh, S., Tanaka, K., Setoyama, M., Nagamura, F., Asano, S., and Kamada, N. (1999). Fusion of ETV6 to neurotrophin-3 receptor TRKC in acute myeloid leukemia with t(12;15)(p13;q25). *Blood* **93**, 1355-63.
- Eis, P. S., Tam, W., Sun, L., Chadburn, A., Li, Z., Gomez, M. F., Lund, E., and Dahlberg, J. E. (2005). Accumulation of miR-155 and BIC RNA in human B cell lymphomas. *Proc Natl Acad Sci U S A* **102**, 3627-32.
- Eletto, D., Russo, G., Passiatore, G., Del Valle, L., Giordano, A., Khalili, K., Gualco, E., and Peruzzi, F. (2008). Inhibition of SNAP25 expression by HIV-1 Tat involves the activity of mir-128a. *J Cell Physiol* **216**, 764-70.
- Encinas, M., Iglesias, M., Llecha, N., and Comella, J. X. (1999). Extracellular-regulated kinases and phosphatidylinositol 3-kinase are involved in brain-derived neurotrophic factor-mediated survival and neuritogenesis of the neuroblastoma cell line SH-SY5Y. *J Neurochem* **73**, 1409-21.
- Enright, A. J., John, B., Gaul, U., Tuschl, T., Sander, C., and Marks, D. S. (2003). MicroRNA targets in Drosophila. *Genome Biol* **5**, R1.



- Entschladen, F., Palm, D., Niggemann, B., and Zaenker, K. S. (2008). The cancer's nervous tooth: Considering the neuronal crosstalk within tumors. *Semin Cancer Biol* **18**, 171-5.
- Esau, C., Davis, S., Murray, S. F., Yu, X. X., Pandey, S. K., Pear, M., Watts, L., Booten, S. L., Graham, M., McKay, R., Subramaniam, A., Propp, S., Lollo, B. A., Freier, S., Bennett, C. F., Bhanot, S., and Monia, B. P. (2006). miR-122 regulation of lipid metabolism revealed by in vivo antisense targeting. *Cell Metab* **3**, 87-98.
- Esteban, P. F., Yoon, H. Y., Becker, J., Dorsey, S. G., Caprari, P., Palko, M. E., Coppola, V., Saragovi, H. U., Randazzo, P. A., and Tessarollo, L. (2006). A kinase-deficient TrkC receptor isoform activates Arf6-Rac1 signaling through the scaffold protein tamalin. *J Cell Biol* **173**, 291-9.
- Ferno, J., Skrede, S., Vik-Mo, A. O., Havik, B., and Steen, V. M. (2006). Drug-induced activation of SREBP-controlled lipogenic gene expression in CNS-related cell lines: marked differences between various antipsychotic drugs. *BMC Neurosci* **7**, 69.
- Filipowicz, W., Bhattacharyya, S. N., and Sonenberg, N. (2008). Mechanisms of post-transcriptional regulation by microRNAs: are the answers in sight? *Nat Rev Genet* **9**, 102-14.
- Fiore, R., and Schratt, G. (2007). MicroRNAs in vertebrate synapse development. *ScientificWorldJournal* **7**, 167-77.
- Geetha, T., Jiang, J., and Wooten, M. W. (2005). Lysine 63 polyubiquitination of the nerve growth factor receptor TrkA directs internalization and signaling. *Mol Cell* **20**, 301-12.
- Giraldez, A. J., Cinalli, R. M., Glasner, M. E., Enright, A. J., Thomson, J. M., Baskerville, S., Hammond, S. M., Bartel, D. P., and Schier, A. F. (2005). MicroRNAs regulate brain morphogenesis in zebrafish. *Science* **308**, 833-8.
- Griffiths-Jones, S. (2006). miRBase: the microRNA sequence database. *Methods Mol Biol* **342**, 129-38.
- Hallbook, F. (1999). Evolution of the vertebrate neurotrophin and Trk receptor gene families. *Curr Opin Neurobiol* **9**, 616-21.
- Hansen, T., Olsen, L., Lindow, M., Jakobsen, K. D., Ullum, H., Jonsson, E., Andreassen, O. A., Djurovic, S., Melle, I., Agartz, I., Hall, H., Timm, S., Wang, A. G., and Werge, T. (2007). Brain expressed microRNAs implicated in schizophrenia etiology. *PLoS ONE* **2**, e873.
- Harrington, A. W., Kim, J. Y., and Yoon, S. O. (2002). Activation of Rac GTPase by p75 is necessary for c-jun N-terminal kinase-mediated apoptosis. *J Neurosci* **22**, 156-66.
- He, A., Zhu, L., Gupta, N., Chang, Y., and Fang, F. (2007a). Overexpression of micro ribonucleic acid 29, highly up-regulated in diabetic rats, leads to insulin resistance in 3T3-L1 adipocytes. *Mol Endocrinol* **21**, 2785-94.

## References

---

- He, H., Jazdzewski, K., Li, W., Liyanarachchi, S., Nagy, R., Volinia, S., Calin, G. A., Liu, C. G., Franssila, K., Suster, S., Kloos, R. T., Croce, C. M., and de la Chapelle, A. (2005). The role of microRNA genes in papillary thyroid carcinoma. *Proc Natl Acad Sci U S A* **102**, 19075-80.
- He, L., and Hannon, G. J. (2004). MicroRNAs: small RNAs with a big role in gene regulation. *Nat Rev Genet* **5**, 522-31.
- He, L., He, X., Lim, L. P., de Stanchina, E., Xuan, Z., Liang, Y., Xue, W., Zender, L., Magnus, J., Ridzon, D., Jackson, A. L., Linsley, P. S., Chen, C., Lowe, S. W., Cleary, M. A., and Hannon, G. J. (2007b). A microRNA component of the p53 tumour suppressor network. *Nature* **447**, 1130-4.
- He, X. L., and Garcia, K. C. (2004). Structure of nerve growth factor complexed with the shared neurotrophin receptor p75. *Science* **304**, 870-5.
- Hetman, M., Kanning, K., Cavanaugh, J. E., and Xia, Z. (1999). Neuroprotection by brain-derived neurotrophic factor is mediated by extracellular signal-regulated kinase and phosphatidylinositol 3-kinase. *J Biol Chem* **274**, 22569-80.
- Hillebrand, J., Barbee, S. A., and Ramaswami, M. (2007). P-body components, microRNA regulation, and synaptic plasticity. *ScientificWorldJournal* **7**, 178-90.
- Holgado-Madruga, M., Moscatello, D. K., Emlet, D. R., Dieterich, R., and Wong, A. J. (1997). Grb2-associated binder-1 mediates phosphatidylinositol 3-kinase activation and the promotion of cell survival by nerve growth factor. *Proc Natl Acad Sci U S A* **94**, 12419-24.
- Hudder, A., and Novak, R. F. (2008). miRNAs: effectors of environmental influences on gene expression and disease. *Toxicol Sci* **103**, 228-40.
- Hutvagner, G., and Simard, M. J. (2008). Argonaute proteins: key players in RNA silencing. *Nat Rev Mol Cell Biol* **9**, 22-32.
- Ichinose, T., and Snider, W. D. (2000). Differential effects of TrkC isoforms on sensory axon outgrowth. *J Neurosci Res* **59**, 365-71.
- Jensen, K. P., Covault, J., Conner, T. S., Tennen, H., Kranzler, H. R., and Furneaux, H. M. (2008). A common polymorphism in serotonin receptor 1B mRNA moderates regulation by miR-96 and associates with aggressive human behaviors. *Mol Psychiatry*.
- Jin, P., Zarnescu, D. C., Ceman, S., Nakamoto, M., Mowrey, J., Jongens, T. A., Nelson, D. L., Moses, K., and Warren, S. T. (2004). Biochemical and genetic interaction between the fragile X mental retardation protein and the microRNA pathway. *Nat Neurosci* **7**, 113-7.
- John, B., Enright, A. J., Aravin, A., Tuschl, T., Sander, C., and Marks, D. S. (2004). Human MicroRNA targets. *PLoS Biol* **2**, e363.

- Johnson, S. M., Grosshans, H., Shingara, J., Byrom, M., Jarvis, R., Cheng, A., Labourier, E., Reinert, K. L., Brown, D., and Slack, F. J. (2005). RAS is regulated by the let-7 microRNA family. *Cell* **120**, 635-47.
- Johnston, R. J., and Hobert, O. (2003). A microRNA controlling left/right neuronal asymmetry in *Caenorhabditis elegans*. *Nature* **426**, 845-9.
- Kanamoto, T., Mota, M., Takeda, K., Rubin, L. L., Miyazono, K., Ichijo, H., and Bazenet, C. E. (2000). Role of apoptosis signal-regulating kinase in regulation of the c-Jun N-terminal kinase pathway and apoptosis in sympathetic neurons. *Mol Cell Biol* **20**, 196-204.
- Kaplan, D. R., Matsumoto, K., Lucarelli, E., and Thiele, C. J. (1993). Induction of TrkB by retinoic acid mediates biologic responsiveness to BDNF and differentiation of human neuroblastoma cells. Eukaryotic Signal Transduction Group. *Neuron* **11**, 321-31.
- Kaplan, D. R., and Miller, F. D. (1997). Signal transduction by the neurotrophin receptors. *Curr Opin Cell Biol* **9**, 213-21.
- Kaplan, D. R., and Miller, F. D. (2000). Neurotrophin signal transduction in the nervous system. *Curr Opin Neurobiol* **10**, 381-91.
- Karege, F., Vaudan, G., Schwald, M., Perroud, N., and La Harpe, R. (2005). Neurotrophin levels in postmortem brains of suicide victims and the effects of antemortem diagnosis and psychotropic drugs. *Brain Res Mol Brain Res* **136**, 29-37.
- Kawaji, H., and Hayashizaki, Y. (2008). Exploration of small RNAs. *PLoS Genet* **4**, e22.
- Kawamata, J., and Shimohama, S. (2002). Association of novel and established polymorphisms in neuronal nicotinic acetylcholine receptors with sporadic Alzheimer's disease. *J Alzheimers Dis* **4**, 71-6.
- Kermani, P., Rafii, D., Jin, D. K., Whitlock, P., Schaffer, W., Chiang, A., Vincent, L., Friedrich, M., Shido, K., Hackett, N. R., Crystal, R. G., Rafii, S., and Hempstead, B. L. (2005). Neurotrophins promote revascularization by local recruitment of TrkB+ endothelial cells and systemic mobilization of hematopoietic progenitors. *J Clin Invest* **115**, 653-63.
- Kim, J., Inoue, K., Ishii, J., Vanti, W. B., Voronov, S. V., Murchison, E., Hannon, G., and Abeliovich, A. (2007). A MicroRNA feedback circuit in midbrain dopamine neurons. *Science* **317**, 1220-4.
- Kim, V. N. (2005). Small RNAs: classification, biogenesis, and function. *Mol Cells* **19**, 1-15.
- Kim, V. N., and Nam, J. W. (2006). Genomics of microRNA. *Trends Genet* **22**, 165-73.
- Kiriakidou, M., Nelson, P. T., Kouranov, A., Fitziev, P., Bouyioukos, C., Mourelatos, Z., and Hatzigeorgiou, A. (2004). A combined computational-experimental approach predicts human microRNA targets. *Genes Dev* **18**, 1165-78.

## References

---

- Kiriakidou, M., Tan, G. S., Lamprinaki, S., De Planell-Saguer, M., Nelson, P. T., and Mourelatos, Z. (2007). An mRNA m7G cap binding-like motif within human Ago2 represses translation. *Cell* **129**, 1141-51.
- Klattenhoff, C., and Theurkauf, W. (2008). Biogenesis and germline functions of piRNAs. *Development* **135**, 3-9.
- Koh, J. Y., Gwag, B. J., Lobner, D., and Choi, D. W. (1995). Potentiated necrosis of cultured cortical neurons by neurotrophins. *Science* **268**, 573-5.
- Koponen, E., Voikar, V., Riekkki, R., Saarelainen, T., Rauramaa, T., Rauvala, H., Taira, T., and Castren, E. (2004). Transgenic mice overexpressing the full-length neurotrophin receptor trkB exhibit increased activation of the trkB-PLCgamma pathway, reduced anxiety, and facilitated learning. *Mol Cell Neurosci* **26**, 166-81.
- Kosik, K. S. (2006). The neuronal microRNA system. *Nat Rev Neurosci* **7**, 911-20.
- Krek, A., Grun, D., Poy, M. N., Wolf, R., Rosenberg, L., Epstein, E. J., MacMenamin, P., da Piedade, I., Gunsalus, K. C., Stoffel, M., and Rajewsky, N. (2005). Combinatorial microRNA target predictions. *Nat Genet* **37**, 495-500.
- Krichevsky, A. M., Sonntag, K. C., Isacson, O., and Kosik, K. S. (2006). Specific microRNAs modulate embryonic stem cell-derived neurogenesis. *Stem Cells* **24**, 857-64.
- Krishnan, V., Han, M. H., Graham, D. L., Berton, O., Renthal, W., Russo, S. J., Laplant, Q., Graham, A., Lutter, M., Lagace, D. C., Ghose, S., Reister, R., Tannous, P., Green, T. A., Neve, R. L., Chakravarty, S., Kumar, A., Eisch, A. J., Self, D. W., Lee, F. S., Tamminga, C. A., Cooper, D. C., Gershenfeld, H. K., and Nestler, E. J. (2007). Molecular adaptations underlying susceptibility and resistance to social defeat in brain reward regions. *Cell* **131**, 391-404.
- Kruttgen, A., Schneider, I., and Weis, J. (2006). The dark side of the NGF family: neurotrophins in neoplasias. *Brain Pathol* **16**, 304-10.
- Kye, M. J., Liu, T., Levy, S. F., Xu, N. L., Groves, B. B., Bonneau, R., Lao, K., and Kosik, K. S. (2007). Somatodendritic microRNAs identified by laser capture and multiplex RT-PCR. *Rna* **13**, 1224-34.
- Lachyankar, M. B., Condon, P. J., Quesenberry, P. J., Litofsky, N. S., Recht, L. D., and Ross, A. H. (1997). Embryonic precursor cells that express Trk receptors: induction of different cell fates by NGF, BDNF, NT-3, and CNTF. *Exp Neurol* **144**, 350-60.
- Lagos-Quintana, M., Rauhut, R., Yalcin, A., Meyer, J., Lendeckel, W., and Tuschl, T. (2002). Identification of tissue-specific microRNAs from mouse. *Curr Biol* **12**, 735-9.
- Lai, E. C., Wiel, C., and Rubin, G. M. (2004). Complementary miRNA pairs suggest a regulatory role for miRNA:miRNA duplexes. *Rna* **10**, 171-5.

- Landthaler, M., Yalcin, A., and Tuschl, T. (2004). The human DiGeorge syndrome critical region gene 8 and Its D. melanogaster homolog are required for miRNA biogenesis. *Curr Biol* **14**, 2162-7.
- Laneve, P., Di Marcotullio, L., Gioia, U., Fiori, M. E., Ferretti, E., Gulino, A., Bozzoni, I., and Caffarelli, E. (2007). The interplay between microRNAs and the neurotrophin receptor tropomyosin-related kinase C controls proliferation of human neuroblastoma cells. *Proc Natl Acad Sci U S A* **104**, 7957-62.
- Lee, R., Kermani, P., Teng, K. K., and Hempstead, B. L. (2001). Regulation of cell survival by secreted proneurotrophins. *Science* **294**, 1945-8.
- Lewis, B. P., Burge, C. B., and Bartel, D. P. (2005). Conserved seed pairing, often flanked by adenosines, indicates that thousands of human genes are microRNA targets. *Cell* **120**, 15-20.
- Lewis, B. P., Shih, I. H., Jones-Rhoades, M. W., Bartel, D. P., and Burge, C. B. (2003). Prediction of mammalian microRNA targets. *Cell* **115**, 787-98.
- Licatalosi, D. D., and Darnell, R. B. (2006). Splicing regulation in neurologic disease. *Neuron* **52**, 93-101.
- Liebl, D. J., Tessarollo, L., Palko, M. E., and Parada, L. F. (1997). Absence of sensory neurons before target innervation in brain-derived neurotrophic factor-, neurotrophin 3-, and TrkC-deficient embryonic mice. *J Neurosci* **17**, 9113-21.
- Liepinsh, E., Ilag, L. L., Otting, G., and Ibanez, C. F. (1997). NMR structure of the death domain of the p75 neurotrophin receptor. *Embo J* **16**, 4999-5005.
- Lillevali, K., Kulla, A., and Ord, T. (2001). Comparative expression analysis of the genes encoding polypyrimidine tract binding protein (PTB) and its neural homologue (brPTB) in prenatal and postnatal mouse brain. *Mech Dev* **101**, 217-20.
- Lim, L. P., Lau, N. C., Garrett-Engele, P., Grimson, A., Schelter, J. M., Castle, J., Bartel, D. P., Linsley, P. S., and Johnson, J. M. (2005). Microarray analysis shows that some microRNAs downregulate large numbers of target mRNAs. *Nature* **433**, 769-73.
- Lin, M. I., Das, I., Schwartz, G. M., Tsoulfas, P., Mikawa, T., and Hempstead, B. L. (2000). Trk C receptor signaling regulates cardiac myocyte proliferation during early heart development in vivo. *Dev Biol* **226**, 180-91.
- Lin, P. Y., and Tsai, G. (2004). Meta-analyses of the association between genetic polymorphisms of neurotrophic factors and schizophrenia. *Schizophr Res* **71**, 353-60.
- Lindow, M., and Gorodkin, J. (2007). Principles and limitations of computational microRNA gene and target finding. *DNA Cell Biol* **26**, 339-51.
- Lovat, P. E., Pearson, A. D., Malcolm, A., and Redfern, C. P. (1993). Retinoic acid receptor expression during the in vitro differentiation of human neuroblastoma. *Neurosci Lett* **162**, 109-13.

## References

---

- Lu, B., Pang, P. T., and Woo, N. H. (2005). The yin and yang of neurotrophin action. *Nat Rev Neurosci* **6**, 603-14.
- Lukiw, W. J. (2007). Micro-RNA speciation in fetal, adult and Alzheimer's disease hippocampus. *Neuroreport* **18**, 297-300.
- Mahony, S., Corcoran, D. L., Feingold, E., and Benos, P. V. (2007). Regulatory conservation of protein coding and microRNA genes in vertebrates: lessons from the opossum genome. *Genome Biol* **8**, R84.
- Makeyev, E. V., Zhang, J., Carrasco, M. A., and Maniatis, T. (2007). The MicroRNA miR-124 promotes neuronal differentiation by triggering brain-specific alternative pre-mRNA splicing. *Mol Cell* **27**, 435-48.
- Maroney, P. A., Yu, Y., Fisher, J., and Nilsen, T. W. (2006). Evidence that microRNAs are associated with translating messenger RNAs in human cells. *Nat Struct Mol Biol* **13**, 1102-7.
- Meister, G., and Tuschl, T. (2004). Mechanisms of gene silencing by double-stranded RNA. *Nature* **431**, 343-9.
- Menn, B., Timsit, S., Calothy, G., and Lamballe, F. (1998). Differential expression of TrkC catalytic and noncatalytic isoforms suggests that they act independently or in association. *J Comp Neurol* **401**, 47-64.
- Menn, B., Timsit, S., Represa, A., Mateos, S., Calothy, G., and Lamballe, F. (2000). Spatiotemporal expression of noncatalytic TrkC NC2 isoform during early and late CNS neurogenesis: a comparative study with TrkC catalytic and p75NTR receptors. *Eur J Neurosci* **12**, 3211-23.
- Michael, M. Z., SM, O. C., van Holst Pellekaan, N. G., Young, G. P., and James, R. J. (2003). Reduced accumulation of specific microRNAs in colorectal neoplasia. *Mol Cancer Res* **1**, 882-91.
- Middleton, G., Hamanoue, M., Enokido, Y., Wyatt, S., Pennica, D., Jaffray, E., Hay, R. T., and Davies, A. M. (2000). Cytokine-induced nuclear factor kappa B activation promotes the survival of developing neurons. *J Cell Biol* **148**, 325-32.
- Miranda, K. C., Huynh, T., Tay, Y., Ang, Y. S., Tam, W. L., Thomson, A. M., Lim, B., and Rigoutsos, I. (2006). A pattern-based method for the identification of MicroRNA binding sites and their corresponding heteroduplexes. *Cell* **126**, 1203-17.
- Muiños-Gimeno, M., Guidi, M., Kagerbauer, B., Martin-Santos, R., Navinés, R., Alonso, P., Menchón, J. M., Gratacòs, M., Estivill, X., and Espinosa-Parrilla, Y. (2008). Allele variants in functional microRNA target sites of the neurotrophin-3 receptor gene (NTRK3) contribute to the susceptibility to anxiety disorders *Submitted*.
- Mukai, J., Suvant, P., and Sato, T. A. (2003). Nerve growth factor-dependent regulation of NADE-induced apoptosis. *Vitam Horm* **66**, 385-402.

- Narla, G., DiFeo, A., Yao, S., Banno, A., Hod, E., Reeves, H. L., Qiao, R. F., Camacho-Vanegas, O., Levine, A., Kirschenbaum, A., Chan, A. M., Friedman, S. L., and Martignetti, J. A. (2005). Targeted inhibition of the KLF6 splice variant, KLF6 SV1, suppresses prostate cancer cell growth and spread. *Cancer Res* **65**, 5761-8.
- Nestler, E. J., Barrot, M., DiLeone, R. J., Eisch, A. J., Gold, S. J., and Monteggia, L. M. (2002). Neurobiology of depression. *Neuron* **34**, 13-25.
- Novotny, G. W., Nielsen, J. E., Sonne, S. B., Skakkebaek, N. E., Rajpert-De Meyts, E., and Leffers, H. (2007). Analysis of gene expression in normal and neoplastic human testis: new roles of RNA. *Int J Androl* **30**, 316-26; discussion 326-7.
- Numan, S., Lane-Ladd, S. B., Zhang, L., Lundgren, K. H., Russell, D. S., Seroogy, K. B., and Nestler, E. J. (1998). Differential regulation of neurotrophin and trk receptor mRNAs in catecholaminergic nuclei during chronic opiate treatment and withdrawal. *J Neurosci* **18**, 10700-8.
- O'Donnell, K. A., Wentzel, E. A., Zeller, K. I., Dang, C. V., and Mendell, J. T. (2005). c-Myc-regulated microRNAs modulate E2F1 expression. *Nature* **435**, 839-43.
- Oppenheim, R. W. (1991). Cell death during development of the nervous system. *Annu Rev Neurosci* **14**, 453-501.
- Palko, M. E., Coppola, V., and Tessarollo, L. (1999). Evidence for a role of truncated trkC receptor isoforms in mouse development. *J Neurosci* **19**, 775-82.
- Papadia, S., Soriano, F. X., Leveille, F., Martel, M. A., Dakin, K. A., Hansen, H. H., Kaindl, A., Sifringer, M., Fowler, J., Stefovaska, V., McKenzie, G., Craigon, M., Corriveau, R., Ghazal, P., Horsburgh, K., Yankner, B. A., Wyllie, D. J., Ikonomidou, C., and Hardingham, G. E. (2008). Synaptic NMDA receptor activity boosts intrinsic antioxidant defenses. *Nat Neurosci* **11**, 476-87.
- Park, J. K., Liu, X., Strauss, T. J., McKearin, D. M., and Liu, Q. (2007). The miRNA pathway intrinsically controls self-renewal of Drosophila germline stem cells. *Curr Biol* **17**, 533-8.
- Pasquale, E. B. (2008). Eph-ephrin bidirectional signaling in physiology and disease. *Cell* **133**, 38-52.
- Penagarikano, O., Mulle, J. G., and Warren, S. T. (2007). The pathophysiology of fragile x syndrome. *Annu Rev Genomics Hum Genet* **8**, 109-29.
- Perkins, D. O., Jeffries, C. D., Jarskog, L. F., Thomson, J. M., Woods, K., Newman, M. A., Parker, J. S., Jin, J., and Hammond, S. M. (2007). microRNA expression in the prefrontal cortex of individuals with schizophrenia and schizoaffective disorder. *Genome Biol* **8**, R27.
- Pierson, J., Hostager, B., Fan, R., and Vibhakar, R. (2008). Regulation of cyclin dependent kinase 6 by microRNA 124 in medulloblastoma. *J Neurooncol* **90**, 1-7.



- Poy, M. N., Eliasson, L., Krutzfeldt, J., Kuwajima, S., Ma, X., Macdonald, P. E., Pfeffer, S., Tuschl, T., Rajewsky, N., Rorsman, P., and Stoffel, M. (2004). A pancreatic islet-specific microRNA regulates insulin secretion. *Nature* **432**, 226-30.
- Psilopanagioti, A., Papadaki, H., Kranioti, E. F., Alexandrides, T. K., and Varakis, J. N. (2008). Expression of Adiponectin and Adiponectin Receptors in Human Pituitary Gland and Brain. *Neuroendocrinology*.
- Rayet, B., and Gelinas, C. (1999). Aberrant rel/nfkb genes and activity in human cancer. *Oncogene* **18**, 6938-47.
- Rehmsmeier, M., Steffen, P., Hochsmann, M., and Giegerich, R. (2004). Fast and effective prediction of microRNA/target duplexes. *Rna* **10**, 1507-17.
- Reichardt, L. F. (2006). Neurotrophin-regulated signalling pathways. *Philos Trans R Soc Lond B Biol Sci* **361**, 1545-64.
- Ribases, M., Gratacos, M., Fernandez-Aranda, F., Bellodi, L., Boni, C., Anderluh, M., Cavallini, M. C., Cellini, E., Di Bella, D., Erzegovesi, S., Foulon, C., Gabrovsek, M., Gorwood, P., Hebebrand, J., Hinney, A., Holliday, J., Hu, X., Karwautz, A., Kipman, A., Komel, R., Nacmias, B., Remschmidt, H., Ricca, V., Sorbi, S., Wagner, G., Treasure, J., Collier, D. A., and Estivill, X. (2004). Association of BDNF with anorexia, bulimia and age of onset of weight loss in six European populations. *Hum Mol Genet* **13**, 1205-12.
- Ro, S., Park, C., Sanders, K. M., McCarrey, J. R., and Yan, W. (2007). Cloning and expression profiling of testis-expressed microRNAs. *Dev Biol* **311**, 592-602.
- Rodriguez, A., Griffiths-Jones, S., Ashurst, J. L., and Bradley, A. (2004). Identification of mammalian microRNA host genes and transcription units. *Genome Res* **14**, 1902-10.
- Rodriguez-Tebar, A., Dechant, G., and Barde, Y. A. (1990). Binding of brain-derived neurotrophic factor to the nerve growth factor receptor. *Neuron* **4**, 487-92.
- Rougvie, A. E. (2001). Control of developmental timing in animals. *Nat Rev Genet* **2**, 690-701.
- Saarelainen, T., Hendolin, P., Lucas, G., Koponen, E., Sairanen, M., MacDonald, E., Agerman, K., Haapasalo, A., Nawa, H., Aloyz, R., Ernfors, P., and Castren, E. (2003). Activation of the TrkB neurotrophin receptor is induced by antidepressant drugs and is required for antidepressant-induced behavioral effects. *J Neurosci* **23**, 349-57.
- Sadakata, T., Kakegawa, W., Mizoguchi, A., Washida, M., Katoh-Semba, R., Shutoh, F., Okamoto, T., Nakashima, H., Kimura, K., Tanaka, M., Sekine, Y., Itohara, S., Yuzaki, M., Nagao, S., and Furuichi, T. (2007). Impaired cerebellar development and function in mice lacking CAPS2, a protein involved in neurotrophin release. *J Neurosci* **27**, 2472-82.
- Sahun, I., Gallego, X., Gratacos, M., Murtra, P., Trullas, R., Maldonado, R., Estivill, X., and Diernsen, M. (2007). Differential responses to anxiogenic drugs in a



- mouse model of panic disorder as revealed by Fos immunocytochemistry in specific areas of the fear circuitry. *Amino Acids* **33**, 677-88.
- Saile, B., Matthes, N., El Armouche, H., Neubauer, K., and Ramadori, G. (2001). The bcl, NFkappaB and p53/p21WAF1 systems are involved in spontaneous apoptosis and in the anti-apoptotic effect of TGF-beta or TNF-alpha on activated hepatic stellate cells. *Eur J Cell Biol* **80**, 554-61.
- Schaefer, A., O'Carroll, D., Tan, C. L., Hillman, D., Sugimori, M., Llinas, R., and Greengard, P. (2007). Cerebellar neurodegeneration in the absence of microRNAs. *J Exp Med* **204**, 1553-8.
- Schratt, G. M., Tuebing, F., Nigh, E. A., Kane, C. G., Sabatini, M. E., Kiebler, M., and Greenberg, M. E. (2006). A brain-specific microRNA regulates dendritic spine development. *Nature* **439**, 283-9.
- Schulte, J. H., Horn, S., Schlierf, S., Schramm, A., Heukamp, L. C., Christiansen, H., Buettner, R., Berwanger, B., and Eggert, A. (2008). MicroRNAs in the pathogenesis of neuroblastoma. *Cancer Lett.*
- Schulte-Herbruggen, O., Braun, A., Rochlitzer, S., Jockers-Scherubl, M. C., and Hellweg, R. (2007). Neurotrophic factors--a tool for therapeutic strategies in neurological, neuropsychiatric and neuroimmunological diseases? *Curr Med Chem* **14**, 2318-29.
- Sempere, L. F., Freemantle, S., Pitha-Rowe, I., Moss, E., Dmitrovsky, E., and Ambros, V. (2004). Expression profiling of mammalian microRNAs uncovers a subset of brain-expressed microRNAs with possible roles in murine and human neuronal differentiation. *Genome Biol* **5**, R13.
- Sethupathy, P., Megraw, M., and Hatzigeorgiou, A. G. (2006). A guide through present computational approaches for the identification of mammalian microRNA targets. *Nat Methods* **3**, 881-6.
- Shelton, D. L., Sutherland, J., Gripp, J., Camerato, T., Armanini, M. P., Phillips, H. S., Carroll, K., Spencer, S. D., and Levinson, A. D. (1995). Human trks: molecular cloning, tissue distribution, and expression of extracellular domain immunoadhesins. *J Neurosci* **15**, 477-91.
- Sigrist, S. J., Thiel, P. R., Reiff, D. F., Lachance, P. E., Lasko, P., and Schuster, C. M. (2000). Postsynaptic translation affects the efficacy and morphology of neuromuscular junctions. *Nature* **405**, 1062-5.
- Silber, J., Lim, D. A., Petritsch, C., Persson, A. I., Maunakea, A. K., Yu, M., Vandenberg, S. R., Ginzinger, D. G., James, C. D., Costello, J. F., Bergers, G., Weiss, W. A., Alvarez-Buylla, A., and Hodgson, J. G. (2008). miR-124 and miR-137 inhibit proliferation of glioblastoma multiforme cells and induce differentiation of brain tumor stem cells. *BMC Med* **6**, 14.
- Smirnova, L., Grafe, A., Seiler, A., Schumacher, S., Nitsch, R., and Wulczyn, F. G. (2005). Regulation of miRNA expression during neural cell specification. *Eur J Neurosci* **21**, 1469-77.

## References

---

- Smith, M. A., Makino, S., Altemus, M., Michelson, D., Hong, S. K., Kvetnansky, R., and Post, R. M. (1995). Stress and antidepressants differentially regulate neurotrophin 3 mRNA expression in the locus coeruleus. *Proc Natl Acad Sci U S A* **92**, 8788-92.
- Song, M. S., and Posse de Chaves, E. I. (2003). Inhibition of rat sympathetic neuron apoptosis by ceramide. Role of p75NTR in ceramide generation. *Neuropharmacology* **45**, 1130-50.
- Stark, A., Brennecke, J., Bushati, N., Russell, R. B., and Cohen, S. M. (2005). Animal MicroRNAs confer robustness to gene expression and have a significant impact on 3'UTR evolution. *Cell* **123**, 1133-46.
- Stern-Ginossar, N., Elefant, N., Zimmermann, A., Wolf, D. G., Saleh, N., Biton, M., Horwitz, E., Prokocimer, Z., Prichard, M., Hahn, G., Goldman-Wohl, D., Greenfield, C., Yagel, S., Hengel, H., Altuvia, Y., Margalit, H., and Mandelboim, O. (2007). Host immune system gene targeting by a viral miRNA. *Science* **317**, 376-81.
- Strohmaier, C., Carter, B. D., Urfer, R., Barde, Y. A., and Dechant, G. (1996). A splice variant of the neurotrophin receptor trkB with increased specificity for brain-derived neurotrophic factor. *Embo J* **15**, 3332-7.
- Suh, M. R., Lee, Y., Kim, J. Y., Kim, S. K., Moon, S. H., Lee, J. Y., Cha, K. Y., Chung, H. M., Yoon, H. S., Moon, S. Y., Kim, V. N., and Kim, K. S. (2004). Human embryonic stem cells express a unique set of microRNAs. *Dev Biol* **270**, 488-98.
- Sutton, M. A., and Schuman, E. M. (2006). Dendritic protein synthesis, synaptic plasticity, and memory. *Cell* **127**, 49-58.
- Szymanski, M., Barciszewska, M. Z., Erdmann, V. A., and Barciszewski, J. (2005). A new frontier for molecular medicine: noncoding RNAs. *Biochim Biophys Acta* **1756**, 65-75.
- Tadokoro, K., Hashimoto, R., Tatsumi, M., Kamijima, K., and Kunugi, H. (2004). Analysis of enhancer activity of a dinucleotide repeat polymorphism in the neurotrophin-3 gene and its association with bipolar disorder. *Neuropsychobiology* **50**, 206-10.
- Taganov, K. D., Boldin, M. P., Chang, K. J., and Baltimore, D. (2006). NF-kappaB-dependent induction of microRNA miR-146, an inhibitor targeted to signaling proteins of innate immune responses. *Proc Natl Acad Sci U S A* **103**, 12481-6.
- Takamizawa, J., Konishi, H., Yanagisawa, K., Tomida, S., Osada, H., Endoh, H., Harano, T., Yatabe, Y., Nagino, M., Nimura, Y., Mitsudomi, T., and Takahashi, T. (2004). Reduced expression of the let-7 microRNAs in human lung cancers in association with shortened postoperative survival. *Cancer Res* **64**, 3753-6.
- Tsoufas, P., Stephens, R. M., Kaplan, D. R., and Parada, L. F. (1996). TrkC isoforms with inserts in the kinase domain show impaired signaling responses. *J Biol Chem* **271**, 5691-7.

- van Rooij, E., and Olson, E. N. (2007). microRNAs put their signatures on the heart. *Physiol Genomics* **31**, 365-6.
- Visvanathan, J., Lee, S., Lee, B., Lee, J. W., and Lee, S. K. (2007). The microRNA miR-124 antagonizes the anti-neural REST/SCP1 pathway during embryonic CNS development. *Genes Dev* **21**, 744-9.
- Wang, G., van der Walt, J. M., Mayhew, G., Li, Y. J., Zuchner, S., Scott, W. K., Martin, E. R., and Vance, J. M. (2008a). Variation in the miRNA-433 binding site of FGF20 confers risk for Parkinson disease by overexpression of alpha-synuclein. *Am J Hum Genet* **82**, 283-9.
- Wang, P., Wang, X., Wang, F., Cai, T., and Luo, Y. (2006a). Interaction between Mnk2 and CBC(VHL) ubiquitin ligase E3 complex. *Sci China C Life Sci* **49**, 265-73.
- Wang, W. X., Rajeev, B. W., Stromberg, A. J., Ren, N., Tang, G., Huang, Q., Rigoutsos, I., and Nelson, P. T. (2008b). The expression of microRNA miR-107 decreases early in Alzheimer's disease and may accelerate disease progression through regulation of beta-site amyloid precursor protein-cleaving enzyme 1. *J Neurosci* **28**, 1213-23.
- Wang, Y., Luo, W., Wartmann, T., Halangk, W., Sahin-Toth, M., and Reiser, G. (2006b). Mesotrypsin, a brain trypsin, activates selectively proteinase-activated receptor-1, but not proteinase-activated receptor-2, in rat astrocytes. *J Neurochem* **99**, 759-69.
- Wu, L., and Belasco, J. G. (2005). Micro-RNA regulation of the mammalian lin-28 gene during neuronal differentiation of embryonal carcinoma cells. *Mol Cell Biol* **25**, 9198-208.
- Xie, X., Lu, J., Kulbokas, E. J., Golub, T. R., Mootha, V., Lindblad-Toh, K., Lander, E. S., and Kellis, M. (2005). Systematic discovery of regulatory motifs in human promoters and 3' UTRs by comparison of several mammals. *Nature* **434**, 338-45.
- Yamashiro, D. J., Liu, X. G., Lee, C. P., Nakagawara, A., Ikegaki, N., McGregor, L. M., Baylin, S. B., and Brodeur, G. M. (1997). Expression and function of Trk-C in favourable human neuroblastomas. *Eur J Cancer* **33**, 2054-7.
- Yamashita, T., Tucker, K. L., and Barde, Y. A. (1999). Neurotrophin binding to the p75 receptor modulates Rho activity and axonal outgrowth. *Neuron* **24**, 585-93.
- Yao, R., and Cooper, G. M. (1995). Requirement for phosphatidylinositol-3 kinase in the prevention of apoptosis by nerve growth factor. *Science* **267**, 2003-6.
- Yekta, S., Shih, I. H., and Bartel, D. P. (2004). MicroRNA-directed cleavage of HOXB8 mRNA. *Science* **304**, 594-6.
- Yoon, S., and De Micheli, G. (2006). Computational identification of microRNAs and their targets. *Birth Defects Res C Embryo Today* **78**, 118-28.

## References

---

- Youn, Y. H., Feng, J., Tessarollo, L., Ito, K., and Sieber-Blum, M. (2003). Neural crest stem cell and cardiac endothelium defects in the TrkC null mouse. *Mol Cell Neurosci* **24**, 160-70.
- Yuan, X. B., Jin, M., Xu, X., Song, Y. Q., Wu, C. P., Poo, M. M., and Duan, S. (2003). Signalling and crosstalk of Rho GTPases in mediating axon guidance. *Nat Cell Biol* **5**, 38-45.
- Zhang, B., Tan, Z., Zhang, C., Shi, Y., Lin, Z., Gu, N., Feng, G., and He, L. (2002). Polymorphisms of chromogranin B gene associated with schizophrenia in Chinese Han population. *Neurosci Lett* **323**, 229-33.
- Zhang, Y., Chao, T., Li, R., Liu, W., Chen, Y., Yan, X., Gong, Y., Yin, B., Liu, W., Qiang, B., Zhao, J., Yuan, J., and Peng, X. (2008). MicroRNA-128 inhibits glioma cells proliferation by targeting transcription factor E2F3a. *J Mol Med*.
- Zhou, X., Ruan, J., Wang, G., and Zhang, W. (2007). Characterization and identification of microRNA core promoters in four model species. *PLoS Comput Biol* **3**, e37.

# Abbreviations

|                 |                                          |
|-----------------|------------------------------------------|
| AD              | Alzheimer's disease                      |
| Ago             | Argonaute                                |
| BDNF            | brain-derived neurotrophic factor        |
| bp              | base pair                                |
| CDK             | cyclin-dependent Kinase                  |
| CLL             | chronic lymphocytic leukemia             |
| CNS             | central nervous system                   |
| Ct              | crossing point                           |
| Da, kDa         | Dalton, kiloDalton                       |
| DMEM            | Dulbecco's modified Eagle's medium       |
| dsRNA           | double-stranded RNA                      |
| EC cells        | embryonic carcinoma cells                |
| ECL             | enhanced chemiluminescence               |
| ERK             | extracellular signal-regulated kinase    |
| ES cells        | embryonic stem cells                     |
| EST             | expressed sequence tag                   |
| FBS             | fetal bovine serum                       |
| FX              | Fragile X                                |
| FL-NTRK3        | full-length NTRK3                        |
| GAPDH           | glyceraldehyde 3-phosphate dehydrogenase |
| GBM             | glioblastoma                             |
| IPA             | Ingenuity pathway analysis               |
| MAPK            | mitogen activated protein kinase         |
| MDB             | medulloblastoma                          |
| mfe             | minimum free energy                      |
| miRNA           | microRNA                                 |
| mL, $\mu$ L     | milliliter, microliter                   |
| mM, $\mu$ M, nM | millimolar, micromolar, nanomolar        |

|             |                                              |
|-------------|----------------------------------------------|
| NB          | neuroblastoma                                |
| ncRNA       | non-coding RNA                               |
| NGF         | neurotrophic growth factor                   |
| nt          | nucleotide                                   |
| NT3         | neurotrophin-3                               |
| NT4/5       | neurotrophin 4/5                             |
| NTRK1       | neurotrophic tyrosine kinase receptor type 1 |
| NTRK2       | neurotrophic tyrosine kinase receptor type 2 |
| NTRK3       | neurotrophic tyrosine kinase receptor type 3 |
| ON          | overnight                                    |
| p75NTR      | p75 neurotrophin receptor                    |
| P-body      | processing body                              |
| PCR         | polymerase chain reaction                    |
| PD          | Parkinson's disease                          |
| PI3K        | phosphoinositide 3-kinase                    |
| piRNA       | Piwi interacting RNA                         |
| PLC         | phospholipase C                              |
| PNS         | peripheral nervous system                    |
| pre-miRNA   | precursor miRNA                              |
| pri-miRNA   | primary miRNA                                |
| PTBP1       | polypyrimidine tract-binding protein 1       |
| RA          | retinoic acid                                |
| RISC        | RNA-induced silencing complex                |
| RNP complex | ribonucleoprotein complex                    |
| RT          | room temperature                             |
| RT-PCR      | reverse transcription PCR                    |
| SE          | standard error                               |
| SG          | stress granule                               |
| siRNA       | small interfering RNA                        |
| TK          | tyrosine kinase                              |
| TR-NTRK3    | truncated NTRK3                              |
| U           | enzyme unit                                  |
| UTR         | untranslated region                          |
| WB          | Western blot                                 |







